

## INFORMATION TO USERS

This material was produced from a microfilm copy of the original document. While the most advanced technological means to photograph and reproduce this document have been used, the quality is heavily dependent upon the quality of the original submitted.

The following explanation of techniques is provided to help you understand markings or patterns which may appear on this reproduction.

1. The sign or "target" for pages apparently lacking from the document photographed is "Missing Page(s)". If it was possible to obtain the missing page(s) or section, they are spliced into the film along with adjacent pages. This may have necessitated cutting thru an image and duplicating adjacent pages to insure you complete continuity.
2. When an image on the film is obliterated with a large round black mark, it is an indication that the photographer suspected that the copy may have moved during exposure and thus cause a blurred image. You will find a good image of the page in the adjacent frame.
3. When a map, drawing or chart, etc., was part of the material being photographed the photographer followed a definite method in "sectioning" the material. It is customary to begin photoing at the upper left hand corner of a large sheet and to continue photoing from left to right in equal sections with a small overlap. If necessary, sectioning is continued again – beginning below the first row and continuing on until complete.
4. The majority of users indicate that the textual content is of greatest value, however, a somewhat higher quality reproduction could be made from "photographs" if essential to the understanding of the dissertation. Silver prints of "photographs" may be ordered at additional charge by writing the Order Department, giving the catalog number, title, author and specific pages you wish reproduced.
5. PLEASE NOTE: Some pages may have indistinct print. Filmed as received.

**Xerox University Microfilms**

300 North Zeeb Road  
Ann Arbor, Michigan 48106

76-8338

MUHLENKAMP, Sam Paul, 1947-  
PYROLYSIS OF LIVING WILDLAND FUELS.

The University of Oklahoma, Ph.D., 1975  
Engineering, chemical

**Xerox University Microfilms**, Ann Arbor, Michigan 48106

THIS DISSERTATION HAS BEEN MICROFILMED EXACTLY AS RECEIVED.

THE UNIVERSITY OF OKLAHOMA

GRADUATE COLLEGE

PYROLYSIS OF LIVING WILDLAND FUELS

A DISSERTATION

SUBMITTED TO THE GRADUATE FACULTY

in partial fulfillment of the requirements for the

degree of

DOCTOR OF PHILOSOPHY

BY

SAM PAUL MUHLENKAMP

Norman, Oklahoma

1975

PYROLYSIS OF LIVING WILDLAND FUELS

APPROVED BY

C.M. Sheppard  
J. E. Wilber  
Carl E. Forke  
John J. ...  
J.M. Townsend

DISSERTATION COMMITTEE

## ABSTRACT

Freeze-drying as a method of preparation of living plant samples has been validated by comparison of thermogravimetric measurements of fresh and freeze-dried plant samples. Validation measurements were made on pine needles, spruce needles, and holly leaves.

Weight loss and rate of weight loss measurements have been made in a nitrogen atmosphere on freeze-dried samples at heating rates of 10, 40, and 160°C/min. These freeze-dried samples include Ponderosa pine needles, aspen leaves, Douglas fir needles, lodgepole pine needles, chamise foliage, and manzanita leaves.

Energy changes during pyrolysis were measured on the freeze-dried samples at 40 and 160°C/min in a nitrogen atmosphere using a differential scanning calorimeter. Energy measurements on the ether extractive of Ponderosa pine indicate that the extractives have an important effect on the pyrolysis of freeze-dried plant samples.

Thermogravimetric data of cellulose and punky wood have been analyzed at individual heating rates. These results indicate that the heating rate has an effect upon the kinetic parameters of pyrolysis.

## ACKNOWLEDGMENTS

I am grateful to many people for their contributions to me during this research. Of all these people, the following certainly deserve individual recognition.

Dr. C. M. Sliepcevich, George Lynn Cross Research Professor of Engineering, for his support and interest.

Dr. J. R. Welker, Associate Director of the Flame Dynamics Laboratory, for his innumerable ideas and great assistance in all facets of this research.

Dr. T. J. Love, Jr., Dr. F. M. Townsend, and Dr. C. E. Locke for their service on my dissertation committee.

Mr. K. Z. Iqbal for his assistance with the experimental data.

Ms. Bobbie Everidge for her excellent work in preparing this manuscript.

I would like to express appreciation to the Northern Forest Fire Laboratory of the National Forest Service for their financial support.

Finally, I would like to acknowledge my wife, Marcia, and son, Gregory, for their sacrifices and support during this project.

Sam P. Muhlenkamp

## TABLE OF CONTENTS

	Page
LIST OF TABLES . . . . .	vii
LIST OF ILLUSTRATIONS . . . . .	viii
Chapter	
I. INTRODUCTION . . . . .	1
II. REVIEW OF PREVIOUS WORK . . . . .	4
Studies Using Non-Commercial Equipment . . . . .	4
Thermal Analysis Using Commercial Instruments . . . . .	13
Thermal Properties of Wood and Plant Samples . . . . .	44
III. EXPERIMENTAL PROCEDURE . . . . .	48
Preparation of Living Plant Samples . . . . .	48
Thermogravimetric Balance . . . . .	53
Differential Scanning Calorimeter . . . . .	61
IV. RESULTS AND DISCUSSION . . . . .	71
The Heating Rate Dependency of Cellulose and Punky Wood Kinetics . . . . .	71
Analysis of Living Plant Samples . . . . .	78
V. CONCLUSIONS AND SUGGESTIONS FOR FURTHER WORK . . . . .	90
BIBLIOGRAPHY . . . . .	92
APPENDICES . . . . .	96
A: WEIGHT LOSS AND RATE OF WEIGHT LOSS CURVES . . . . .	97
B: DATA ON FREEZE-DRIED SAMPLE COLLECTION . . . . .	102

TABLE OF CONTENTS--Continued

Appendix	Page
C: DATA FROM WEIGHT LOSS MEASUREMENTS . . . . .	104
D: DATA OF ENERGY MEASUREMENTS . . . . .	107
E: WEIGHT LOSS CURVES FOR FREEZE-DRIED ASPEN LEAVES, DOUGLAS FIR NEEDLES, LODGEPOLE PINE NEEDLES, CHAMISE FOLIAGE, AND MANZANITA LEAVES . . . . .	109
F: RATE OF WEIGHT LOSS CURVES FOR FREEZE-DRIED ASPEN LEAVES, DOUGLAS FIR NEEDLES, LODGEPOLE PINE NEEDLES, CHAMISE FOLIAGE, AND MANZANITA LEAVES . . . . .	115
G: DIFFERENTIAL ENERGY CURVES OF FREEZE-DRIED ASPEN LEAVES, DOUGLAS FIR NEEDLES, LODGEPOLE PINE NEEDLES, CHAMISE FOLIAGE, AND MANZANITA LEAVES . . . . .	121
H: TOTAL ENERGY CURVES OF FREEZE-DRIED ASPEN LEAVES, DOUGLAS FIR NEEDLES, LODGEPOLE PINE NEEDLES, CHAMISE FOLIAGE, AND MANZANITA LEAVES . . . . .	132

LIST OF TABLES

Table	Page
II- 1. Data of Stamm (37) . . . . .	9
II- 2. Kinetic Parameters of Pyrolysis from Dynamic Thermogravimetry . . . . .	28
II- 3. Heat of Pyrolysis . . . . .	29
II- 4. Average Activation Energy . . . . .	31
II- 5. Frequency Factor and Order of Reaction . .	31
II- 6. Kinetic Parameters for Cellulose and Punky Wood (7) . . . . .	35
II- 7. Specific Heat and Energy of Pyrolysis of Cellulose and Punky Wood . . . . .	38
II- 8. Effect of Thermal Properties on Rate of Pyrolysis (17) . . . . .	45
II- 9. Specific Heat Measurements of Wood and Plant Samples . . . . .	47
III- 1. Calibration Standards for TGS-1 Furnace .	58
III- 2. Settings for TGS-1 Furnace Calibration . .	59
III- 3. Transition Temperatures and Energies of DSC Calibration Standards . . . . .	65
III- 4. Calibration of DSC Heat of Transition . .	66
IV- 1. Kinetic Parameters for Cellulose . . . . .	75
IV- 2. Kinetic Parameters for Punky Wood . . . . .	75
IV- 3. Parameters for Equation IV-10 . . . . .	75

## LIST OF ILLUSTRATIONS

Figure	Page
II- 1. Computer and Measured Central Temperature-Time Curves (1) . . . . .	5
II- 2. Temperature Profiles of Murty and Blackshear (24) . . . . .	11
II- 3. Schematic Representation of DTA and DSC and of DSC Sample Holders, Sensors, and Heaters . . . . .	15
II- 4. Differential Thermal Analysis of Alpha-Cellulose by Tang and Neill (40) . . . . .	20
II- 5. DTA Results of Broido (3) for Cellulose in Nitrogen and Air . . . . .	21
II- 6. DTA (Solid Lines) and TGS (Broken Lines) Results of Browne and Tang (6) . . . . .	23
II- 7. Differential Thermal Analysis Curve of Beall (2) . . . . .	25
II- 8. Kinetics of Weight Loss Plots for Wood, Alpha-Cellulose and Lignin (38) . . . . .	27
II- 9. Energy Capacity of Oak Wood as a Function of Temperature in Nitrogen Atmosphere . . . . .	33
II-10. Energy Capacity of Pine Wood as a Function of Temperature in Nitrogen Atmosphere . . . . .	34
II-11. Weight Loss and Rate of Weight Loss for Cellulose. Heating Rate, 40°C/min . . . . .	36
II-12. Weight Loss and Rate of Weight Loss for Punky Wood from Douglas Fir Snags. Heating Rate, 40°C/min . . . . .	37

LIST OF ILLUSTRATIONS--Continued

Figure		Page
II-13.	Weight Loss and Rate of Weight Loss for Excelsior. Heating Rate, 40°C/min . . .	39
II-14.	Differential Energy of Cellulose (40°C/min) . . . . .	40
II-15.	Differential Energy of Lignin (40°C/min) .	41
II-16.	Calculated and Experimental Total Energy for Dry Excelsior (40°C/min) . . . . .	43
III- 1.	Weight Loss and Rate of Weight Loss for Fresh Pine Needles. Heating Rate, 10°C/min . . . . .	51
III- 2.	Weight Loss and Rate of Weight Loss for Freeze-Dried Pine Needles. Heating Rate, 10°C/min . . . . .	52
III- 3.	Perkin-Elmer TGS-1 Thermobalance and UU-1 Temperature Controller . . . . .	54
III- 4.	Schematic of Perkin-Elmer TGS-1 Furnace and Weigh Assembly . . . . .	55
III- 5.	Schematic of TGS-1 Temperature Calibra- tion System . . . . .	57
III- 6.	Calibration Curve for TGS-1 Furnace . . .	60
III- 7.	Perkin-Elmer Differential Scanning Calorimeter DSC-2 . . . . .	62
III- 8.	DSC-2 Sample Holder Assembly . . . . .	64
III- 9.	Specific Heat Curve for Sapphire (12) . .	69
IV- 1.	Effect of Heating Rate on Kinetic Param- eters for Cellulose . . . . .	76
IV- 2.	Effect of Heating Rate on Kinetic Parameters of Punky Wood . . . . .	77
IV- 3.	Weight Loss of Freeze-Dried Ponderosa Pine Needles . . . . .	79
IV- 4.	Rate of Weight Loss of Freeze-Dried Ponderosa Pine Needles . . . . .	80

LIST OF ILLUSTRATIONS--Continued

Figure	Page
IV- 5. Weight Loss and Rate of Weight Loss for Cellulose and Holocellulose. Heating Rate, 40°C/min . . . . .	82
IV- 6. Differential Energy of Freeze-Dried Ponderosa Pine Needles. Heating Rate, 40°C/min . . . . .	83
IV- 7. Differential Energy of Freeze-Dried Ponderosa Pine Needles. Heating Rate, 160°C/min . . . . .	84
IV- 8. Differential Energy of Living Ponderosa Pine Needle Extractive. Heating Rate, 160°C/min . . . . .	86
IV- 9. Total Energy of Freeze-Dried Ponderosa Pine Needles. Heating Rate, 40°C/min . . . . .	88
IV-10. Total Energy of Freeze-Dried Ponderosa Pine Needles. Heating Rate, 160°C/min . . . . .	89
A- 1. Weight Loss and Rate of Weight Loss for Fresh Holly Leaves. Heating Rate, 10°C/min . . . . .	98
A- 2. Weight Loss and Rate of Weight Loss for Freeze-Dried Holly Leaves. Heating Rate, 10°C/min . . . . .	99
A- 3. Weight Loss and Rate of Weight Loss for Fresh Spruce Needles. Heating Rate, 10°C/min . . . . .	100
A- 4. Weight Loss and Rate of Weight Loss for Freeze-Dried Spruce Needles. Heating Rate, 10°C/min . . . . .	101
E- 1. Weight Loss of Freeze-Dried Aspen Leaves . . . . .	110
E- 2. Weight Loss of Freeze-Dried Douglas Fir Needles . . . . .	111
E- 3. Weight Loss of Freeze-Dried Lodgepole Pine Needles . . . . .	112
E- 4. Weight Loss of Freeze-Dried Chamise Foliage . . . . .	113

LIST OF ILLUSTRATIONS--Continued

Figure	Page
E- 5. Weight Loss of Freeze-Dried Manzanita Leaves . . . . .	114
F- 1. Rate of Weight Loss of Freeze-Dried Aspen Leaves . . . . .	116
F- 2. Rate of Weight Loss of Freeze-Dried Douglas Fir Needles . . . . .	117
F- 3. Rate of Weight Loss of Freeze-Dried Lodgepole Pine Needles . . . . .	118
F- 4. Rate of Weight Loss of Freeze-Dried Chamise Foliage . . . . .	119
F- 5. Rate of Weight Loss of Freeze-Dried Manzanita Leaves . . . . .	120
G- 1. Differential Energy of Freeze-Dried Aspen Leaves. Heating Rate, 40°C/min . . . .	122
G- 2. Differential Energy of Freeze-Dried Aspen Leaves. Heating Rate, 160°C/min . . . .	123
G- 3. Differential Energy of Freeze-Dried Douglas Fir Needles. Heating Rate, 40°C/min . . . . .	124
G- 4. Differential Energy of Freeze-Dried Douglas Fir Needles. Heating Rate, 160°C/min . . . . .	125
G- 5. Differential Energy of Freeze-Dried Lodgepole Pine Needles. Heating Rate, 40°C/min . . . . .	126
G- 6. Differential Energy of Freeze-Dried Lodgepole Pine Needles. Heating Rate, 160°C/min . . . . .	127
G- 7. Differential Energy of Freeze-Dried Chamise Foliage. Heating Rate, 40°C/min	128
G- 8. Differential Energy of Freeze-Dried Chamise Foliage. Heating Rate, 160°C/min . . . . .	129

LIST OF ILLUSTRATIONS--Continued

Figure		Page
G- 9.	Differential Energy of Freeze-Dried Manzanita Leaves. Heating Rate, 40°C/min . . . . .	130
G-10.	Differential Energy of Freeze-Dried Manzanita Leaves. Heating Rate, 160°C/min . . . . .	131
H- 1.	Total Energy of Freeze-Dried Aspen Leaves. Heating Rate, 40°C/min . . . . .	133
H- 2.	Total Energy of Freeze-Dried Aspen Leaves. Heating Rate, 160°C/min . . . . .	134
H- 3.	Total Energy of Freeze-Dried Douglas Fir Needles. Heating Rate, 40°C/min . . . .	135
H- 4.	Total Energy of Freeze-Dried Douglas Fir Needles. Heating Rate, 160°C/min . . .	136
H- 5.	Total Energy of Freeze-Dried Lodgepole Pine Needles. Heating Rate, 40°C/min .	137
H- 6.	Total Energy of Freeze-Dried Lodgepole Pine Needles. Heating Rate, 160°C/min .	138
H- 7.	Total Energy of Freeze-Dried Chamise Foliage. Heating Rate, 40°C/min . . . .	139
H- 8.	Total Energy of Freeze-Dried Chamise Foliage. Heating Rate, 160°C/min . . .	140
H- 9.	Total Energy of Freeze-Dried Manzanita Leaves. Heating Rate, 40°C/min . . . .	141
H-10.	Total Energy of Freeze-Dried Manzanita Leaves. Heating Rate, 160°C/min . . . .	142

## CHAPTER I

### INTRODUCTION

Generations of nature's work can be destroyed by a forest fire which leaves behind a wasteland of charred debris. The loss of the wood as a natural resource is only one of the many considerations involved in a forest fire; others are disruption and loss of animal life, expense of fighting the fire, and loss of recreational areas. The containment and control of forest fires and other fires of natural fuels are complicated by the changing ambient conditions and large areas involved in the fires.

Better techniques for predicting the rate of fire spread are not only needed for control of accidental wildland fires but also for the deliberate initiation of prescribed fires in forest management.

To answer this need, a mathematical model for the spread of fires was developed by Rothermel (35) based on earlier work by Frandsen (8). Rothermel's model is

$$R = \frac{(I_p)_o (1 + \phi_w + \phi_s)}{\rho_b \epsilon Q_{ig}} \quad (I-1)$$

where  $P$  = rate of spread (ft/min)  
 $(I_p)_0$  = propagating flux (no wind) (Btu/ft<sup>2</sup>-min)  
 $\phi_w$  = increase in propagating flux due to wind  
 $\phi_s$  = increase in propagating flux due to slope  
 $\rho_b$  = bulk density (lbm/ft<sup>3</sup>)  
 $\epsilon$  = effective heating number  
 $Q_{ig}$  = heat of preignition (Btu/lbm)

Here  $Q_{ig}$  includes the total sensible and transitional heat needed to cause ignition. After considerable experimental work, the parameters in Equation I-1 could be accurately specified with the exception of  $Q_{ig}$ . This value was predicted by

$$Q_{ig} = 250 + 1116 M_f \quad (\text{Btu/lbm}) \quad (\text{I-2})$$

where  $M_f$  = fuel moisture (lbm of water / lbm of dry wood). Equation I-2 assumes that pyrolysis occurs at 320°C and the boiling temperature of water is 100°C. While the amount of water is of primary importance, Rothermel (35) recognizes that the composition and heating rate of the fuel are important parameters in the evaluation of the heat of preignition.

The Flame Dynamics Laboratory at the University of Oklahoma has undertaken much basic research to develop an accurate mathematical model to predict the heat of preignition of wildland fuels. The development of such a model is very complex owing to the large number of components of each plant and to the complexity of each component. Although the primary

application of the model concerns wildland fuels, the research, which is the basis of the model, is applicable to a wide range of wood products.

Upon heating wood, pyrolysis of natural polymers occurs forming volatile gases which can then ignite and burn if oxygen is available. This fundamental concept is the basis for many studies involving flammability. By pyrolyzing samples in an inert atmosphere, it is possible to study the process of pyrolysis apart from combustion.

The goals of this study are:

1. Devise a method of collecting living wildland fuel samples, which does not effect the samples' pyrolysis or composition. However, the method should be of such a nature that the samples do not change during storage.
2. Obtain and analyze pyrolysis data for living aspen leaves, chamise foliage, manzanita leaves, Douglas fir needles, Ponderosa pine needles, and lodgepole pine needles. This pyrolysis data includes weight loss and energy effects upon heating.
3. Investigate pyrolysis effects of extractives of living and dead wildland fuel samples.
4. Improve, if possible, the model of Duvvuri (7).

## CHAPTER II

### REVIEW OF PREVIOUS WORK

Many investigators have studied the pyrolysis and combustion of wood and its components by using either commercial instruments for thermal analysis, such as the thermogravimetric balance (TGS), the differential scanning calorimeter (DSC), and the differential thermal analyzer (DTA), or special equipment designed for a particular purpose.

#### Studies Using Non-Commercial Equipment

In these studies various geometries of samples are used. For example, Bamford, Crank, and Malan (1) used sheets of wood 23 cm square. Each side of the sample was heated by direct contact with flames, and the temperature at the center of the sheet was monitored with a thermocouple. Typical results for the variation of temperature with time for a sheet, 2 cm thick, are shown in Figure II-1. The sudden temperature rise from 600°K to 700°K was assumed to represent the heat of decomposition, which can be calculated from

$$c \rho \Delta T = q w_0 \quad (\text{II-1})$$

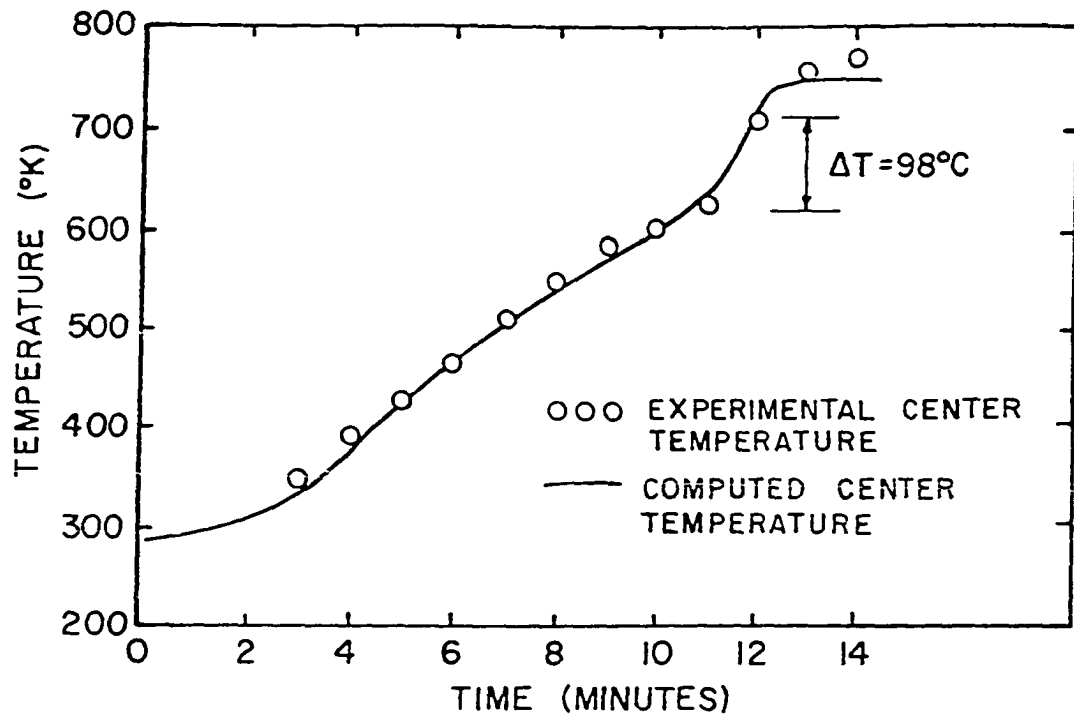


Figure II-1. Computed and Measured Central Temperature-Time Curves (1).

where  $c$  = specific heat (cal/gm-°C)  
 $\rho$  = density (gm/cm<sup>3</sup>)  
 $\Delta T$  = sudden temperature rise (°K)  
 $w_0$  = initial weight of volatile products per cc of  
 wood (gm)  
 $q$  = heat of decomposition (cal/gm)

Using literature values for  $c$  and  $\rho$  and measured values for  $w_0$  (the difference in weight per cc between the original and charred sample) and for  $\Delta T$ ,  $q$  was calculated to be 86 cal/gm exothermic.

The mathematical model was derived by superposition of the heat conduction equation and a production term.

$$K \frac{\partial^2 T}{\partial x^2} = c \rho \frac{\partial T}{\partial t} + q \frac{\partial w}{\partial t} \quad (\text{II-2})$$

where  $K$  = thermal conductivity (cal/cm<sup>2</sup>-sec-(°C/cm))  
 $T$  = temperature (°C)  
 $x$  = distance (cm)  
 $c$  = specific heat (cal/gm-°C)  
 $\rho$  = density (gm/cm<sup>3</sup>)  
 $t$  = time (sec)  
 $q$  = heat of decomposition (cal/gm)  
 $w$  = weight at time  $t$  (gm)

The rate of decomposition was assumed to be first order and given by

$$-\frac{dw}{dt} = A w e^{-E/RT} \quad (\text{II-3})$$

where  $A =$  pre-exponential factor ( $\text{sec}^{-1}$ )

$E =$  activation energy (cal/gm)

Considering only one-half the thickness of the sheet, Equations II-2 and II-3 are subject to the boundary conditions

$$T(x,0) = \text{constant} \quad (\text{II-4})$$

$$w(x,0) = \text{constant} \quad (\text{II-5})$$

$$-K \frac{\partial T}{\partial x} = H(T_0) \text{ for } x = 0, t > 0 \quad (\text{II-6})$$

$$\frac{\partial T}{\partial x} = 0 \text{ for } x = l, t > 0 \quad (\text{II-7})$$

where  $H(T_0)$  is an empirical function of the surface temperature,  $T_0$ , and  $l$  is one-half the thickness of the sheet.

The empirical function of  $H(T_0)$  is assumed to consist of a convection term and a radiation term to and from the sample. The wood is assumed to radiate as a black body. Then

$$H(T_0) = \alpha(T_f - T_0) + \sigma(\epsilon T_f^4 - T_0^4) \quad (\text{II-8})$$

where  $\alpha =$  constant ( $\text{cal/cm}^2\text{-sec-}^\circ\text{C}$ )

$\sigma =$  Stefan-Boltzman constant ( $\text{cal/cm}^2\text{-sec-}^\circ\text{K}^4$ )

$T_f =$  flame temperature ( $^\circ\text{K}$ )

$\epsilon =$  emissivity of the flame (unitless)

$H(300^\circ\text{K})$  was then measured by substituting water in a tin container for the sample and measuring the temperature rise of the water.  $H(800^\circ\text{K})$  was taken as zero since the wood sample would not heat to any higher temperature than  $800^\circ\text{K}$ . With these two values  $\alpha$  and  $\epsilon$  were determined, and  $H(T_0)$

became a known function of surface temperature. E and A were then chosen by a trial and error method. That is, given values for E and A, Equations II-2 and II-3 were solved by a finite-difference scheme. If the calculated values of T did not fit the experimental data, new values of E and A were chosen. The finite difference scheme was solved without the aid of a computer. The final values for E and A were 33,160 cal/gm and  $5.3 \times 10^8 \text{ sec}^{-1}$ , respectively.

Stamm (37) analyzed the data of some previous studies of wood and wood component degradation from the standpoint of reaction kinetics. The data were from isothermal studies ranging in time from 1 min to 2.4 years. The logarithm of the residual weight of each isothermal study was plotted against the heating time resulting in straight lines except at low heating times. This exception was said to be due to loss of absorbed water. The slope of the lines corresponds to the pre-exponential factor, A. The logarithm of A was then plotted versus  $1/T$  for each study, the resulting straight lines having a slope of  $-E/2.3R$ . However, instead of calculating a pre-exponential for an Arrhenius-type rate constant, Stamm (37) merely located  $\log A$  at  $150^\circ\text{C}$ . Some of Stamm's (37) results are listed in Table II-1. Of particular interest is the small range of activation energy values for the various woods and wood components.

Roberts and Clough (33) studied the pyrolysis of beech wood cylinders 2 cm in diameter and 15 cm in length. These

TABLE II-1  
DATA OF STAMM (37)

Material	Time Range	Temp Range (°C)	E ( $\frac{\text{cal}}{\text{mole}}$ )	Log A at 150°C (hours) <sup>-1</sup>
Southern and white pine	1 hr - 2.4 yr	93.5-250	29,500	-3.9
Douglas fir sawdust	16 hr - 64 days	110-220	25,000	-4.0
$\alpha$ -Cellulose from Douglas fir	16 hr - 64 days	110-220	26,000	-4.1
Hemicellulose from Douglas fir	2 hr - 64 days	110-220	26,700	-3.4
Lignin from Douglas fir	16 hr - 64 days	110-220	23,000	-4.3

samples were tested in an apparatus corresponding to a thermo-balance. Five thermocouples were located at various radii of the cylinders. The weight loss equation was assumed to be first-order and of the form

$$-\frac{dw}{dt} = (w - w') A \exp(-E/RT) \quad (\text{II-9})$$

where  $w$  = weight of sample at time  $t$  (gm)

$w'$  = final weight of sample (gm)

$A$  = pre-exponential factor ( $\text{min}^{-1}$ )

$E$  = activation energy (cal/gm)

$R$  = gas constant (cal/gm-°K)

$T$  = absolute temperature (°K)

Equation II-9 is then integrated and applied separately to five different annular sections corresponding to the five different depths of the thermocouples. The values of the kinetic parameters,  $E$  and  $A$ , were then chosen by a trial and error method. First, the value of  $E$  was chosen. Having done that, a value of  $A$  was chosen so that the total calculated weight loss matched the experimental total weight loss. If Equation II-9 did not predict the intermediate weight losses of each experiment, different values of  $E$  and  $A$  were chosen. The values of  $E = 15,000$  cal/mole and  $A = 9.1 \times 10^4$  min<sup>-1</sup> fit 4 out of 5 experiments fairly well.

Murty and Blackshear (24) performed an experiment similar to that of Roberts and Clough (33) by pyrolyzing a cylindrical sample of alpha-cellulose monitored by thermocouples at seven different radii. During heating, the samples were weighed as well as X-rayed to determine density changes. A time-temperature history is given in Figure II-2. Plateaus occur at 125°C and 375°C at the inner radii. Beyond 400°C, the temperature rise is faster. Murty and Blackshear (24) speculate that the plateaus are caused by migrating pyrolysis vapors. These vapors migrate to the cooler interior of the cylinder by diffusion. When cooled enough, the vapors condense. Then as the interior gets hotter, the condensates vaporize causing heat sinks at 125°C and 375°C.

As pyrolysis took place, the X-ray photographs showed a distinct advancing char layer. However, the density

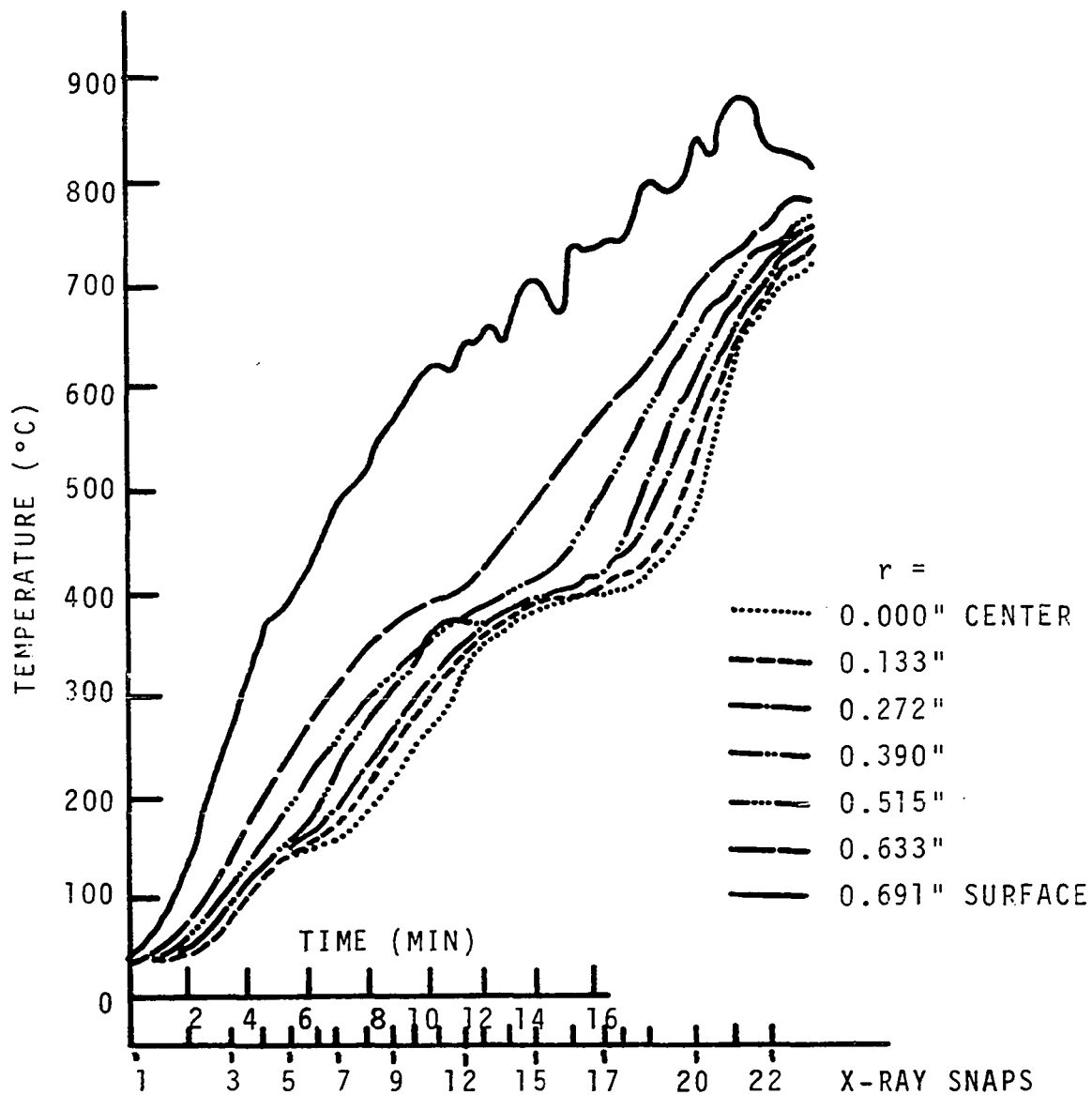


Figure II-2. Temperature Profiles of Murty and Blackshear (24).

measurements showed a density variation in front of the char layer. Murty and Blackshear (24) theorize that the density variation is due to loss of moisture bonded to the alpha-cellulose since the samples were thoroughly dried at 105°C before pyrolysis. The data were graphically fitted to the following equation.

$$\frac{\partial \rho}{\partial t} = -A (\rho - \rho_{\text{char}}) e^{-E/RT} \quad (\text{II-10})$$

where  $\rho$  = density (gm/cm<sup>3</sup>)  
 $t$  = time (sec)  
 $A$  = pre-exponential (sec<sup>-1</sup>)  
 $\rho_{\text{char}}$  = density of char (gm/cm<sup>3</sup>)  
 $E$  = activation energy (cal/mole)  
 $T$  = temperature (°K)

The logarithm of  $[(\partial \rho / \partial t) / (\rho - \rho_{\text{char}})]$  versus  $1/T$  was graphed for the various thermocouple locations resulting in values for  $E$  and  $A$ . The values of  $E$  varied with radius from 13 kcal/mole at the center of the sample to 22 kcal/mole at the surface. The values of  $A$  varied irregularly from  $10^4$  sec<sup>-1</sup> to  $10^7$  sec<sup>-1</sup>. Murty and Blackshear (24) attribute the variation of  $E$  with radius to the fact that "the interior layers are soaked by the migrating condensates and incubated at elevated temperatures for longer times than the outer layers." After plotting  $E$  as a function of temperature, the graph yields

$$E \text{ (kcal/mole)} = 5.08 + 0.0214 T \text{ (°K)} \quad (\text{II-11})$$

Equation II-11 implies that either the structure of the alpha-cellulose was changed by the "migrating condensates" or at higher temperatures different reactions take place. Underlying the entire theory of "migrating condensates" is the possibility that the plateau at 125°C in Figure II-2 is merely the result of the heat of vaporization of any residual water in the sample. Furthermore, since many investigators (2, 4, 7, 14, 19, 39, 40) have measured endothermic heats of pyrolysis for wood samples, the plateau at 375°C could be due to pyrolysis.

#### Thermal Analysis Using Commercial Instruments

In more recent years, many investigators have turned to the commercially available thermogravimetric balance (TGS), differential thermal analyzer (DTA), and differential scanning calorimeter (DSC) to study the reaction kinetics and heat effects of wood pyrolysis. An explanation of the basic principles of these instruments will facilitate the understanding of the studies for which they were used.

#### Basic Principles of Commercial Instruments

The thermogravimetric balance (TGS), as the name implies, measures weight loss as a function of temperature. Since the TGS is operated with a temperature programmer, dynamic temperature studies are usually made at constant heating rates. The TGS also has the ability to measure rate of weight loss. All weighings are made automatically and continuously.

The DSC and the DTA have many similarities in that both instruments have reference cells and a programmed temperature rise. To avoid confusing these two instruments, the basic differences will be explained. Both instruments are used to measure thermal effects of the samples; however, the outputs are different. As shown in Figure II-3a, the DTA has a single heating source for the sample and the reference holder; the temperature difference between the sample and reference holders is recorded during a temperature rise. However, the DSC, Figure II-3b, has individual heaters for both the sample and the reference holders, and the difference in the rate of energy input to each holder is recorded during a temperature rise. The continuous adjustment of electrical power to the sample holder heater to keep the sample holder at the programmed temperature is equivalent to the thermal behavior of the sample. This adjustment is accomplished through the use of a negative feedback signal to the temperature programmer.

Without a feedback signal, the temperature difference between the sample and reference pans is given by

$$\Delta T = Q_s R \quad (\text{II-12})$$

where  $\Delta T$  = temperature difference between pans (without feedback)

$Q_s$  = thermal effect of sample

$R$  = thermal resistance between sample and surroundings

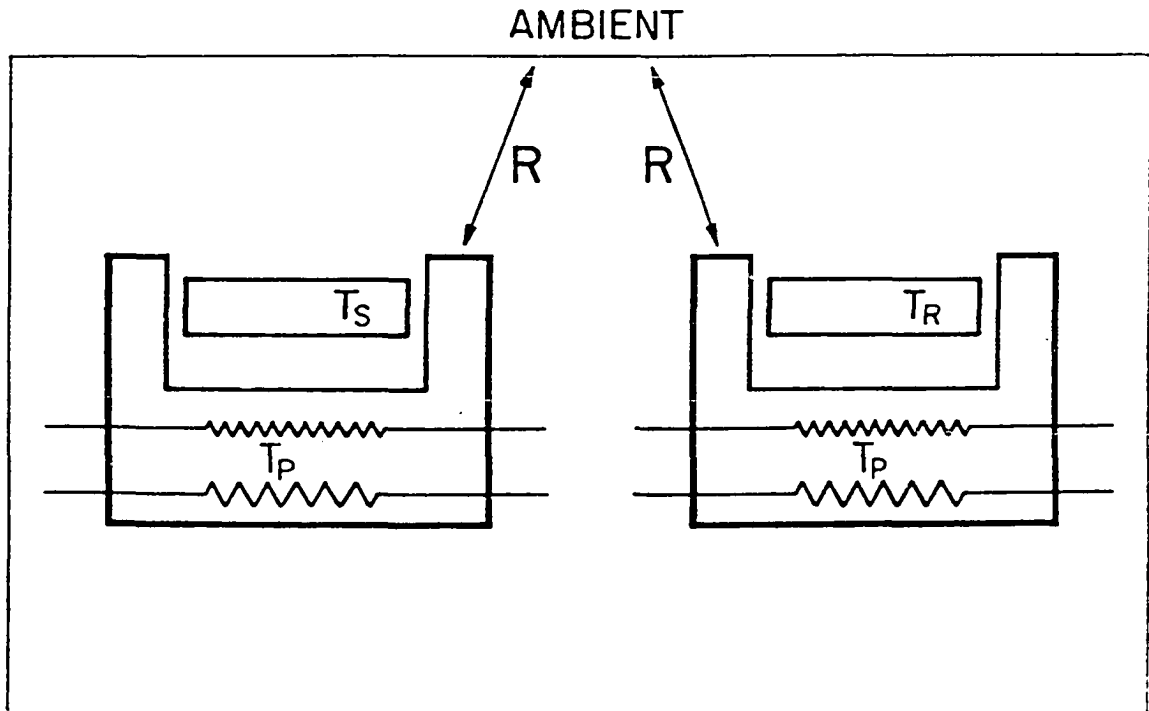
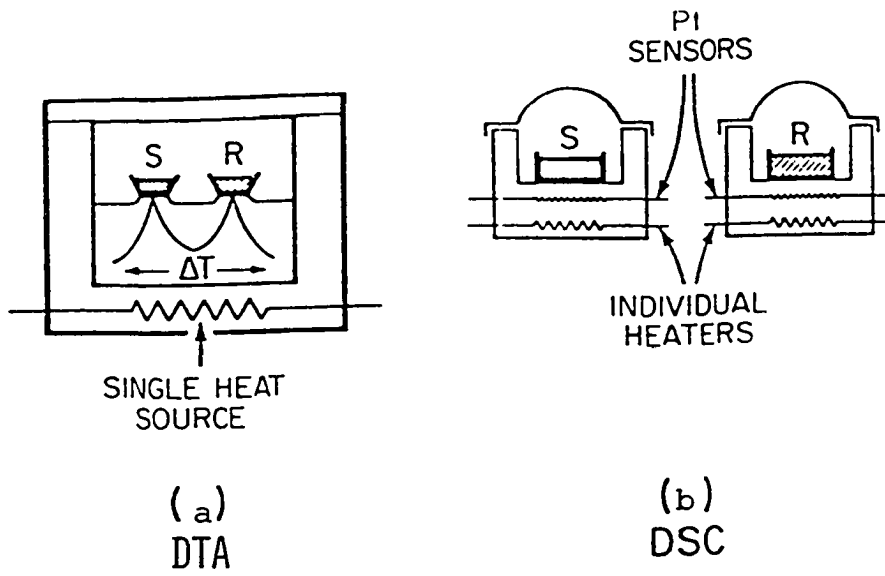


Figure II-3. Schematic Representation of DTA and DSC and of DSC Sample Holders, Sensors, and Heaters.

With feedback control, the instantaneous amount of energy to the sample pan is governed by

$$Q = -G \Delta T' \quad (\text{II-13})$$

where  $Q$  = energy from temperature programmer

$G$  = amplifier gain

$\Delta T'$  = temperature difference between sample and reference holders with feedback

Since the temperature difference with feedback is determined by the net heat flow rate, the equivalent to Equation II-12 for the closed-loop system is

$$\Delta T' = (Q_s + Q) R \quad (\text{II-14})$$

Combining with Equation II-13,

$$-\frac{Q}{G} = (Q_s + Q) R \quad (\text{II-15})$$

Solving for  $Q$

$$Q = -Q_s \left( \frac{1}{1 + (1/GR)} \right) \quad (\text{II-16})$$

Now as  $G \rightarrow \infty$ ,  $Q \rightarrow -Q_s$ ; that is, as the amplifier gain gets very large, the power from the heater is essentially equal to and opposite to the heat effect of the sample. The large value of  $R$ , the thermal resistance between the sample holders and the surroundings, also has an advantageous effect on  $Q$ .

Substituting  $Q$  from Equation II-16 into Equation II-14, we obtain

$$\Delta T' = \frac{Q_s}{G} \left( \frac{1}{1 + \frac{1}{GR}} \right) \quad (\text{II-17})$$

Now as  $G \rightarrow \infty$ ,  $\Delta T' \rightarrow 0$ .

In actual practice, the heater power,  $Q$ , is split between the sample and reference holder. For example, when the sample absorbs energy from the holder at a rate  $\Delta Q_s$ ,  $\Delta Q/2$  additional power is added to the sample holder and  $\Delta Q/2$  less power to the reference holder. The rate at which energy is supplied to the sample holder is recorded.

The DTA records specific heat changes, thermal transitions, and mass changes as temperature differences between the sample holder and reference holder. If more than one change or transition occurs in a sample run, the results are reduced to strictly qualitative analysis. Since the thermal properties of most materials vary with temperature, most DTA studies of transitions are suitable for qualitative analysis only. Furthermore, in the case of pyrolysis specific heat and mass changes of the sample can both occur during the transition.

#### Pyrolysis Studies Using Differential Thermal Analysis

Many investigators use thermogravimetric analysis (TGA) with differential thermal analysis (DTA) in their studies. This enables them to obtain weight loss and energy data on the samples. One such study is Tang and Neill's (40) study of the

effects of flame retardants on pyrolysis and combustion of alpha-cellulose. Based on their TGA results, the flame retardants cause decomposition to occur at a lower temperature and at a lower rate leaving a greater percentage of the sample as char. The TGA data were analyzed to extract kinetic parameters by the method of Freeman and Carroll (9) who derived the equation:

$$\frac{-E}{2.3R} \Delta(T^{-1}) = -n + \frac{\Delta \log (dw/dt)}{\Delta \log w_r} \quad (\text{II-18})$$

where  $E$  = activation energy (cal/mole)

$n$  = kinetic order (unitless)

$T$  = absolute temperature ( $^{\circ}\text{K}$ )

$R$  = gas constant (cal/gm- $^{\circ}\text{K}$ )

$w_r$  = weight remaining at time  $t$  (gm)

A plot of  $[\Delta \log (dw/dt)]/[\Delta \log w_r]$  versus  $[\Delta(T^{-1})]/[\Delta \log w_r]$  results in a linear plot having a slope of  $-E/2.3R$  and an intercept corresponding to  $n$ . This graphical method resulted in an activation energy for alpha-cellulose of 33.1 - 35.2 kcal/mole and a reaction order of 1. All samples were heated at  $3^{\circ}\text{C}/\text{min}$  in a partial vacuum of 0.3 mm Hg absolute.

Due to the method of sample preparation, the DTA results are of particular interest. The DTA experiments were run on a mixture of sample (8 percent) and inert material (92 percent). The weight of the sample mixture was 100 mg. Therefore, when pyrolysis occurred the change in mass was only

approximately 8 percent of the material in the sample holder, which allowed more accurate analysis of the thermograms. Since both the sample and reference cells in the DTA have the same energy source, large mass losses in the sample cell cause the remaining material to heat up faster than the reference material indicating a false exothermic heat of pyrolysis. All thermograms were obtained at 12°C/min in helium and in air. Figure II-4 shows the DTA results for alpha-cellulose. The heat of pyrolysis for alpha-cellulose was found to be  $88. \pm 3.6$  cal/gm endothermic, while the heat of combustion was  $3540 \pm 140$  cal/gm exothermic. The samples treated with flame retardants had lower heats of pyrolysis and similar values for heats of combustion. The DTA thermograms of all samples were similar in overall shape to those shown in Figure II-4.

With the same apparatus used by Tang and Neill, Broido (3) studied the effect of potassium bicarbonate on the pyrolysis of cellulose. Instead of mixing the sample with an inert material, Broido (3) tested a pure 5 gm sample of cellulose. Therefore, when pyrolysis occurred approximately 100 percent of the material in the sample holder was pyrolyzed. Figure II-5 shows Broido's (3) TGA and DTA results for cellulose in nitrogen and air. An endothermic reaction is shown up to about 320°C; beyond this point an exothermic reaction is indicated. These results are in conflict with those of Tang and Neill (40). Using a pure sample, instead of mixing

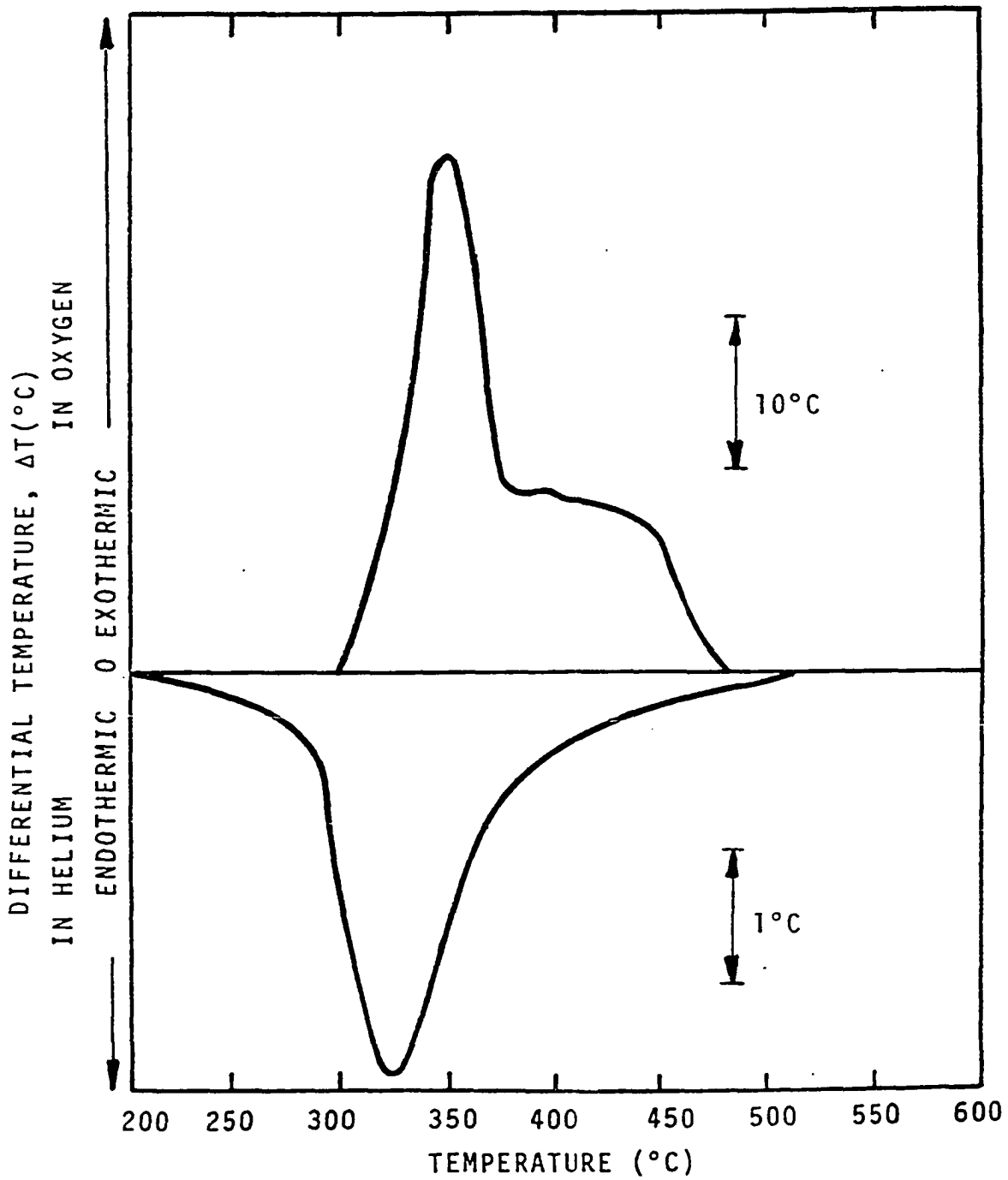


Figure II-4. Differential Thermal Analysis of  $\alpha$ -Cellulose by Tang and Neill (40).

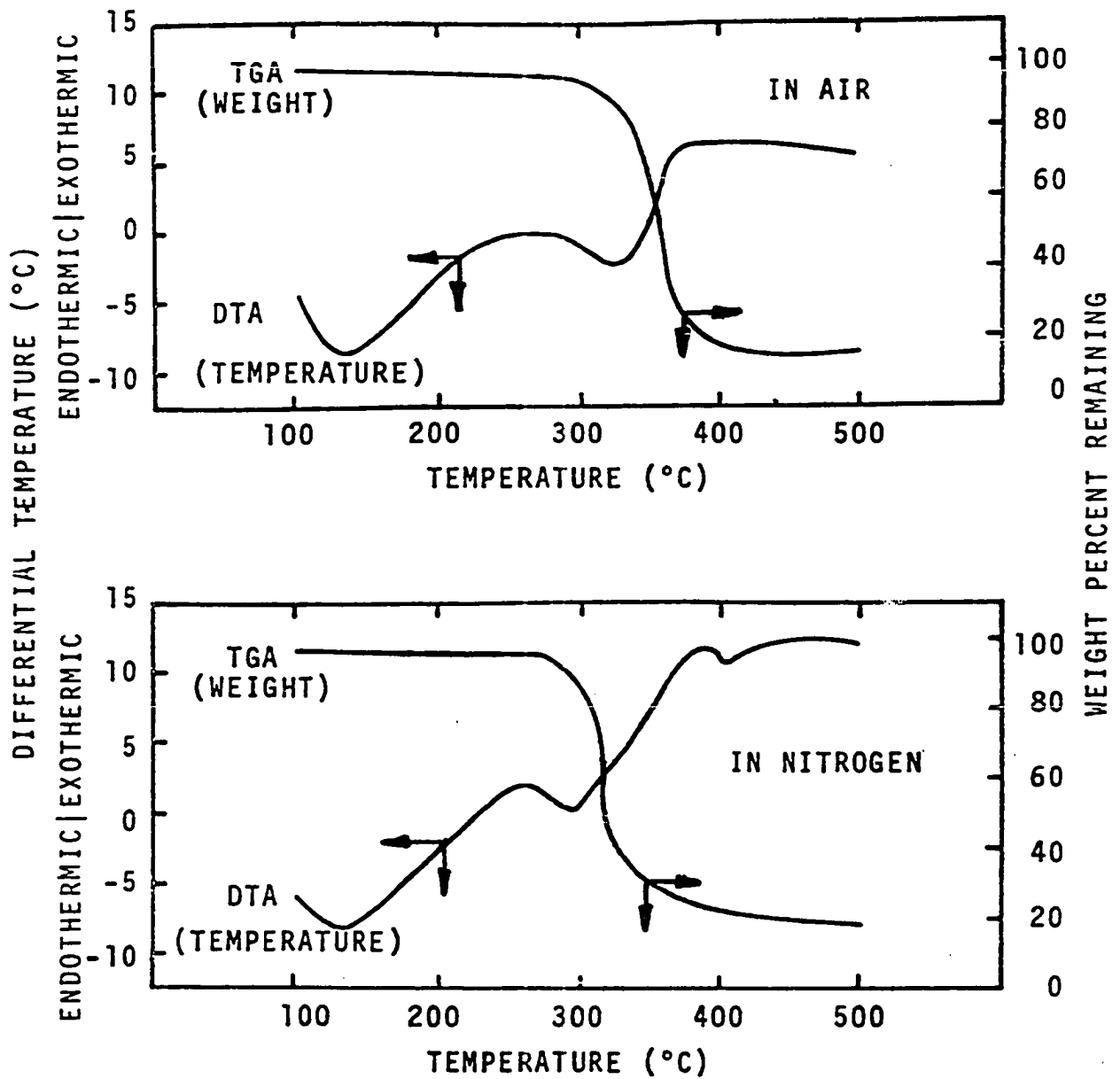


Figure II-5. DTA Results of Broido (3) for Cellulose in Nitrogen and Air.

the sample with an inert, may have caused an exothermic reaction to be falsely indicated as previously described; in reality, the exothermic indication is merely the result of a mass loss in the sample holder. The total heats of pyrolysis and combustion were not computed.

A study of the pyrolysis of wood and wood treated with inorganic salts was made by Browne and Tang (6). All experiments used 5 gm samples pyrolyzed in nitrogen at 12°C/min. Of primary interest are the TGS and DTA results on wood and its two major components, alpha-cellulose and lignin shown in Figure II-6. All the materials exhibit an endothermic peak at approximately 130°C which is associated with the loss of moisture; however, the expected weight loss due to water at 130°C is not shown. At the temperature of greatest weight loss, the wood and lignin exhibit an apparent exothermic pyrolysis. The alpha-cellulose exhibits a strong endotherm before lapsing into an apparently exothermic pyrolysis. As in the study of Broido (3), the apparent exotherms may be merely the result of the large mass loss in the sample holder. The mass loss causes the remaining material in the sample holder to be heated to a higher temperature for the same heat flux to the sample. An activation energy of 35.8 kcal/gm was found for the Ponderosa pine wood samples. Heats of pyrolysis were not calculated for the materials studied.

Beall's (2) study uses an instrument referred to as a differential calorimetric analyzer (DCA). This instrument is an improvement over the DTA since it controls the heat flux

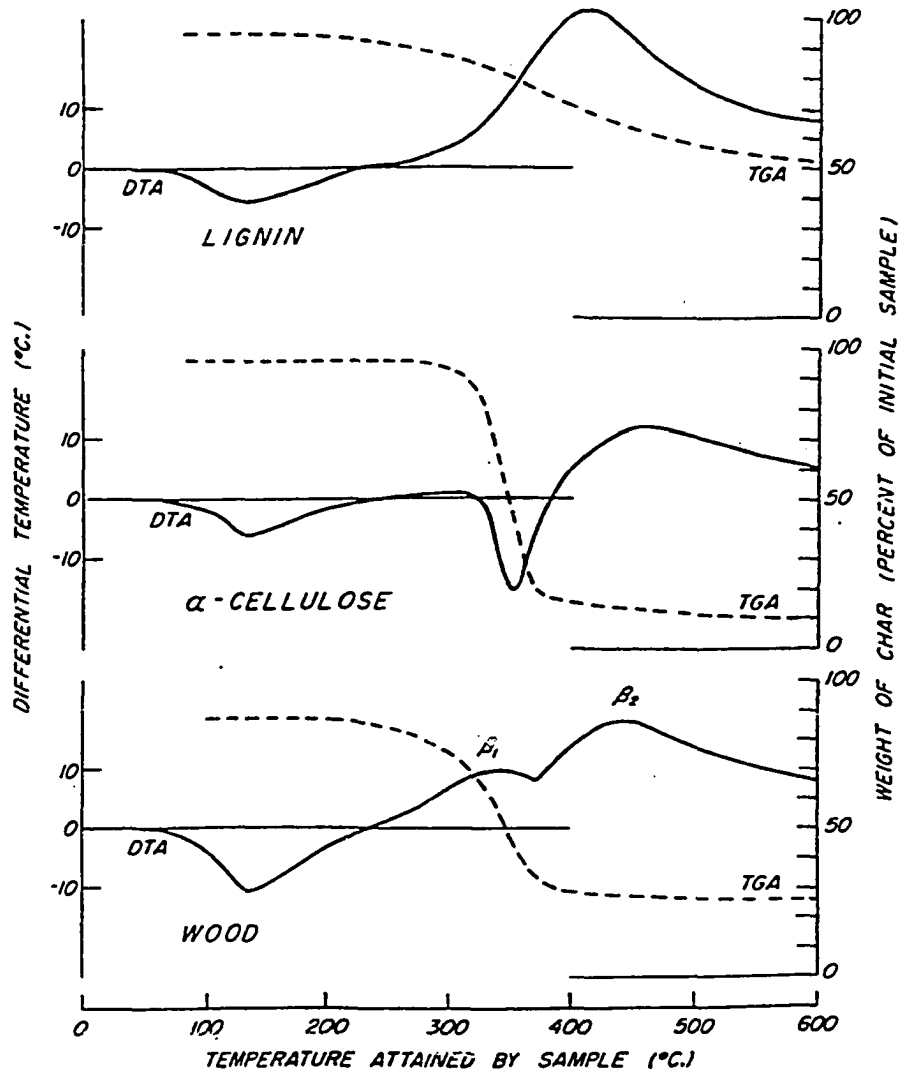


Figure II-6. DTA (Solid Lines) and TGS (Broken Lines) Results of Browne and Tang (6).

to the sample and reference holders better. A small sample of approximately 5 mg is used in the DCA to minimize any heat transfer problems. Beall (2) states that "any changes in sample mass, porosity, or thermal conductivity can cause either a baseline drift or an instability." Throughout the study great attention was paid to the problem of baseline stability in order to avoid erroneous results. Baseline drift is described as "one of the most troublesome effects of the equipment." The most difficult form of baseline drift was caused by changes in specific heat of the sample with temperature. The use of a reference material with similar characteristics was used to minimize the problem.

Figure II-7 shows Beall's (2) DCA results for cellulose. The calculation of the heat of pyrolysis involves the comparison of areas under the  $\Delta T$  versus temperature curve of a standard transition and that of the pyrolyzed sample. However, instead of actually measuring the area under the curve, the curve was photocopied, and the area was determined by cutting out the portion of the paper under the curve and then weighing the paper. By this method the heat of pyrolysis was found to be 55.0 cal/gm endothermic.

A study of the effects of inorganic salts on the pyrolysis of Ponderosa pine wood, alpha-cellulose, and lignin was made by Tang (38) and Tang and Eickner (39). The TGS data were analyzed by the difference method of Freeman and Carroll (9). The order of reaction was found to be pseudo first-order.

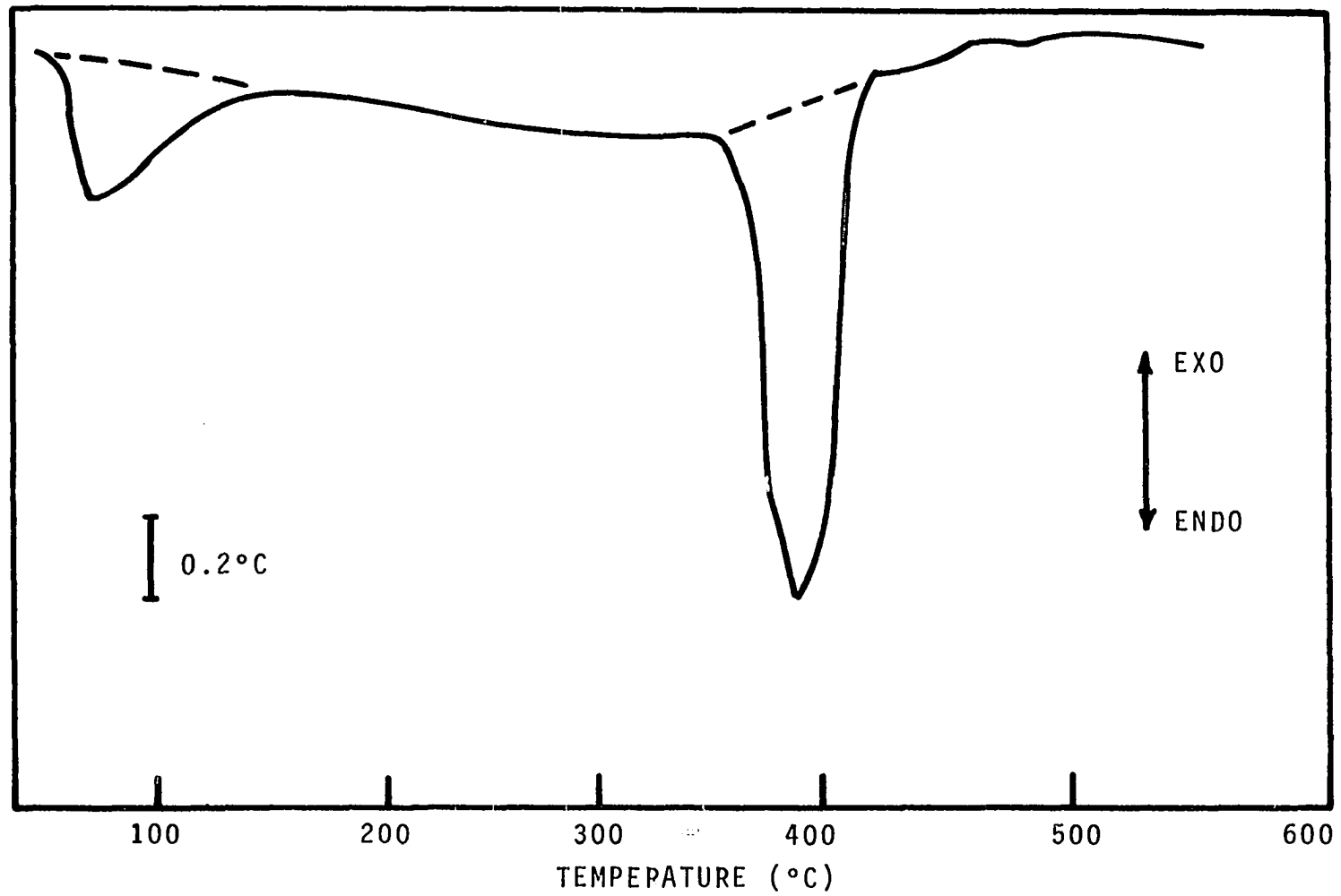


Figure II-7. Differential Thermal Analysis Curve of Beall (2).

Figure II-8 shows the plot of  $\log A$  versus  $1/T$  for alpha-cellulose, Ponderosa pine wood, and lignin. Table II-2 gives the kinetic parameters for results shown in Figure II-8. The TGS data were obtained on 100 mg samples at a heating rate of  $3^{\circ}\text{C}/\text{min}$  in a vacuum of 0.3 mm Hg.

The DTA portion of this study is similar to that of Tang and Neill (39) since 92 percent inerts were used in the sample holder. The wood and lignin samples had an endothermic and exothermic portion on the DTA curve, while the alpha-cellulose was entirely endothermic. Table II-3 gives the results of the heat of pyrolysis calculations.

Philpot (27, 28, 29, 30, 31) has conducted a number of studies on various types of wood using DTA and thermogravimetry. These studies included pyrolysis of cottonwood and the effect of mineral content on the pyrolysis of plant materials. In the latter investigation, samples of 21 different plants of varying mineral content were studied. While the results obtained were of a quantitative nature, little attempt was made to correlate them.

Thermogravimetric analysis was made on samples of filter paper by Sardesai (36) using the Friedman (10) method of analysis. The filter paper samples were pyrolyzed at 20, 40, 80, and  $160^{\circ}\text{C}/\text{min}$  in air and in nitrogen. Five grades of Whatman filter paper were analyzed.

The Friedman (10) method of analysis is based on an Arrhenius-type decomposition equation proposed by Goldfarb (13):

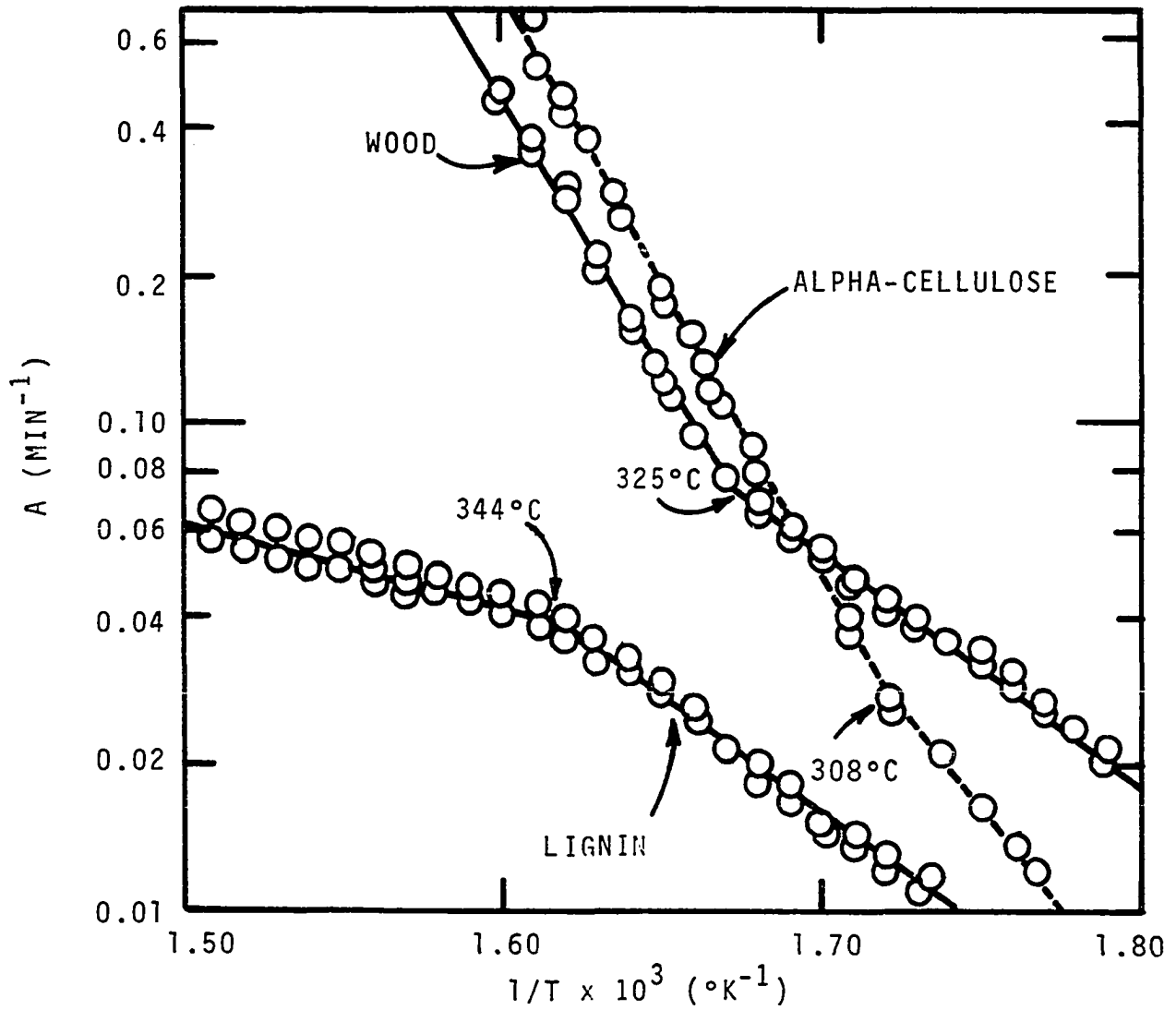


Figure II-8. Kinetics of Weight Loss Plots for Wood, Alpha-Cellulose, and Lignin (38).

TABLE II-2  
 KINETIC PARAMETERS OF PYROLYSIS FROM DYNAMIC THERMOGRAVIMETRY\*  
 [Tang (38)]

Material	First Stage			Second Stage		
	T (°C)	A <sub>1</sub> <sup>-1</sup> (min <sup>-1</sup> )	E <sub>1</sub> (kcal/gm-mole)	T (°C)	A <sub>2</sub> <sup>-1</sup> (min <sup>-1</sup> )	E <sub>2</sub> (kcal/gm-mole)
Pine wood	280-325	1.98 x 10 <sup>7</sup>	23	325-350	3.92 x 10 <sup>18</sup>	54
α-Cellulose	240-308	3.85 x 10 <sup>11</sup>	35	308-360	2.37 x 10 <sup>19</sup>	54
Lignin	280-344	9.86 x 10 <sup>5</sup>	21	344-435	5.6 x 10 <sup>10</sup>	9

\*For 100 mg samples in vacuum (0.3 mm Hg absolute).

TABLE II-3

HEAT OF PYROLYSIS  
[Tang and Eickner (39)]

Material	Temperature Range (°C)	Heat of Pyrolysis (cal/gm)
Wood	200-390	77 (endo)
	390-500	31 (exo)
$\alpha$ -Cellulose	240-450	88 (endo)
Lignin	190-345	19 (endo)
	345-500	40 (exo)

$$-\frac{dW}{dt} = A e^{-E/RT} F(W) \quad (\text{II-19})$$

where  $W = (w - w_f)/(w_o - w_f)$  = weight fraction (dimensionless)

$t$  = time (sec)

$A$  = pre-exponential factor ( $\text{sec}^{-1}$ )

$E$  = activation energy (cal/gm)

$T$  = absolute temperature ( $^{\circ}\text{K}$ )

$F(W)$  = function of  $W$

$w$  = weight at time  $t$  (mg)

$w_f$  = final weight of sample (mg)

$w_o$  = initial weight of sample (mg)

Putting the weight in dimensional form, Equation II-19

becomes

$$-\frac{1}{w_o - w_f} \frac{dw}{dt} = A e^{-E/RT} F\left(\frac{w - w_f}{w_o - w_f}\right) \quad (\text{II-20})$$

Taking logarithms

$$\ln \left[ -\frac{1}{w_o - w_f} \frac{dw}{dt} \right] = \ln A + \ln F \left[ \frac{w - w_f}{w_o - w_f} \right] - \frac{E}{RT} \quad (\text{II-21})$$

Plotting  $\ln [-1/(w_o - w_f) \cdot dw/dt]$  at a particular conversion versus  $1/T$  for all heating rates gives straight lines of slope  $-E/R$  and intercept  $\ln [A F(W)]$ . By plotting at various levels of conversion, an activation energy can be calculated at each conversion. Now  $F(W)$  is assumed to be of the form

$$F(W) = \left[ \frac{w - w_f}{w_o - w_f} \right]^n \quad (\text{II-22})$$

Then

$$\ln A F(W) = \ln A + n \ln \left[ \frac{w - w_f}{w_o - w_f} \right] \quad (\text{II-23})$$

A plot of the previously determined values of  $\ln [A F(W)]$  versus  $\ln [(w - w_f)/(w_o - w_f)]$  now gives straight lines of slope  $n$ , order of reaction, and intercept  $\ln A$ . The kinetic parameters obtained at each conversion are then averaged to obtain the kinetic parameters of the sample. Sardesai's (36) results are shown in Tables II-4 and II-5.

#### Pyrolysis Studies Using Differential Scanning Calorimetry

As part of the development of a mathematical model to describe the decomposition of wood, Havens (14) used a differential scanning calorimeter (DSC) to measure "energy capacity." Havens' (14) "energy capacity" is defined to include all heat effects, due both to sensible heat and to any transition energy, as a function of temperature. The DSC then measures

TABLE II-4  
AVERAGE ACTIVATION ENERGY

Sample	Atmosphere	
	N <sub>2</sub> cal/g-mole	Air Kcal/g-mole
Whatman 54	28.61	18.68
Whatman 40	29.11	20.85
Whatman 6	29.86	19.87
Whatman 1	29.17	19.77
Whatman 115	25.36	13.25

TABLE II-5  
FREQUENCY FACTOR AND ORDER OF REACTION

Sample	Order of Reaction		Frequency Factor, sec <sup>-1</sup>	
	N <sub>2</sub>	Air	N <sub>2</sub>	Air
Whatman 54	0.97	1.0	8.6 x 10 <sup>13</sup>	1.86 x 10 <sup>11</sup>
Whatman 6	0.96	1.02	8.4 x 10 <sup>13</sup>	9.43 x 10 <sup>11</sup>
Whatman 40	0.98	0.91	6.2 x 10 <sup>13</sup>	1.24 x 10 <sup>12</sup>
Whatman 1	0.92	0.95	6.3 x 10 <sup>13</sup>	9.34 x 10 <sup>11</sup>
Whatman 115	0.93	0.90	6.1 x 10 <sup>12</sup>	9.4 x 10 <sup>9</sup>

"energy capacity." After overcoming some problems with volatile products which condensed on the lids of the DSC, thereby changing the radiation characteristics of the sample holder, Havens (14) measured the "energy capacity" of milled oak and pine. The "energy capacity" of each sample was then separated into the sensible heat and decomposition heat portions. Havens' (14) results are shown in Figures II-9 and II-10. The endothermic heats of decomposition for oak and pine wood were calculated at 26.6 cal/gm and 47.5 cal/gm, respectively. These same materials were rerun by Brown (4) who found endothermic heat of decomposition values of 27.0 cal/gm and 43.2 cal/gm for oak and pine wood, respectively. These are in good agreement with the results of Havens (14). The remaining work of Havens (14) and Brown (4) concerns the thermal properties of wood and char and will be discussed in a later section.

Duvvuri (7) used thermogravimetric analysis and differential scanning calorimetry to predict the heat of preignition for plant constituents and plant samples. Using the equation of Goldfarb (13), Duvvuri (7) performed a least-squares technique on TGA data for cellulose and punky wood, a biologically decomposed form of Douglas fir snags known to contain a high percentage of lignin. With this technique kinetic parameters were obtained for the decomposition of cellulose and lignin assuming decomposition occurred according to Equation II-19 where  $F(W) = W^n$ . The values of the kinetic

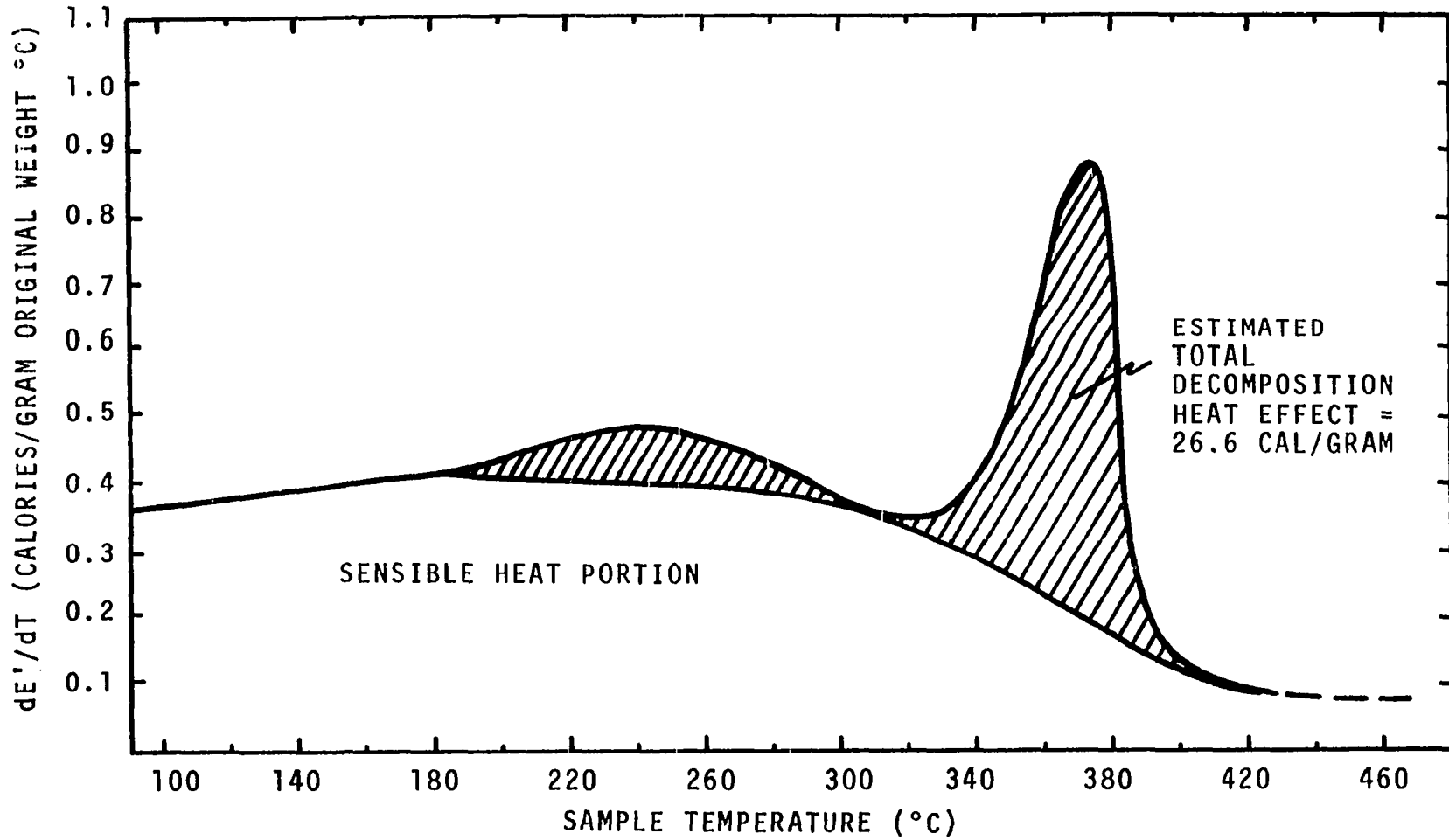


Figure II-9. Energy Capacity of Oak Wood as a Function of Temperature in Nitrogen Atmosphere (from Reference 14).

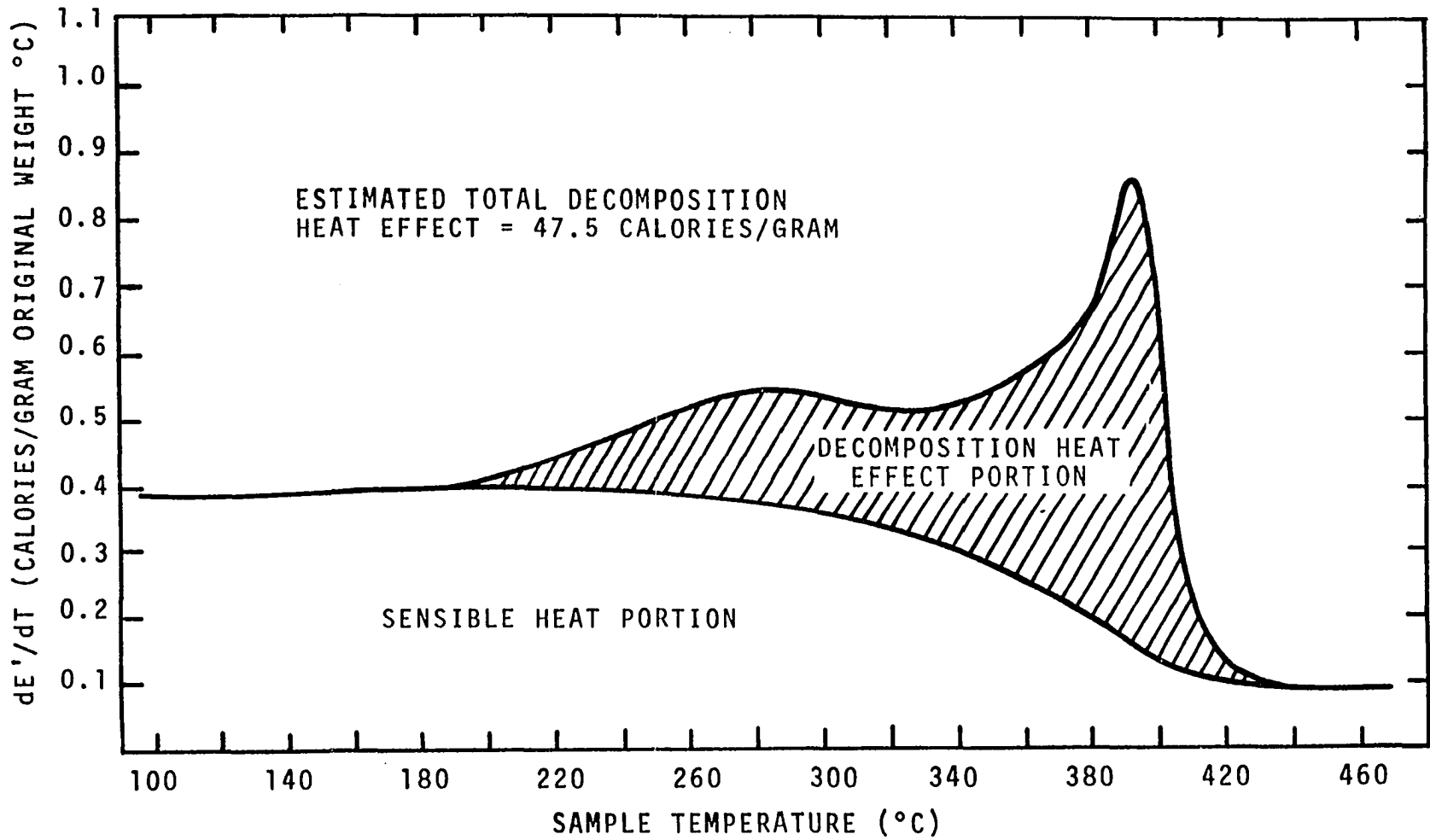


Figure II-10. Energy Capacity of Pine Wood as a Function of Temperature in Nitrogen Atmosphere from Reference (14).

parameters are shown in Table II-6. By numerically integrating Equation II-19 using the kinetic parameters, the weight loss and rate of weight loss for cellulose and punky wood at any heating rate can be calculated. The 40°C/min calculated and experimental curves are shown for cellulose and punky wood in Figures II-11 and II-12. Since the chief constituents of wood are holocellulose and lignin, the weight loss and rate of weight loss of plant samples are modeled as the sum of two weight loss terms having the form

$$-\frac{dW}{dt} = X_H A_H e^{-E_H/RT} (W_H)^{n_H} + X_L A_L e^{-E_L/RT} (W_L)^{n_L} \quad (\text{II-24})$$

where X is the mass fraction and the subscripts refer to holocellulose and lignin. The other symbols are defined as in Equation II-19. The kinetic parameters for cellulose and punky wood are used in Equation II-24 for those of holocellulose and lignin, respectively. Using this method, the

TABLE II-6  
KINETIC PARAMETERS FOR CELLULOSE AND PUNKY WOOD (7)

Kinetic Parameter	Cellulose	Punky Wood
Activation energy (cal/gm-mole)	29,740	21,290
Frequency Factor (l/min)	5.0 x 10 <sup>9</sup>	3.1 x 10 <sup>7</sup>
Order of Reaction	0.79	3.2

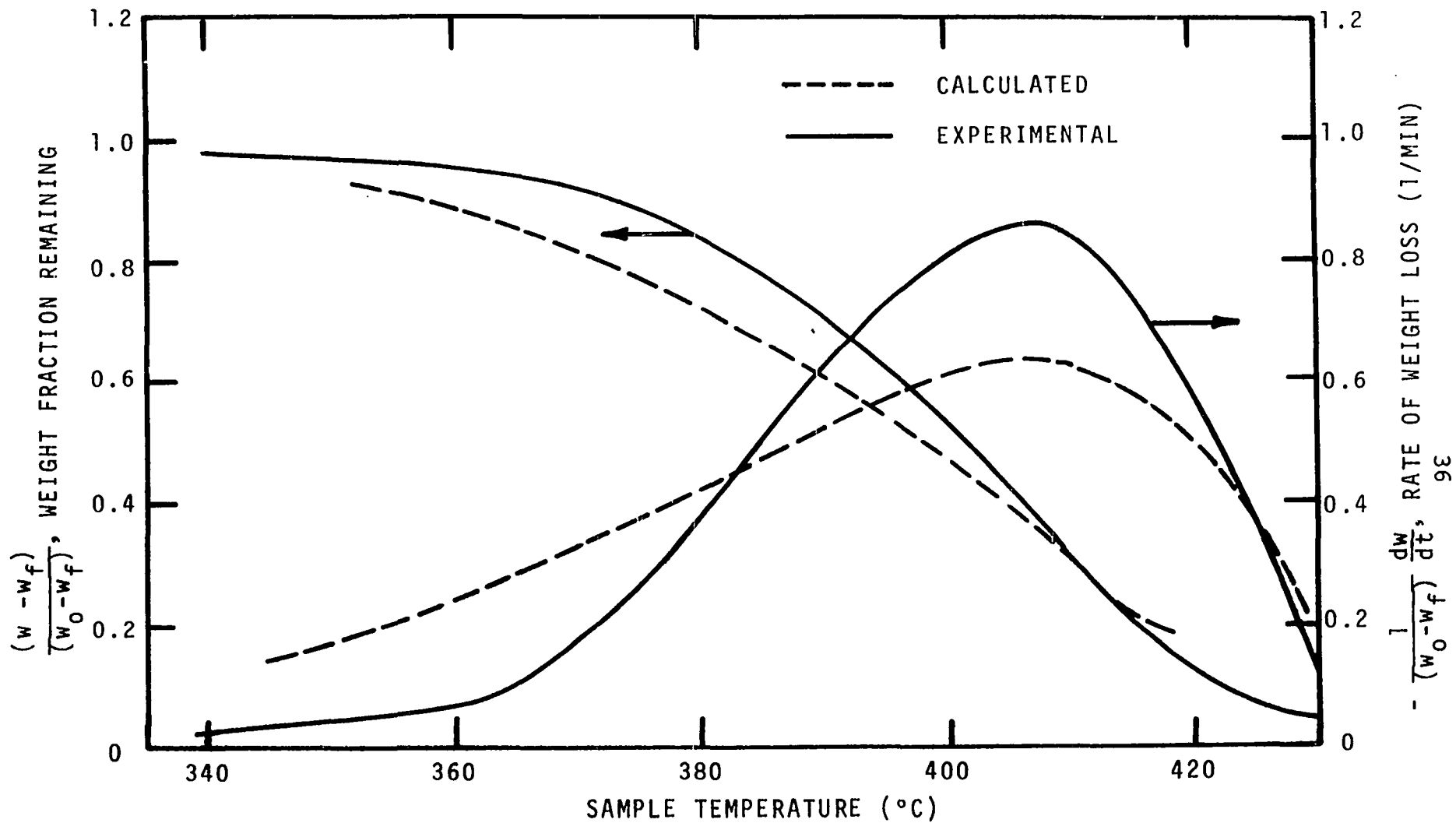


Figure II-11. Weight Loss and Rate of Weight Loss for Cellulose. Heating Rate, 40°C/min. (Reference 7).

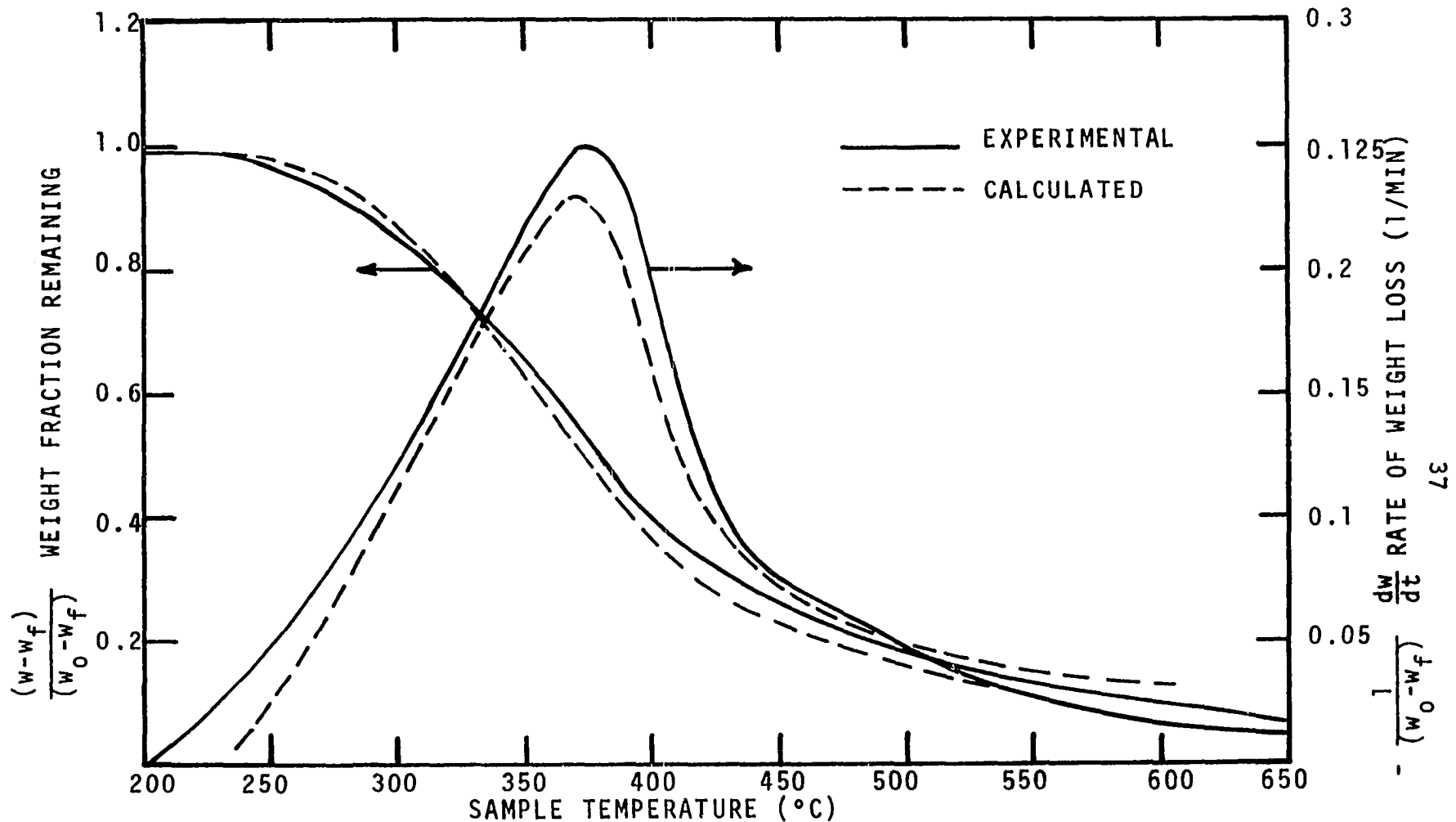


Figure II-12. Weight Loss and Rate of Weight Loss for Punky Wood from Douglas Fir Snags. Heating Rate, 40°C/min. (Reference 7).

calculated and experimental weight loss and rate of weight loss for excelsior are shown in Figure II-13.

Duvvuri (7) then made energy measurements on cellulose and punky wood with the DSC at 40°C/min as shown in Figure II-14 and Figure II-15. The shaded area depicts the energy of pyrolysis. Measurements were also made at heating rates of 80°C/min and 160°C/min; however, the results are similar to those of the 40°C/min scan. The values computed for specific heat and energy of pyrolysis are shown in Table II-7.

TABLE II-7  
SPECIFIC HEAT AND ENERGY OF PYROLYSIS OF CELLULOSE  
AND PUNKY WOOD (7)

Material	C <sub>p</sub> at 25°C (cal/gm-°C)	Energy of Pyrolysis (cal/gm)
Cellulose	0.33	86.0
Punky Wood	0.44	36.0

In order to predict the total energy to pyrolyze a plant sample, the values from Table II-7 were combined with the weight loss calculation in the following equation

$$E' = \left[ \int_0^{500} W C_p dT + \int_0^{500} \Delta H_p \frac{dW}{dt} \frac{dt}{dT} dT \right]_C + \left[ \int_0^{500} W C_p dT + \int_0^{500} \Delta H_p \frac{dW}{dt} \frac{dt}{dT} dT \right]_L \quad (\text{II-25})$$

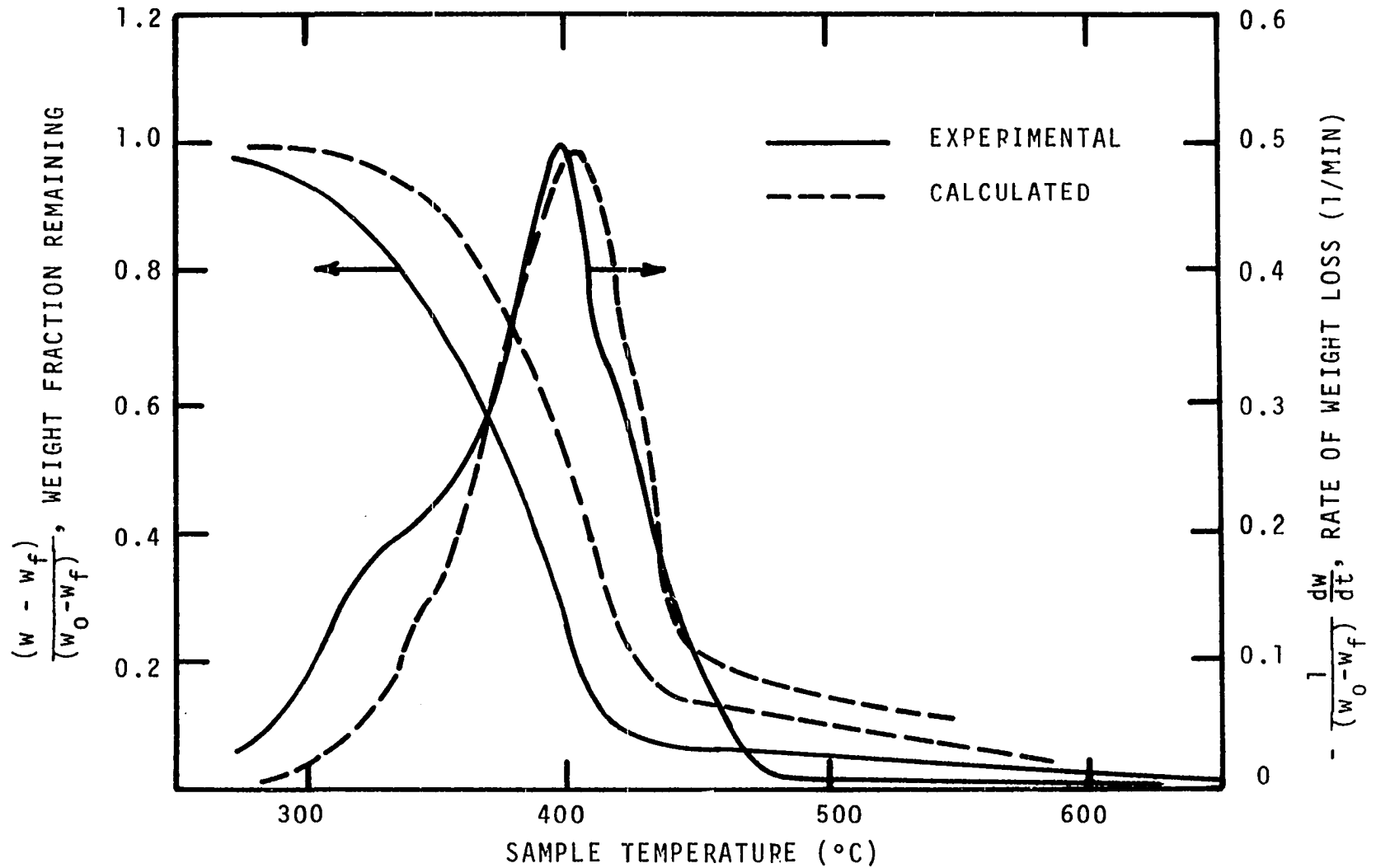


Figure II-13. Weight Loss and Rate of Weight Loss for Excelsior. Heating Rate, 40°C/min.

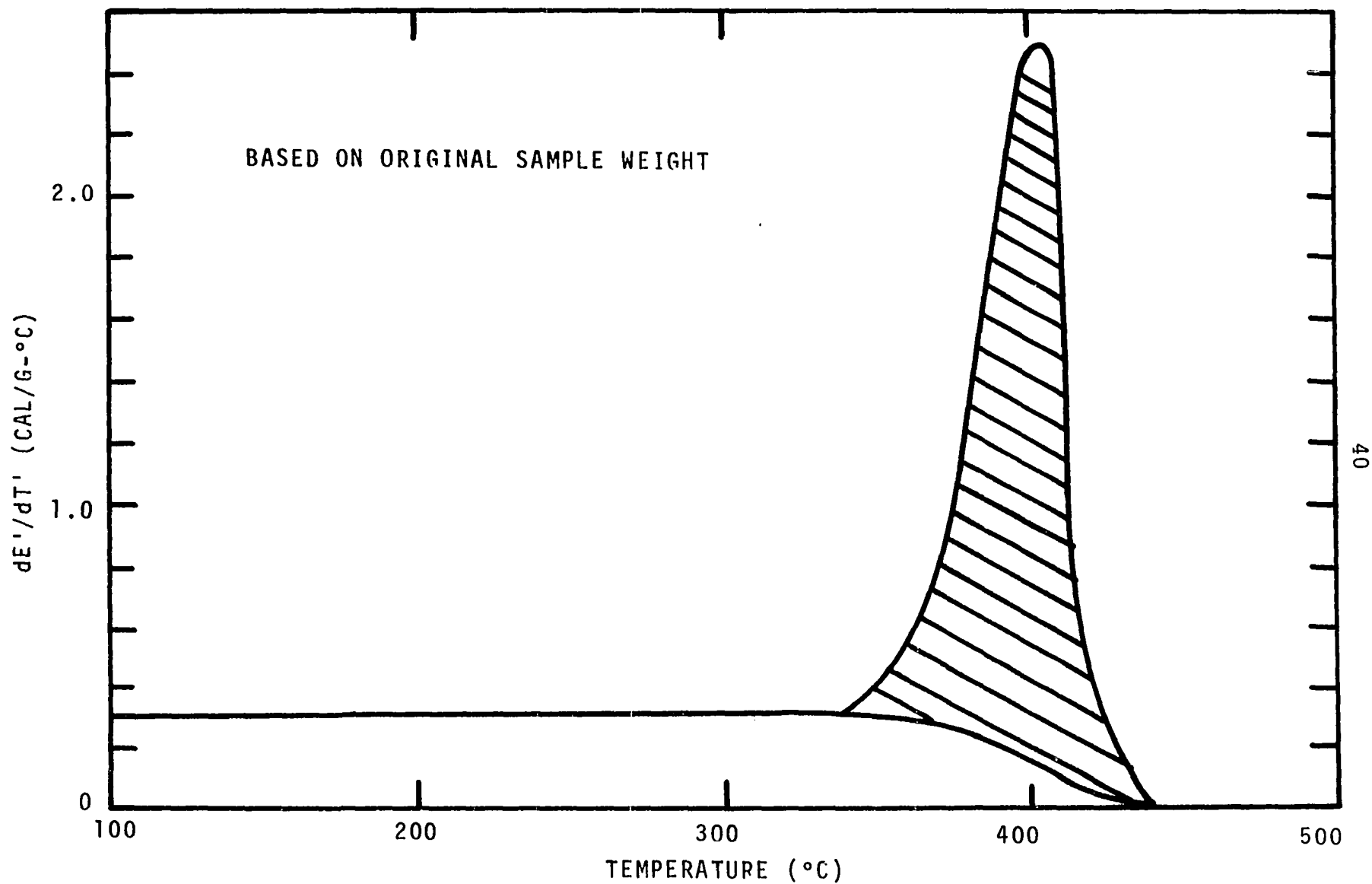


Figure II-14. Differential Energy of Cellulose. Heating Rate,  $40^\circ\text{C}/\text{min}$ . (Reference 7).

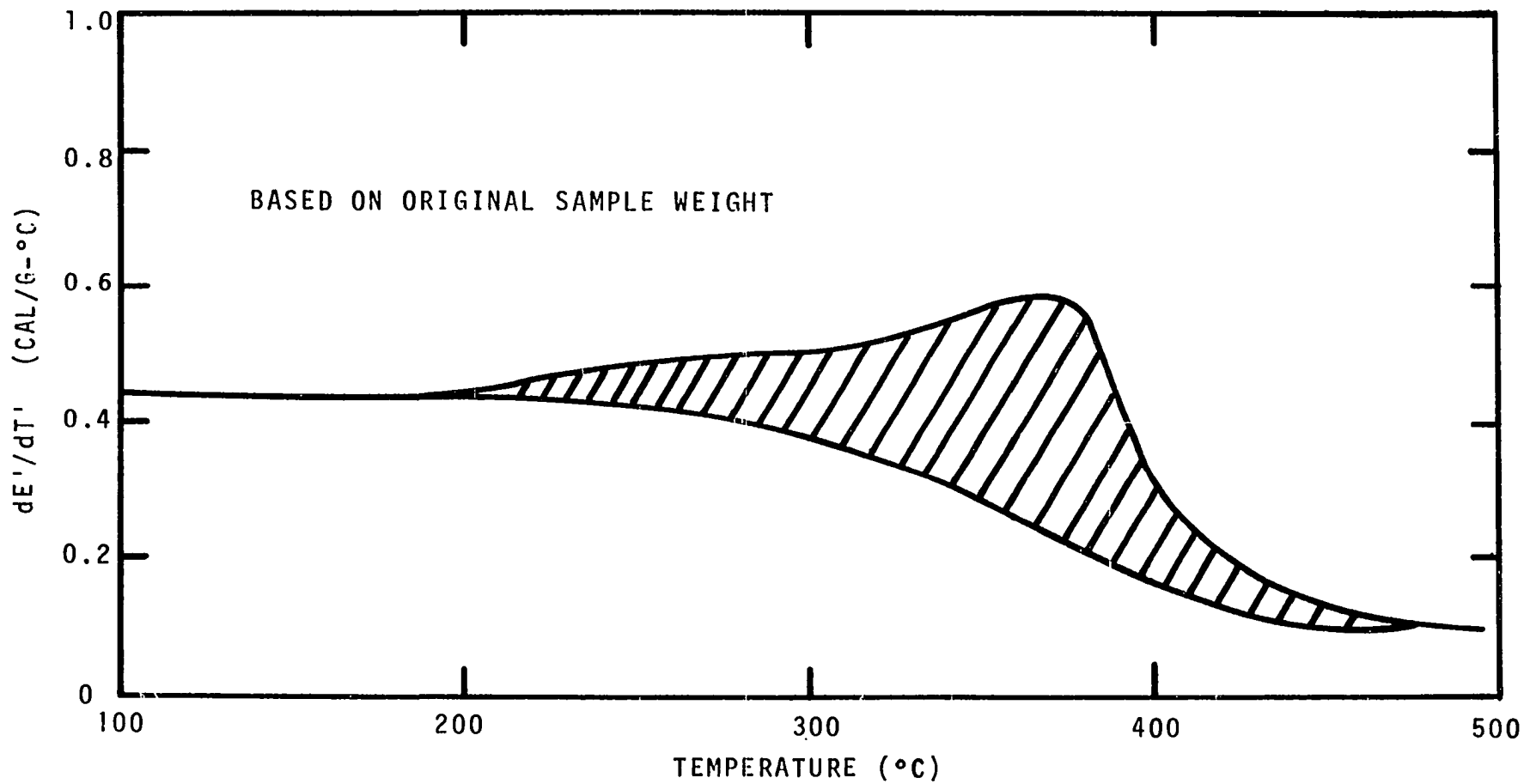


Figure II-15. Differential Energy of Lignin. Heating Rate, 40°C/min. (Reference 7).

where  $W$  = weight (dimensionless)

$E'$  = total energy (cal/gm)

$C_p$  = specific heat (cal/gm-°C)

$\Delta H_p$  = energy of pyrolysis (cal/gm)

$dW/dt$  = calculated rate of weight loss (l/min)

$dt/dT$  = reciprocal of heating rate (min/°C)

C and L refer to cellulose and lignin, respectively. The experimental DSC results for excelsior were integrated numerically to find total energy. A comparison of these experimental results and the calculated results for excelsior is shown in Figure II-16. The agreement between the experimental and calculated results is within 12 percent. The accuracy could possibly be improved by using actual lignin instead of punky wood. Further improvements could be made by including the effect of other chemical components of the plants. As suggested by Duvvuri (7), computations of kinetic parameters for each heating rate could result in better weight loss predictions.

In addition to decomposition studies, differential scanning calorimetry has been used, with slight equipment modifications, for other types of studies. These include determination of emissivities (34), heats of mixing (23), and specific heats of various materials to be discussed in the next section.

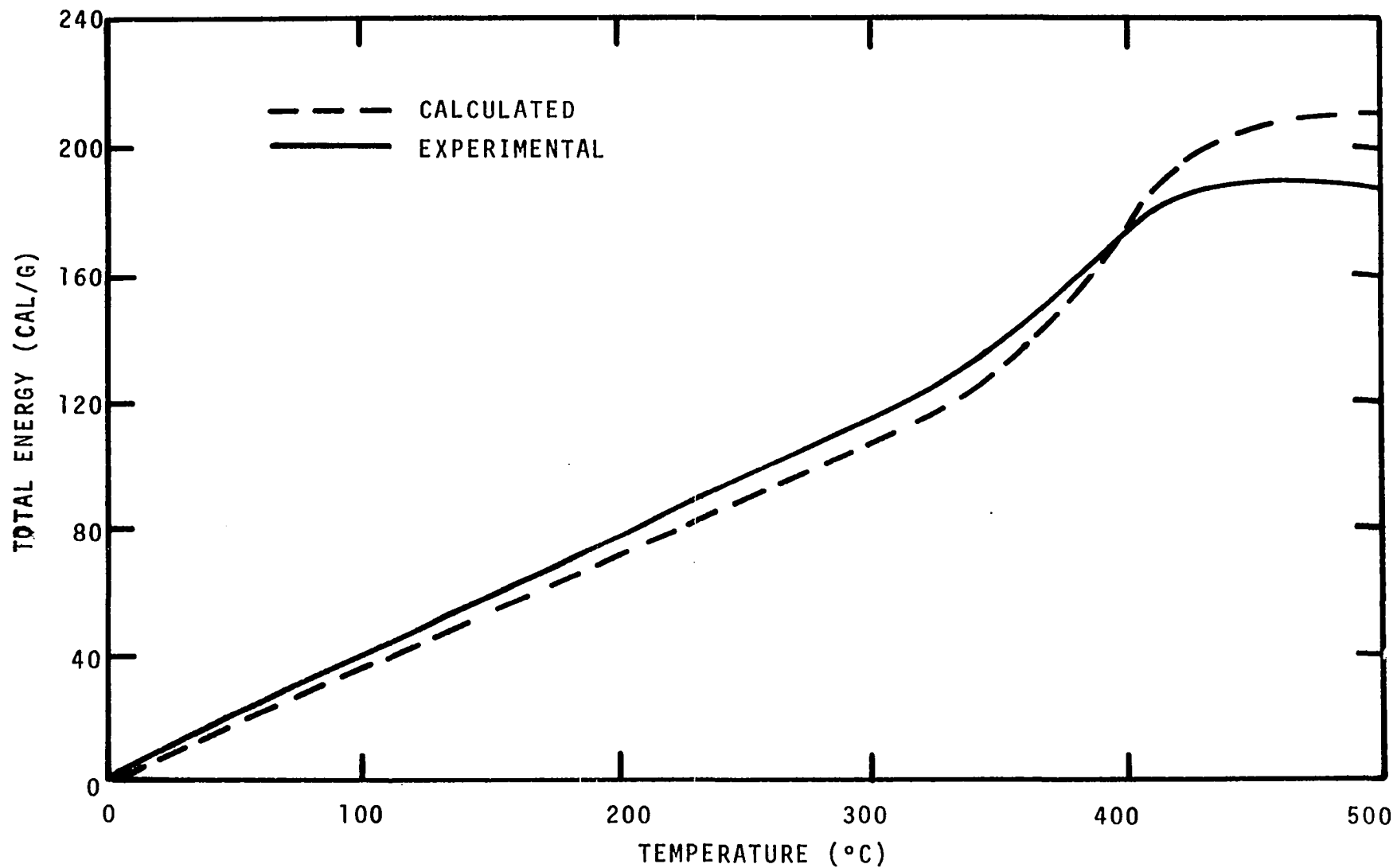


Figure II-16. Calculated and Experimental Total Energy for Dry Excelsior. Heating Rate, 40°C/min. (Reference 7).

Thermal Properties of Wood and Plant Samples

The importance of accurate thermal properties of wood is demonstrated by Kung and Kalelkar (17). In this study a Crank-Nicolson solution for the continuity, energy, and kinetic equations is obtained for the pyrolysis of a wood cylinder. The kinetic parameters and heat of pyrolysis were calculated from the data of Roberts and Clough (33) resulting in an activation energy of 15,140 cal/mole, a pre-exponential factor of  $1.19 \times 10^5 \text{ min}^{-1}$  and a heat of pyrolysis of 48.4 cal/gm endothermic. The study of Roberts and Clough (33) was then simulated with the mathematical model. Calculations for the rate of pyrolysis were made by individually varying the values of char thermal conductivity, char specific heat, wood thermal conductivity, and heat of pyrolysis. The results of these computations are shown in Table II-8. Since the thermal conductivity of the wood was used to non-dimensionalize time in this study, the maximum rate of pyrolysis is shown in dimensional units for that portion of Table II-8. Although the actual values of the calculations have a limited worth, the comparative changes in the rate of pyrolysis with changes in thermal properties indicates the need for accurate values of the thermal properties of the sample.

In his mathematical model for the pyrolysis of wood, Havens (14) used wood and char thermal conductivities calculated from MacLean's (2) density correlation,

$$K = 0.00478(\rho) + 0.000568 \quad (\text{II-26})$$

TABLE II-8

EFFECT OF THERMAL PROPERTIES ON RATE OF PYROLYSIS (17)

Property	Value	dW/dt (max)
Char thermal conductivity	$0.98 \times 10^{-4}$ ( $\frac{\text{cal}}{\text{cm-sec-}^\circ\text{C}}$ )	2.6 (dimensionless)
	$3.0 \times 10^{-4}$	3.3
	$9.0 \times 10^{-4}$	4.6
Char specific heat	0.08 (cal/gm-°C)	6.9 (dimensionless)
	0.16	2.5
	0.33	1.5
Wood thermal conductivity	$1.75 \times 10^{-4}$ ( $\frac{\text{cal}}{\text{cm-sec-}^\circ\text{C}}$ )	0.005 (gm/sec)
	$3.5 \times 10^{-4}$	0.0085
	$7.0 \times 10^{-4}$	0.015
Heat of pyrolysis	24.2 exothermic (cal/gm)	8.0 (dimensionless)
	24.2 endothermic	5.75
	48.4 endothermic	2.5
	96.8 endothermic	1.4

where  $K$  = thermal conductivity ( $\text{cal}/\text{cm}^2\text{-sec-}(\text{°C}/\text{cm})$ )

$\rho$  = density ( $\text{gm}/\text{cm}^3$ )

Using Equation II-26 thermal conductivity values of  $0.00296 \text{ cal}/\text{cm}^2\text{-sec-}(\text{°C}/\text{cm})$  and  $0.000112 \text{ cal}/\text{cm}^2\text{-sec-}(\text{°C}/\text{cm})$  were calculated for pine wood and char, respectively. However, when comparing his calculated temperatures to those of his experiment, Havens (14) found that values of thermal conductivity 15 percent higher than those given by the density correlation fit the data better. These higher values are referred to as an "effective thermal conductivity."

Brown's (4) work was primarily aimed at measuring the thermal conductivity of the charred wood. Values were obtained

which average  $0.000527 \text{ cal/cm}^2\text{-sec-(}^\circ\text{C/cm)}$ . These values are approximately five times as large as those given by MacLean's (20) density correlation and three times as large as Havens' (14) "effective thermal conductivities." However, these values for thermal conductivity, along with corrections for heating rate and bulk flow of gases through the char, gave good agreement between the experimental and calculated temperature profiles.

The specific heat of various wood and plant samples has been determined by many investigators. Most recent studies utilize differential scanning calorimetry. The results of some of the studies are shown in Table II-9. In general, where direct comparisons can be made from different investigators, the agreement is quite good. On the other hand, measurements of the heat of pyrolysis are frequently conflicting. Because there are many species of wood, some recent studies have considered wood on the basis of its components. The pyrolysis of various wood samples is then described by the pyrolysis effects of the various components.

TABLE II-9

SPECIFIC HEAT MEASUREMENTS OF WOOD AND  
PLANT SAMPLES

Investigator	Temperature (°C)	Sample	Specific Heat (cal/gm-°C)
Havens (14)	100	Pine Wood	0.39
	100	Oak Wood	0.37
Brown (4)	100	Pine Wood	0.40
	100	Oak Wood	0.37
Duvvuri (7)	100	Cellulose	0.33
	100	Dead Ponderosa Pine Needles	0.44
	100	Excelsior	0.37
	100	Saltbush Leaves	0.39
	100	Punky Wood	0.44
	100	Punky Wood	0.44
McMillin (21)	60	Loblolly Pine Wood	0.3265
	100	Loblolly Pine Wood	0.3684
	140	Loblolly Pine Wood	0.4024
Koch (16)	60	Spruce Pine Wood	0.3250
	100	Spruce Pine Wood	0.3662
	140	Spruce Pine Wood	0.4053
McMillin (22)	60	Loblolly	
		Holocellulose	0.3110
		α-Cellulose	0.3107
		Lignin	0.3165
	100	Extractives	0.4292
		Loblolly	
		Holocellulose	0.3573
		α-Cellulose	0.3572
	140	Lignin	0.3486
		Extractives	0.4853
		Loblolly	
		Holocellulose	0.3904
		α-Cellulose	0.3900
	Lignin	0.3780	
	Extractives	0.5166	

## CHAPTER III

### EXPERIMENTAL PROCEDURE

The experimental portion of this study can be divided into two sections. The first section consisted of devising a method of preparation for living samples, while the second section consisted of obtaining pyrolysis data on samples supplied by the Northern Forest Fire Laboratory. The samples supplied by the Northern Forest Fire Laboratory were prepared according to the method devised in the initial section of this study. Samples of pine needles, holly leaves, and spruce needles were used in the validation of the sample preparation. The samples sent from the Northern Forest Fire Laboratory consisted of freeze-dried aspen leaves, chamise foliage, manzanita leaves, Douglas fir needles, Ponderosa pine needles, and lodgepole pine needles. Of primary importance is the measurement of the total energy needed to pyrolyze the samples.

#### Preparation of Living Plant Samples

The development of a method for gathering and preparing living plant samples had to conform to the following guidelines:

1. The method must be applicable for the collection of plant samples in remote areas.

2. The resulting samples must be stable for long periods of time.
3. The composition of the resulting samples must be representative of the living plants with the possible exception of water content.

Fresh living samples and prepared samples were compared by testing the samples on a thermogravimetric balance (TGS) to be described in the next section. The choice of instruments was dictated by the large amount of water (about two-thirds by weight) in the fresh samples. Testing the samples on the differential scanning calorimeter (DSC) was impractical due to the large heat of vaporization and sensible heat of water compared to the heat of pyrolysis and sensible heat of the plants. However, the weight losses of the living and prepared samples measured by the TGS are at least of the same order of magnitude.

Since a type of freeze-drying appeared to be a promising method of preparation, the following procedure was employed for the collection and preparation of the samples and the subsequent validation of the method.

1. Samples of a plant were collected, divided into four capped bottles and weighed. Two of the bottled samples were frozen at  $-10^{\circ}\text{F}$ , one sample was retained at room temperature, and one sample was immediately tested on the TGS at a heating rate of  $10^{\circ}\text{C}/\text{min}$ . At this heating rate, separation of the total weight loss into that of the water and that of the plant material was easily accomplished.

2. The following day the room temperature sample and one of the frozen samples were subjected to a partial vacuum of less than 3 mm Hg until no further weight loss was recorded. This partial vacuum was accomplished with the use of a Welch duo-seal vacuum pump, Model 1405, connected to glass bell jars.
3. These samples were then tested on the TGS at a heating rate of 10°C/min and the results were compared to that of the plant material of the fresh sample.

The above procedure was repeated for pine needles, spruce needles, and holly leaves. These plants were chosen for their high degree of homogeneity within that portion of the plant which was tested. Milling the samples would have also insured homogeneity; however, the milled fresh plants would have resulted in a rather "soupy" liquid. Due to the inherent handling problems of such a sample, tests were run on small (2-3 mg) cross-sections of the samples. The method of freezing and then drying with a vacuum, referred to as freeze-drying, was judged to be adequate based on the TGS results. The weight loss and rate of weight loss for fresh (moisture-free basis) and freeze-dried pine needle samples are shown in Figures III-1 and III-2, respectively. The agreement of the results depicted in Figures III-1 and III-2 is excellent, thereby validating freeze-drying as a method of preparing samples which are comparable to the fresh samples. Initial plans to show the fresh and freeze-dried results on a

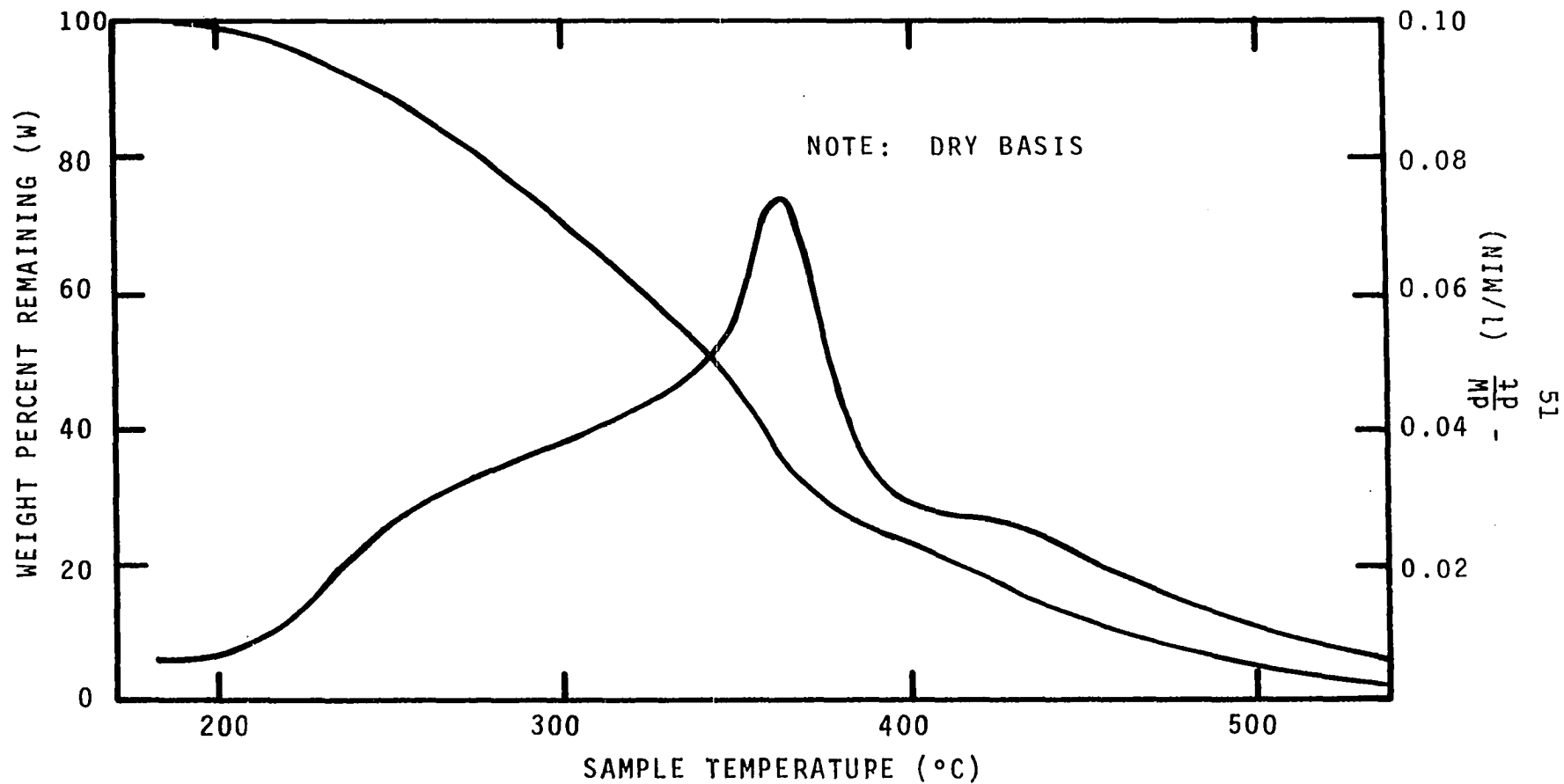


Figure III-1. Weight Loss and Rate of Weight Loss for Fresh Pine Needles. Heating Rate, 10°C/min.

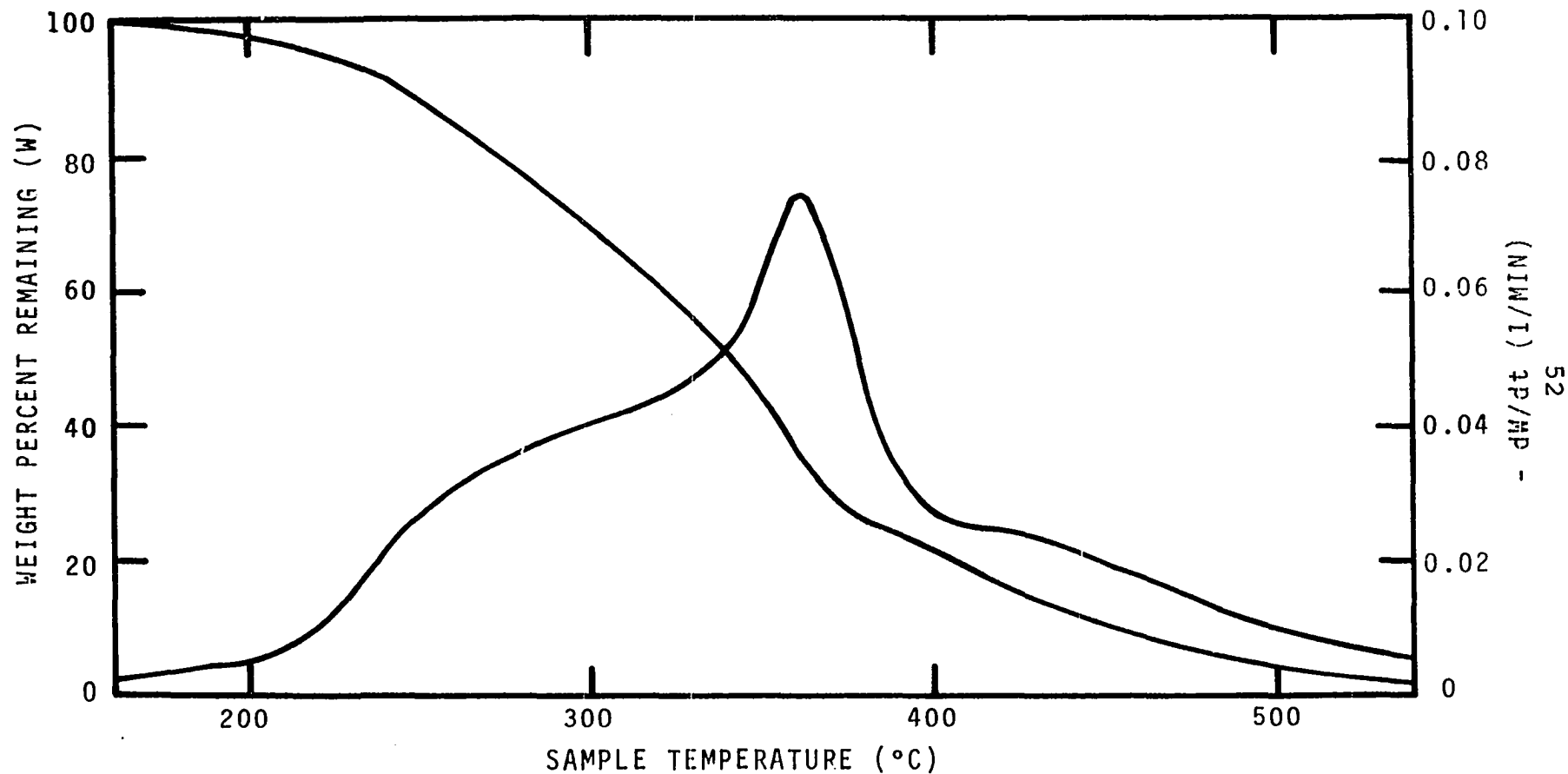


Figure III-2. Weight Loss and Rate of Weight Loss for Freeze-Dried Pine Needles. Heating Rate, 10°C/min.

single figure had to be curtailed since the results were too close to distinguish the curves. The corresponding results for spruce needles and holly leaves are in Appendix A. Comparison of the results of the fresh and freeze-dried spruce needles and holly leaves also indicates excellent agreement.

#### Thermogravimetric Balance

A Perkin-Elmer TGS-1 thermobalance and UU-1 temperature programmer were used to obtain the thermogravimetric data in this study. These are shown in Figure III-3 with a schematic of the sample holder, furnace, and electrobalance shown in Figure III-4. The electrobalance used in the TGS-1 is a Cahn-RG electrobalance. As the temperature programmer heats the furnace, the sample loses weight in the form of gaseous products. This weight loss is continuously monitored by the electrobalance and recorded on a Leeds & Northrup Series XL680 recorder. While it is possible to obtain weight loss and rate of weight loss as output from the TGS, only weight loss was obtained from the TGS. This weight loss signal was then used as input into a Cahn No. 3100 time derivative computer, thereby enabling the weight loss and the rate (or time derivative) of weight loss to be recorded simultaneously.

As shown in Figure III-4, the sample hangs from the electrobalance into the cylindrical furnace on a wire. This nichrome wire is long enough to isolate the electrobalance

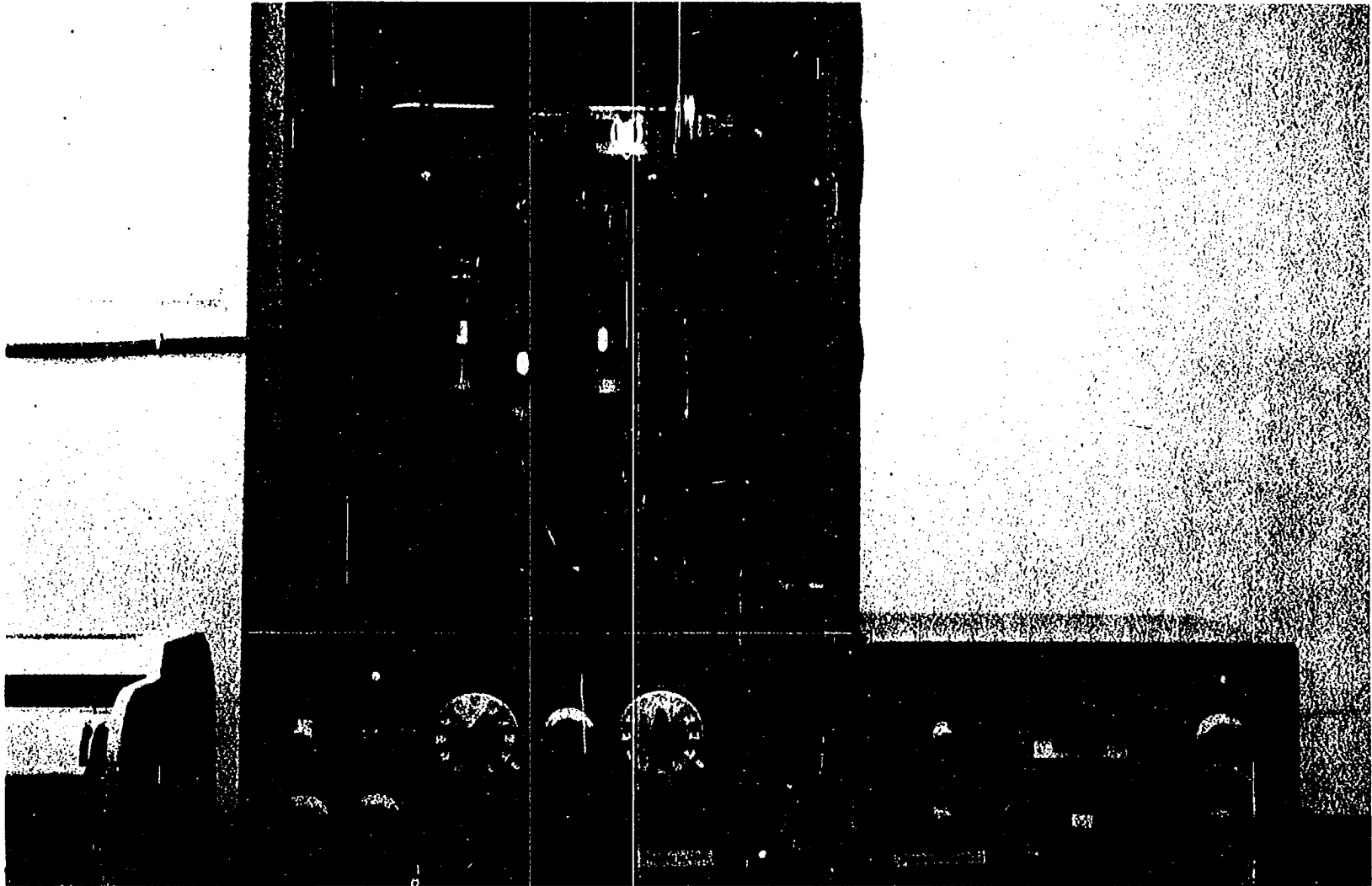


Figure III-3. Perkin-Elmer TGS-1 Thermobalance and UU-1 Temperature Controller.

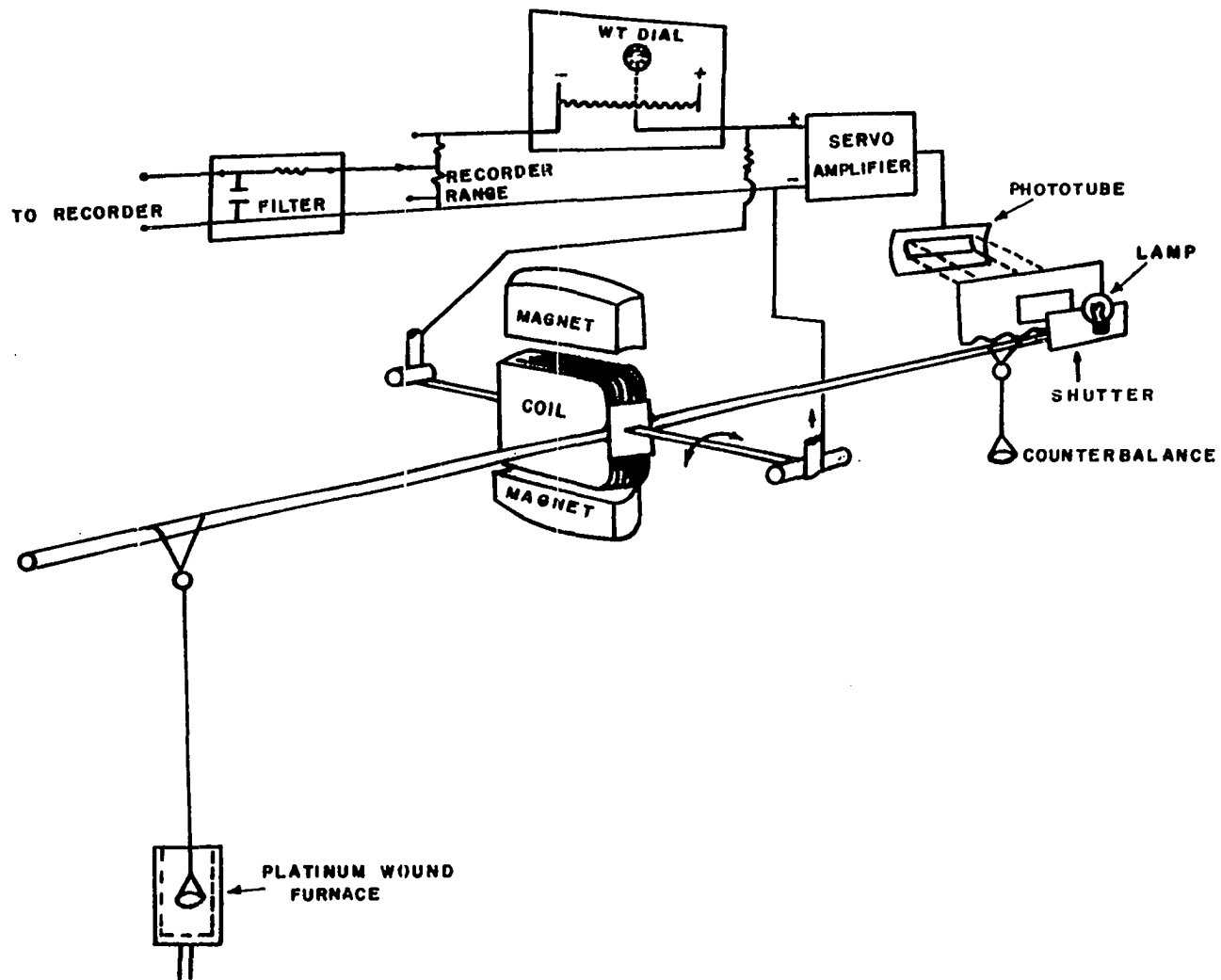


Figure III-4. Schematic of Perkin-Elmer TGS-1 Furnace and Weigh Assembly.

from any heat effects from the furnace. Furthermore, the glass container of the electrobalance is purged with nitrogen in such a manner that the nitrogen sweeps the pyrolysis products away from the balance and out of the glass enclosure. This purge prevents any condensation of pyrolysis products on the delicate parts of the weighing mechanism. However, these gaseous products do collect on the furnace which is made of wound platinum wire. These products can corrode the wire heater unless the heater is protected by a glass wool plug inserted in the bottom of the heater. This modification, introduced by Brown (4), has resulted in a considerable increase in furnace life.

The plant samples were milled to a 20-60 mesh size and ranged from 1 to 2 mg in mass. The use of a very small sample minimizes any heat transfer effects within the sample. The furnace is calibrated at the various heating rates in order to minimize any heat transfer effects from the furnace to the sample.

The furnace calibration is achieved through the application of a property of ferromagnetic alloys. That is, at a known temperature these metal alloys lose their magnetic effect. The calibration is accomplished by placing small samples of the alloys in the sample pan and covering them with aluminum oxide for better heat transfer to the sample. Then a permanent magnet is placed around the "hang-down" tube as in Figure III-5 so as to avoid contact between the sample

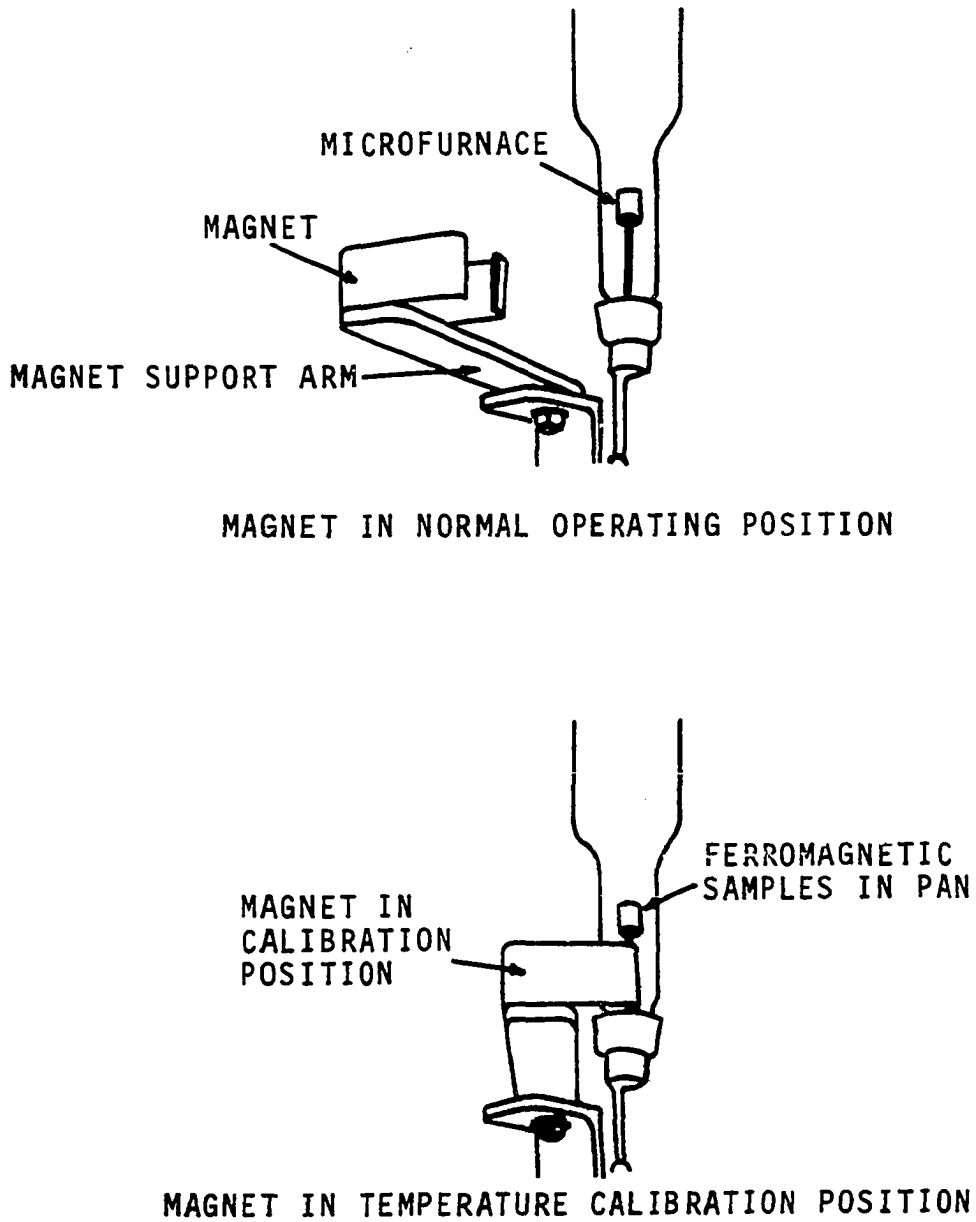


Figure III-5. Schematic of TGS-1 Temperature Calibration System.

pan and the furnace. Any contact is easily recognizable by the excessive noise indicated by the recorder. As the alloy samples are heated by the furnace, the alloys lose their magnetic effect and a sharp weight loss is recorded. In all cases the temperature at which the rate of weight loss peaked was chosen as the indicated magnetic transition temperature. The actual magnetic transition temperatures of these ferromagnetic alloys is shown in Table III-1.

TABLE III-1  
CALIBRATION STANDARDS FOR TGS-1 FURNACE

Metal	Magnetic Transition Temperature (°C)
Monel	65
Alumel	163
Nickel	354
Mumetal	393
Nicoseal	438
Perkalloy	596
Iron	780
Hi-Sat 50	1000

The difference between the actual and indicated temperatures can be minimized by adjustment of the zero, range, and linearity dials on the thermobalance and temperature programmer. In the past, most investigators used one setting of the dials for all heating rates and applied a temperature correction to obtain actual temperatures. In this study the temperature calibration settings were optimized for each heating rate in

addition to performing the temperature correction. The settings for each heating rate are shown in Table III-2.

TABLE III-2  
SETTINGS FOR TGS-1 FURNACE CALIBRATION

Heating Rate	Zero*	Range	Linearity
10	631	860	-3.6
40	643	865	-3.4
160	705	863	-3.55

\*All dial settings are in arbitrary units.

Throughout this study Alumel, nickel, Mumetal, and Perkalloy were used for temperature calibration of the furnace. Although the magnetic transition temperature of Nicoseal is in the temperature range of interest, it was decided not to use Nicoseal for the calibration on the basis that its temperature deviation was always very large compared to that of the other alloys. This behavior can be seen in previous investigations by Woodard (42). Figure III-6 shows the results of the temperature calibration for three heating rates with the settings as shown in Table III-2.

Calibration weights were used initially to insure linearity of the indicated weight loss. The actual weight loss was essentially calibrated each run by weighing the sample before and after each run on an analytical balance. This measured weight loss was then compared to the total span on

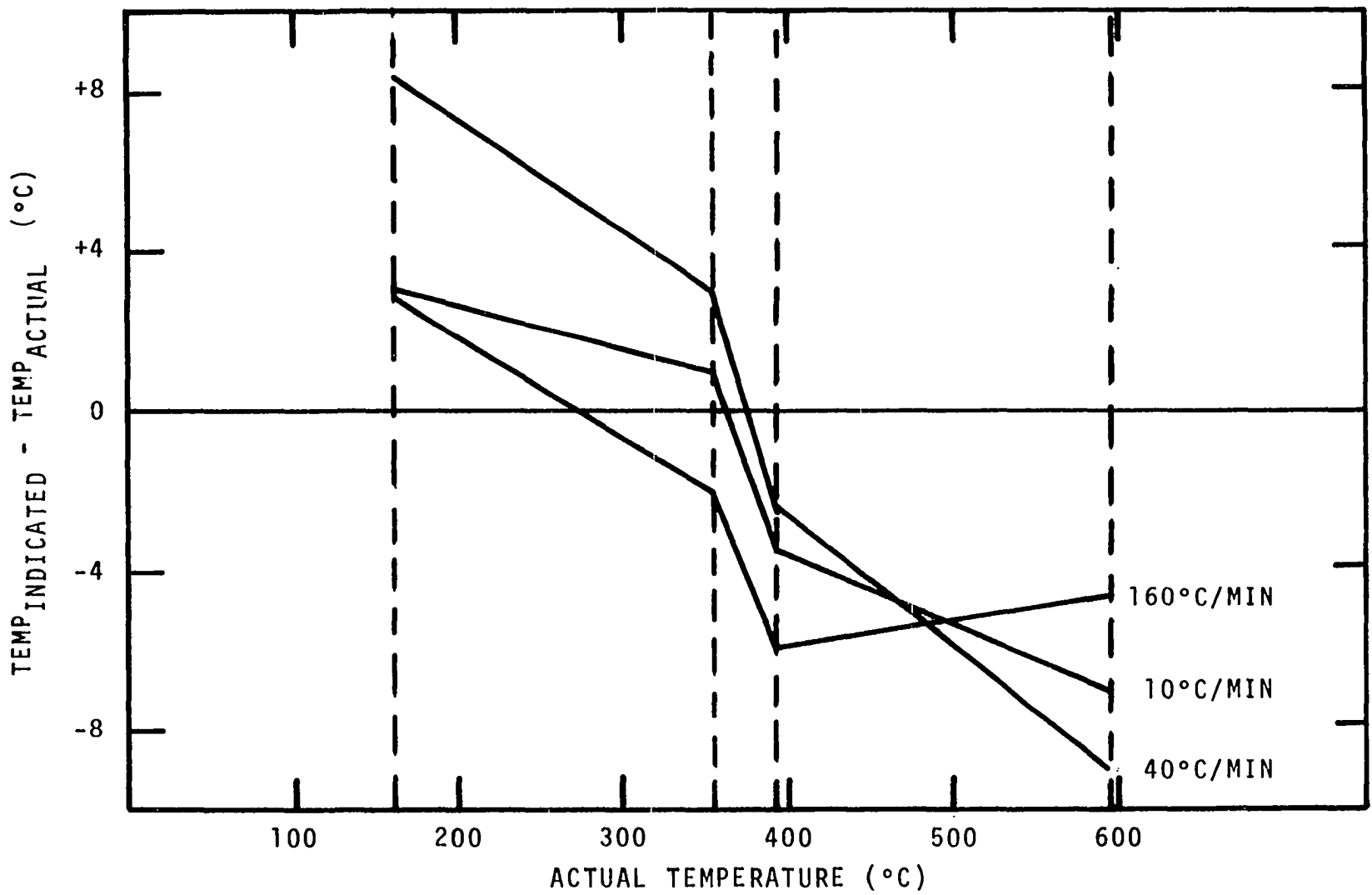


Figure III-6. Calibration Curve for TGS-1 Furnace.

the recorder enabling the calculation of the remaining weight at any point during the pyrolysis of the sample.

The time derivative computer was also calibrated with each run by comparing the total weight loss with the area under the rate of weight loss curve. The time derivative computer has an adjustable "filter" to control the amount of noise in the output. Great care was needed to insure that the derivative computer was not overly "filtered," which would cause the rate of weight loss curve to shift to a higher temperature.

#### Differential Scanning Calorimeter

Energy measurements of the pyrolyzing samples were made on the Perkin-Elmer DSC-2 differential scanning calorimeter shown in Figure III-7. As explained in Chapter II, the DSC measures the differential energy necessary to maintain a sample at the temperature of the empty reference pan during heating. The heating of the sample and reference holders is controlled at constant rates by the temperature controller built into the DSC-2. The DSC-2 has eleven heating or cooling rates from 0.3125 to 320°C/min. Since the DSC-2 can be operated in Fahrenheit, Centigrade, or Kelvin, this corresponds to twenty-two different heating or cooling rates. With the use of a subambient assembly, the DSC-2 has a temperature range of 100°K to 1000°K with the digital temperature readout indicating the temperature to the nearest one-tenth of a degree. The differential energy output ranges vary from 0.1 to 20.0

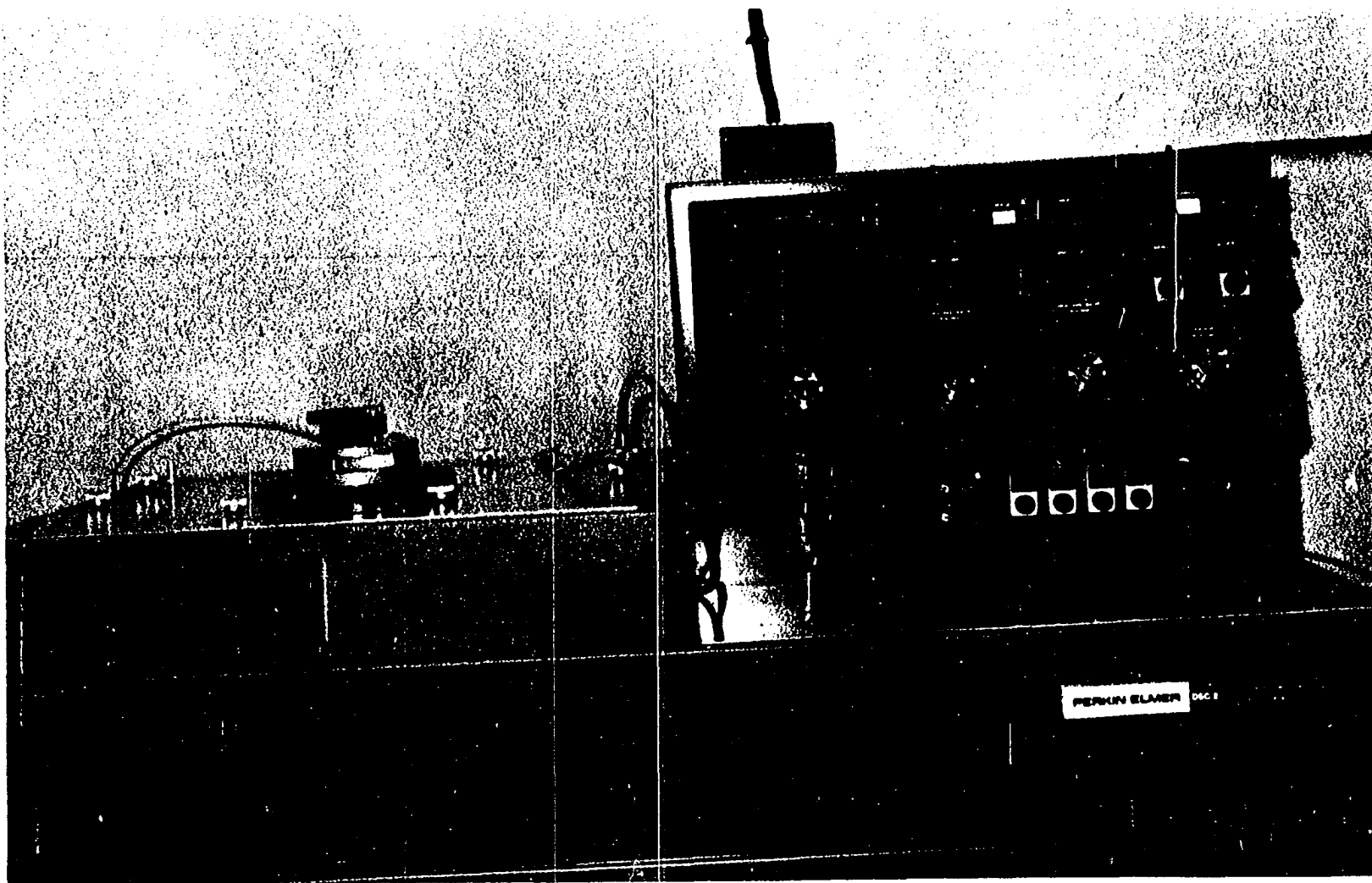


Figure III-7. Perkin-Elmer Differential Scanning Calorimeter  
DSC-2.

mc cal/sec full scale on a 10 mv potentiometric recorder. In order to avoid excessive noise at the low ranges, Perkin-Elmer has designed the instrument to have a maximum noise of  $\pm 0.004$  mc cal/sec at 700°K with no purge. In this study the sample and reference holders were purged with 110 psig of nitrogen. Perkin-Elmer has built into the DSC-2 a special orifice for the purge gas which provides that the pressure in psi corresponds to the flow rate in cc/min. Therefore, the nitrogen flow rate was 110 cc/min in this study.

The sample and reference holders are located in an aluminum block which serves as a heat sink to provide a constant thermal environment. The improvement in the holder assembly, known as the head, is probably the most important improvement in the DSC-2 over the previous model, the DSC-1B. The head is shown in Figure III-8. Each platinum-iridium sample holder contains its own platinum heater and temperature sensor.

The DSC-2 is calibrated for: (1) temperature; (2) energy of transition; and (3) ordinate displacement due to specific heat of the sample. The calibration of the DSC-2 for temperature and energy of transition is accomplished by the melting of various standard calibrating materials, shown in Table III-3. The melting temperature of distilled water, indium, and zinc were used for temperature calibration at 10°C/min at various times within this study. In all cases the indicated temperature was within 1°C of the actual temperature; therefore, no adjustments were made.

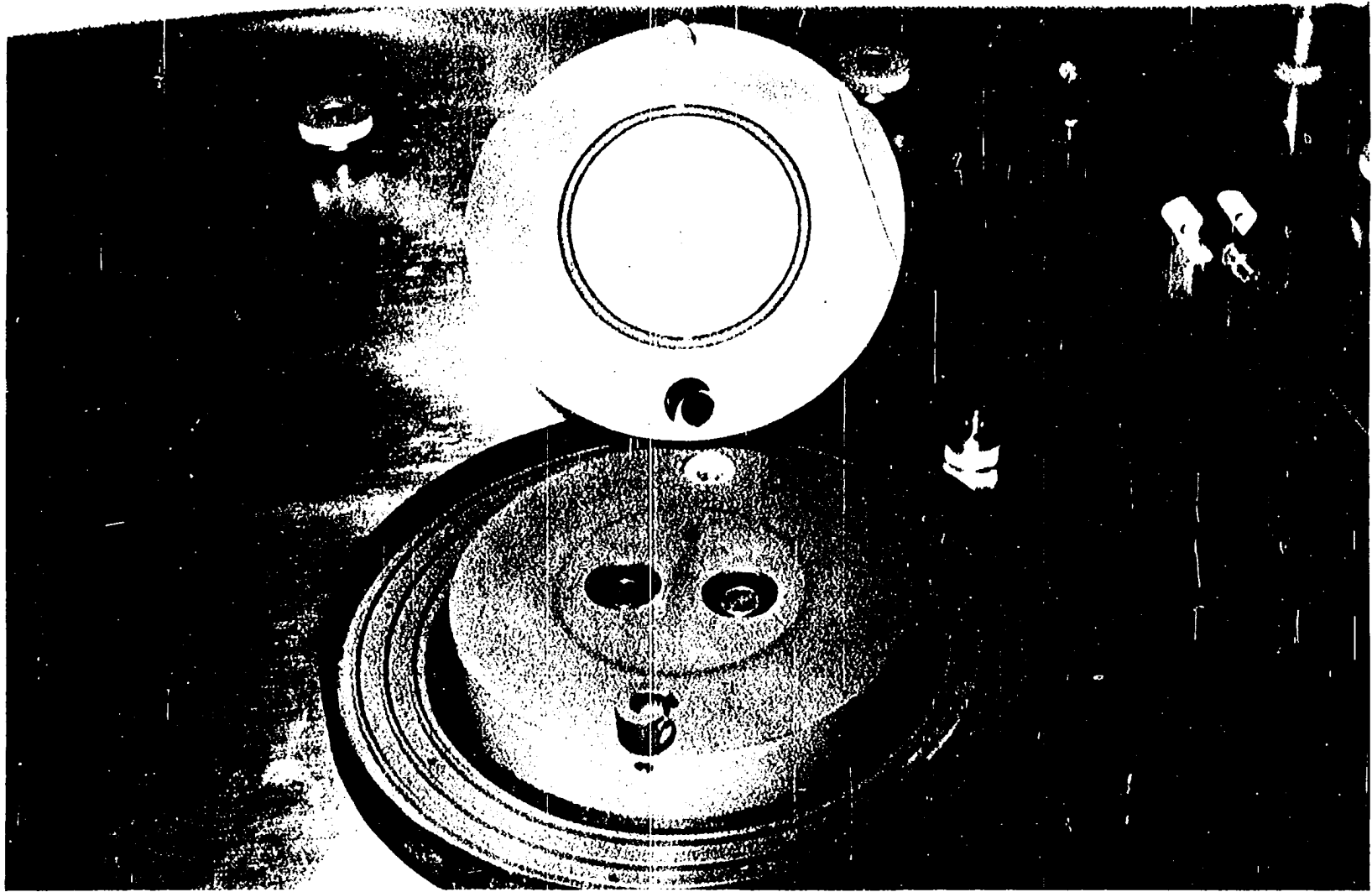


Figure III-8. DSC-2 Sample Holder Assembly.

TABLE III-3

TRANSITION TEMPERATURES AND ENERGIES OF DSC  
CALIBRATION STANDARDS

Material	Transition Temperature (°C)	Transition Energy (cal/gm)
Indium	156.6	6.8
Tin	231.88	14.45
Lead	327.47	5.5
Zinc	419.47	25.9
K <sub>2</sub> SO <sub>4</sub>	585.0±0.5	7.95
K <sub>2</sub> CrO <sub>4</sub>	670.0±0.5	8.50

When a material undergoes a transition in the DSC-2, a peak in the differential energy is recorded. The area under this peak represents the energy of transition (endothermic or exothermic). Therefore, the energy calibration is done by measuring the area under the transition peak of a material of known energy of transition from which the instrument constant,  $C$ , is computed by

$$C = \frac{\Delta H_f W_s S}{R A_s} \quad (\text{III-1})$$

where  $\Delta H_f$  = the heat of transition of the standard (mcal/gm)

$W_s$  = the weight of standard (mg)

$S$  = chart speed (in/sec)

$R$  = range control setting divided by chart span in  
inches (mcal/sec-in)

$A_s$  = area under transition peak of the standard (in<sup>2</sup>)

The indicated range times C then equals the actual range. Throughout this study the value of C was checked on indium three times and on water once. The results of these calibrations are shown in Table III-4.

TABLE III-4  
CALIBRATION OF DSC HEAT OF TRANSITION

Material	H <sub>f</sub> (cal/gm)	W <sub>s</sub> (mg)	R (mcal/sec-in)	S (in/sec)	A <sub>s</sub> (in <sup>2</sup> )	C
Indium	6.8	5.62	0.508	0.0984	7.575	0.977
Indium	6.8	5.62	0.508	0.0984	7.459	0.992
Indium	6.8	5.62	1.016	0.1333	4.864	1.031
Water	79.71	3.34	2.032	0.1333	17.831	0.980

Since the values of C are all near 1, no adjustments were made. However, the transition energies of samples are calculated using the value of C in

$$H_t = \frac{C R A_{\text{sam}}}{W_{\text{sam}} S_{\text{sam}}} \quad (\text{III-2})$$

where  $H_t$  = energy of transition of sample (mcal/mg)  
 $A_{\text{sam}}$  = area under the transition curve of the sample  
(in<sup>2</sup>)  
 $W_{\text{sam}}$  = weight of sample (mg)  
 $S_{\text{sam}}$  = chart speed of sample run (in/sec)

The calibration of the DSC-2 for ordinate displacement is accomplished with a standard material of known specific heat (Al<sub>2</sub>O<sub>3</sub>). Before calibrating the ordinate, the baseline

must be optimized for flatness. The baseline is determined by making a scan over the temperature range with both sample and reference pans empty. This baseline accounts for any differences due to the sample holders and the pans themselves. The following procedure is used to calibrate the DSC for ordinate displacement:

1. A weighed sample of  $\text{Al}_2\text{O}_3$  was placed in a gold sample pan and covered with a gold sample pan lid.
2. The gold sample pan was placed in the left sample holder and a gold reference pan was placed in the right sample holder.
3. The range, purge gas rate, heating rate, and zero were left at the same settings as those of the optimized baseline.
4. After placing platinum holder covers over the sample holders and closing the cover, the pans were allowed to come to equilibrium at the lower temperature limit.
5. The sample holders were then heated to the upper temperature limit at a programmed rate.
6. At a particular temperature, a calibration constant,  $K_d$ , can be computed from

$$K_d = \frac{W_{st} C_{pst}}{D_{st}} \quad (\text{III-3})$$

where  $W_{st}$  = weight of standard (mg)  
 $C_{pst}$  = specific heat of standard (mcal/mg-°C)  
 $D_{st}$  = displacement of calibration scan from  
 baseline scan (mm)

In Equation III-3 the values for  $C_{p_{st}}$  and  $D_{st}$  need to be chosen at the same temperature. The values of specific heat of the  $Al_2O_3$  standard material are shown in Figure III-9. At a heating rate of  $160^\circ C/min$  and a range setting of 20 mcal/sec, five determinations of  $K_d$  averaged  $0.03135$  mcal/mm- $^\circ C$ . This corresponds to an actual range of 20.9 mcal/sec. At  $40^\circ C/min$  the value of  $K_d$  was  $0.06672$  mcal/mm- $^\circ C$  which corresponds to a range of 11.0 mcal/sec for a setting of 10.0 mcal/sec.

Having calculated  $K_d$ , the specific heat of a sample can be measured by repeating the calibration procedure with a sample in place of the standard material. The specific heat of the sample can be computed from

$$C_{p_{sam}} = \frac{K_d D_{sam}}{W_{sam}}$$

where  $D_{sam}$  = displacement of sample scan from baseline scan (mm)

$W_{sam}$  = weight of sample (mg)

$C_{psam}$  = specific heat of sample (cal/gm- $^\circ C$ )

In this study, after running a baseline and a sample run, a run was made on the char only without disturbing the sample pan between the sample and char run to determine if excessive baseline drift had occurred during the sample run. Previous investigators have reported baseline drift, which has been assumed to be due primarily to changes in the radiative characteristics of the sample pans and covers. These

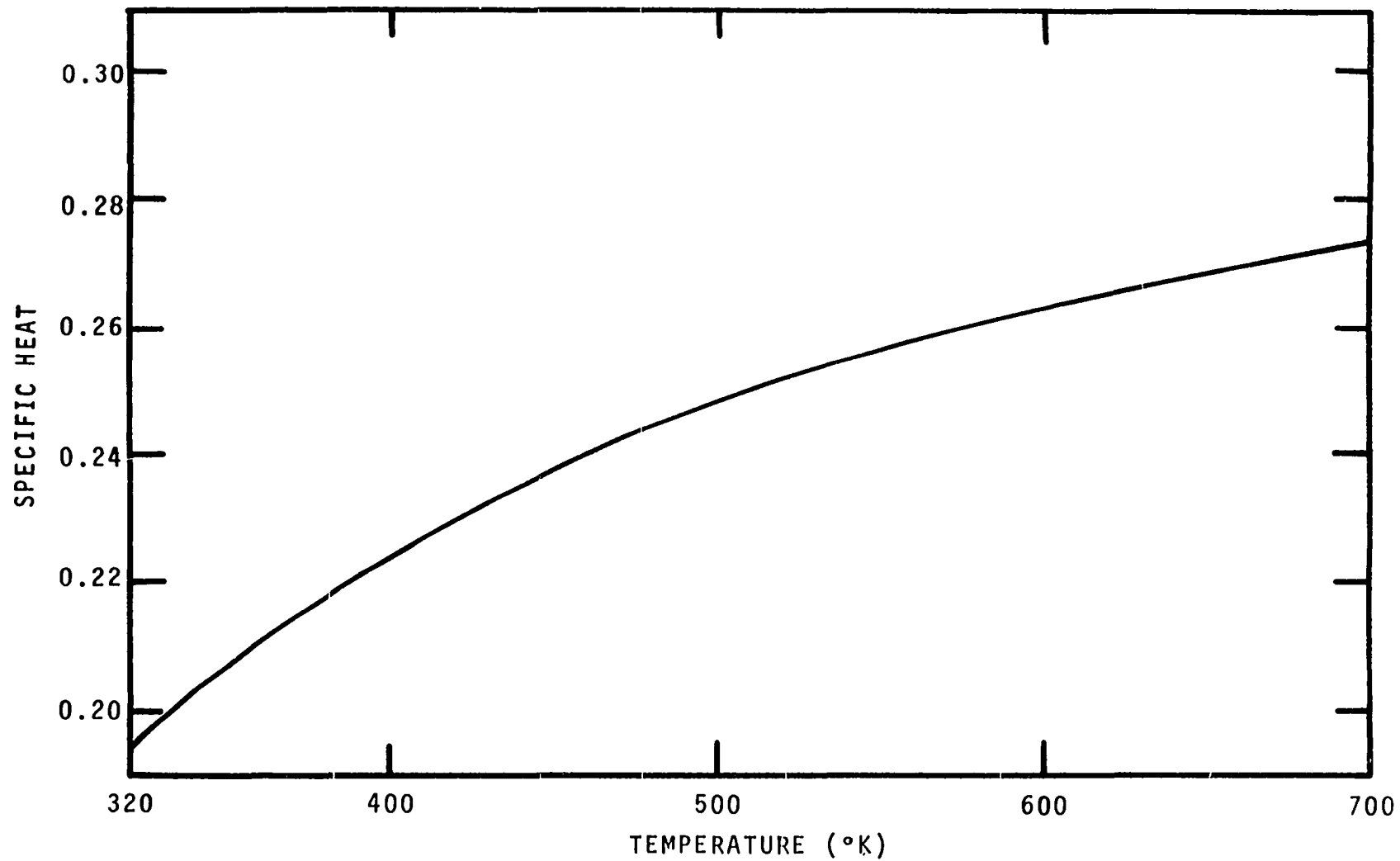


Figure III-9. Specific Heat Curve for Sapphire (12).

changes occur if pyrolysis products condense on the sample pan and holder cover. To combat the change in the radiation characteristics of the sample holder covers, Duvvuri (7) painted the sample holder covers black. This eliminated the large radiation changes due to condensation of pyrolysis products on the covers. However, in this study the covers were not painted since the painted covers resulted in a more curved baseline. Furthermore, the paint had a tendency to come off the covers gradually. With the unpainted covers the pans and covers had to be "conditioned" every one or two sample runs. "Conditioning" consists of heating to 1000°K and introducing air into the head. This procedure burned off any condensed pyrolysis products.

Initially, attempts to optimize the baseline resulted in a straight line which angled across the recorder paper leaving little or no space on the recorder paper for the results of the sample run. Since there was inadequate adjustment in the slope control of the DSC-2, a Brooks Flow Controller, Model 8743, was put into the nitrogen purge line to the reference cell. Adjustment of the flow controller leveled the baseline while maintaining its straightness.

## CHAPTER IV

### RESULTS AND DISCUSSION

This study can be divided into the investigation of the heating rate dependency on the pyrolysis of plant components using the model of Duvvuri (7) and the analysis of freeze-dried plant samples.

#### The Heating Rate Dependency of Cellulose and Punky Wood Kinetics

In a previous study, Duvvuri (7) obtained Thermogravimetric data at 10, 20, 40, 80, and 160°C/min on cellulose and a biologically degraded form of Douglas fir snags known as punky wood. This punky wood consists primarily of lignin which is one of the chief components of plants. Using Duvvuri's (7) data, the reaction kinetics were studied at individual heating rates. Again, the model proposed by Goldfarb (13) was employed.

$$-\frac{dW}{dt} = A e^{-E/RT} F(W) \quad (\text{IV-1})$$

where  $W = (w - w_f)/(w_o - w_f)$  = weight fraction (dimensionless)

$t$  = time (min)

$A$  = pre-exponential factor ( $\text{min}^{-1}$ )

E = activation energy (cal/gm)

T = absolute temperature (°K)

F(W) = function of W

w = weight at time t (mg)

w<sub>f</sub> = final weight of sample (mg)

w<sub>o</sub> = initial weight of sample (mg)

R = gas constant (cal/mole-°K)

It is assumed that F(W) has the form

$$F(W) = W^n \quad (\text{IV-2})$$

where n = order of reaction. Substituting for F(W) and for W, Equation IV-1 becomes

$$-\frac{1}{w_o - w_f} \frac{dw}{dt} = Ae^{-E/RT} \left[ \frac{w - w_f}{w_o - w_f} \right]^n \quad (\text{IV-3})$$

Equation IV-3 is linearized by taking the logarithm of the equation to obtain

$$\log \left[ -\frac{1}{w_o - w_f} \frac{dw}{dt} \right] = \log A - \frac{E}{2.303RT} + n \log \left[ \frac{w - w_f}{w_o - w_f} \right] \quad (\text{IV-4})$$

Equation IV-4 is of the form

$$y = B + Cx + Dz \quad (\text{IV-5})$$

where  $y = \log [-1/(w_o - w_f) \cdot dw/dt]$

$x = 1/2.303RT$

$z = \log [(w - w_f)/(w_o - w_f)]$

$B = \log A$

$$C = -E$$

$$D = n$$

The error at each experimental point is given by

$$R_i = Y_i - Y_{\text{cal}}(x_i, z_i) \quad (\text{IV-6})$$

where  $R_i$  = error at point  $i$

$Y_i$  = experimental value of  $y$  at point  $i$

$Y_{\text{cal}}(x_i, z_i)$  = calculated value of  $y$  using Equation IV-5

The sum of the square of the error at each point is given by

$$S = \sum_{i=1}^N R_i^2 = \sum_{i=1}^N [Y_i - Y_{\text{cal}}(x_i, z_i)]^2 \quad (\text{IV-7})$$

where  $S$  = sum of the square of errors

$N$  = number of data points

Equation IV-7 can be written as

$$S = \sum_{i=1}^N [Y_i - (B + Cx_i + Dz_i)]^2 \quad (\text{IV-8})$$

The values of  $B$ ,  $C$ , and  $D$  which result in a minimum of  $S$  are specified by setting the partial derivative of  $S$  with respect to  $B$ ,  $C$ , and  $D$  to zero, giving three equations in three unknowns,  $B$ ,  $C$ , and  $D$ :

$$BN + C \sum_{i=1}^N x_i + D \sum_{i=1}^N z_i = \sum_{i=1}^N Y_i$$

$$B \sum_{i=1}^N x_i + C \sum_{i=1}^N (x_i)^2 + D \sum_{i=1}^N x_i z_i = \sum_{i=1}^N x_i Y_i$$

$$B \sum_{i=1}^N z_i + C \sum_{i=1}^N x_i z_i + D \sum_{i=1}^N (z_i)^2 = \sum_{i=1}^N Y_i z_i$$

Using a Gauss-Jordan numerical technique, the equations are solved for B, C, and D which correspond to  $\log A$ ,  $-E$ , and  $n$ , respectively. The results of the least-squares determination of A, E, and  $n$  for cellulose and punky wood are presented in Tables IV-1 and IV-2 for individual heating rates and for all heating rates considered collectively. The overall values of the kinetic parameters for cellulose are slightly different from those of Duvvuri (7). One of Duvvuri's (7) fifteen data sets for cellulose decomposition seemed to have a mistake in six of the points. Therefore, that entire set was eliminated from the data and the overall kinetic parameters were calculated with fourteen sets. The elimination of the fifteenth set resulted in slightly different overall kinetic parameters.

In both the cellulose and punky wood data, the overall parameters lie outside the range of values for the individual heating rates. Although this result seems unusual, the combination of the pre-exponential factor, activation energy, and order of reaction in Equation IV-3 is the determining consideration.

The results for cellulose and punky wood are plotted in Figures IV-1 and IV-2, respectively. The lines described by these points are given by equations of the following form:

TABLE IV-1  
KINETIC PARAMETERS FOR CELLULOSE

Heating Rate (°C/min)	Log A	E	n
10	24.4	72200.	1.39
20	21.0	63000.	1.22
40	19.7	59800.	1.30
80	16.9	52300.	1.34
160	15.6	47300.	1.16
Overall	11.1	33900.	0.76

TABLE IV-2  
KINETIC PARAMETERS FOR PUNKY WOOD

Heating Rate (°C/min)	Log A	E	n
10	3.40	11500.	1.85
20	3.22	10700.	1.98
40	3.66	11500.	2.06
80	5.38	15100.	2.71
160	6.61	18000.	2.83
Overall	7.49	21300.	3.20

TABLE IV-3  
PARAMETERS FOR EQUATION IV-10

Material	Kinetic Parameter	m	b
Cellulose	log A	-0.160	1.54
	E	-0.149	5.00
	n	-0.037	0.166
Punky Wood	log A	0.266	0.205
	E	0.178	3.830
	n	0.169	0.081

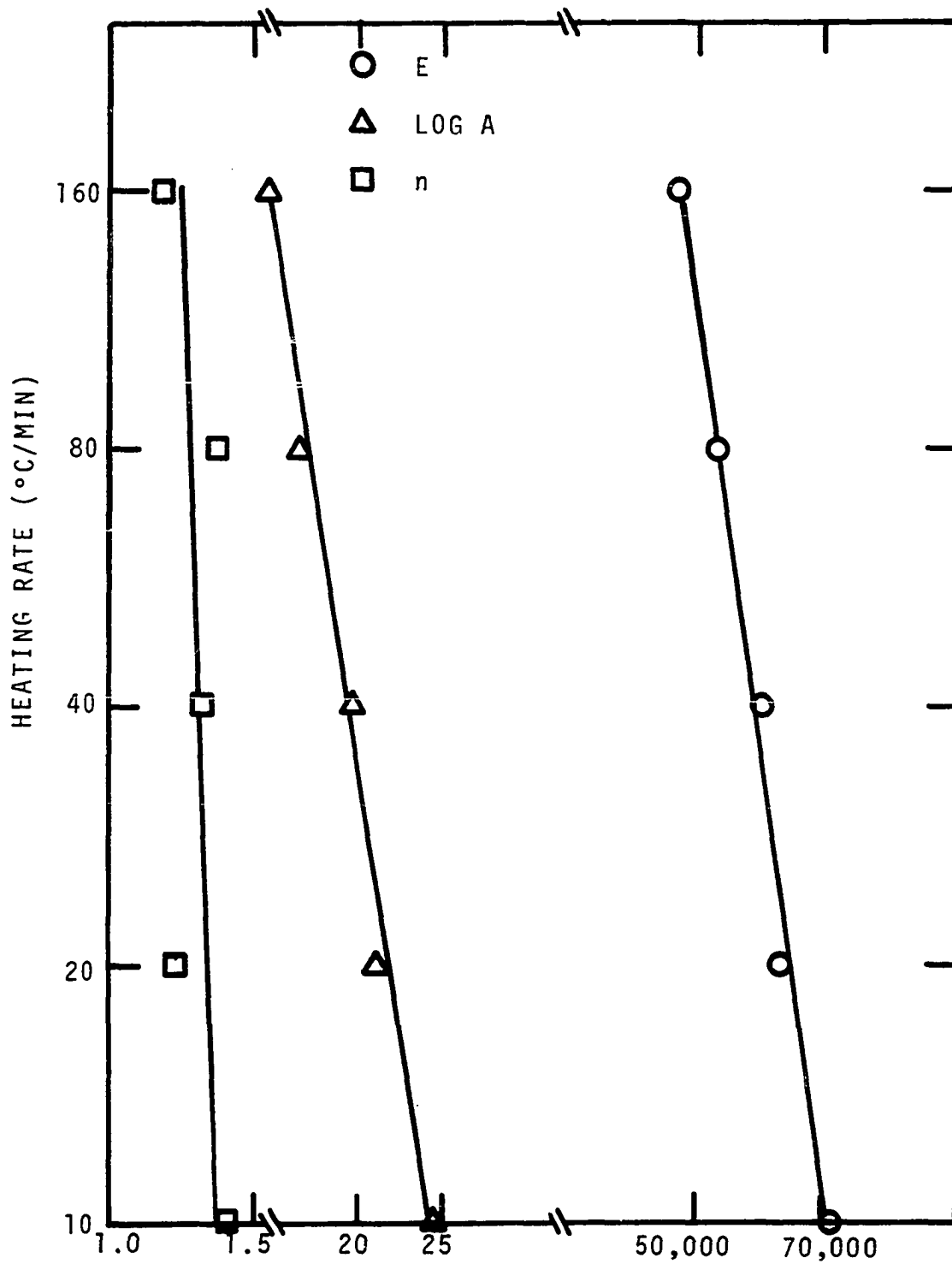


Figure IV-1. Effect of Heating Rate on Kinetic Parameters for Cellulose.

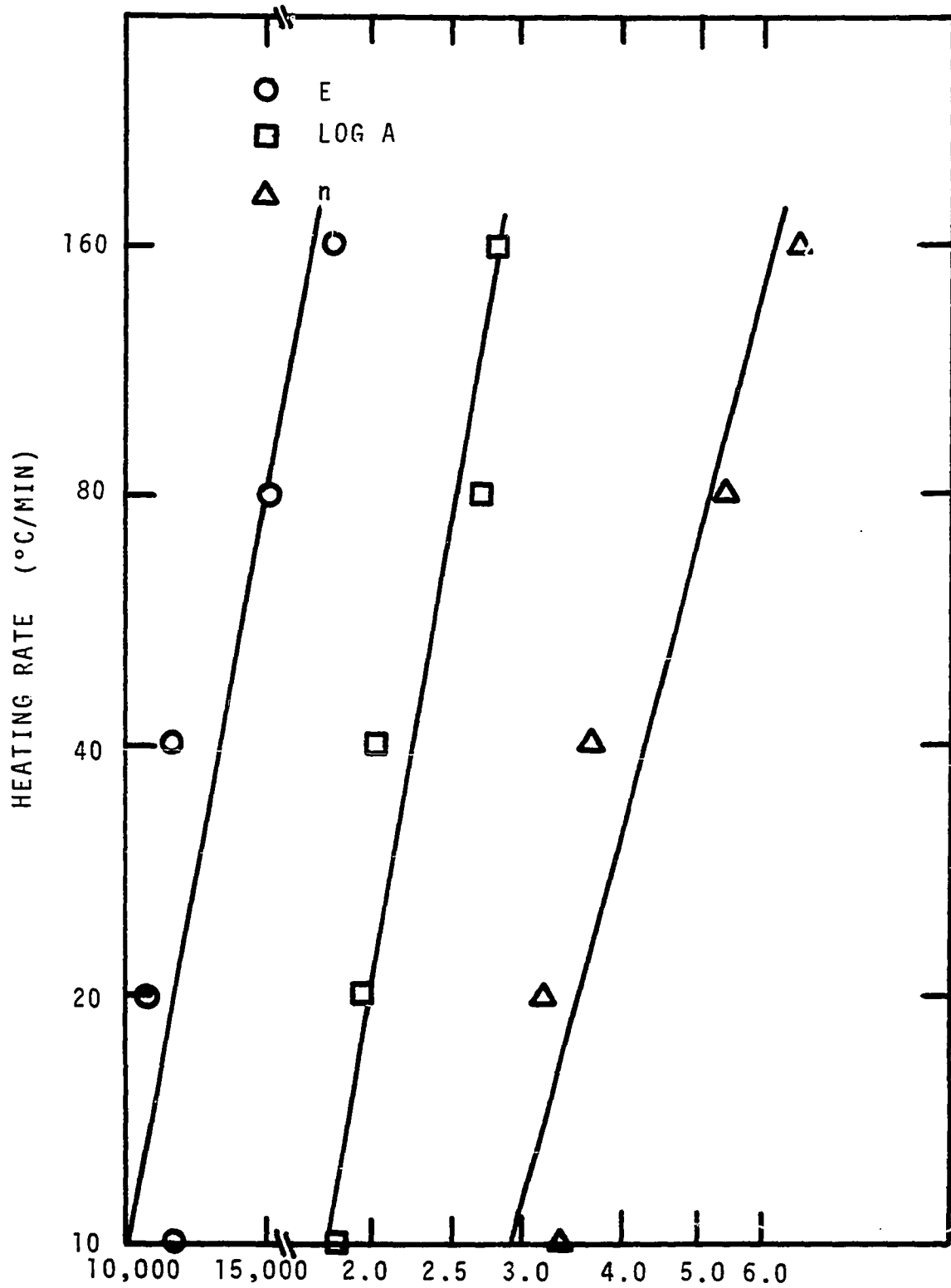


Figure IV-2. Effect of Heating Rate on Kinetic Parameters of Punky Wood.

$$\log (\text{kinetic parameter}) = m \log (\text{heating rate}) + b \quad (\text{IV-10})$$

Table IV-3 gives the values for the slope,  $m$ , and the intercept,  $b$ .

Figures IV-1 and IV-2 indicate that heating rate has a definite effect on the values of the kinetic parameters for cellulose and punky wood. Furthermore, this effect can be expressed by a form of Equation IV-10.

#### Analysis of Living Plant Samples

The weight loss and rate of weight loss of the freeze-dried samples provided by the USDA Forest Service were measured experimentally in the Perkin-Elmer TGS-1 thermobalance at 10, 40, and 160°C/min. Figure IV-3 shows the weight loss results for freeze-dried Ponderosa pine needles, which are typical of the other plant samples. As found by other investigators (4, 7, 14), the higher heating rates tend to shift the weight loss curves to higher temperatures. Weight loss results for freeze-dried chamise foliage, manzanita leaves, Douglas fir needles, aspen leaves, and lodgepole pine needles are shown in Appendix E.

Figure IV-4 shows the rate of weight loss for freeze-dried Ponderosa pine needles at 10, 40, and 160°C/min. The rate of weight loss is expressed as  $-dW/dT \times 10^3$ ; that is, the derivative of the fractional weight loss with respect to temperature. Graphing the results in this manner provides an easy check on the validity of the results since the area under

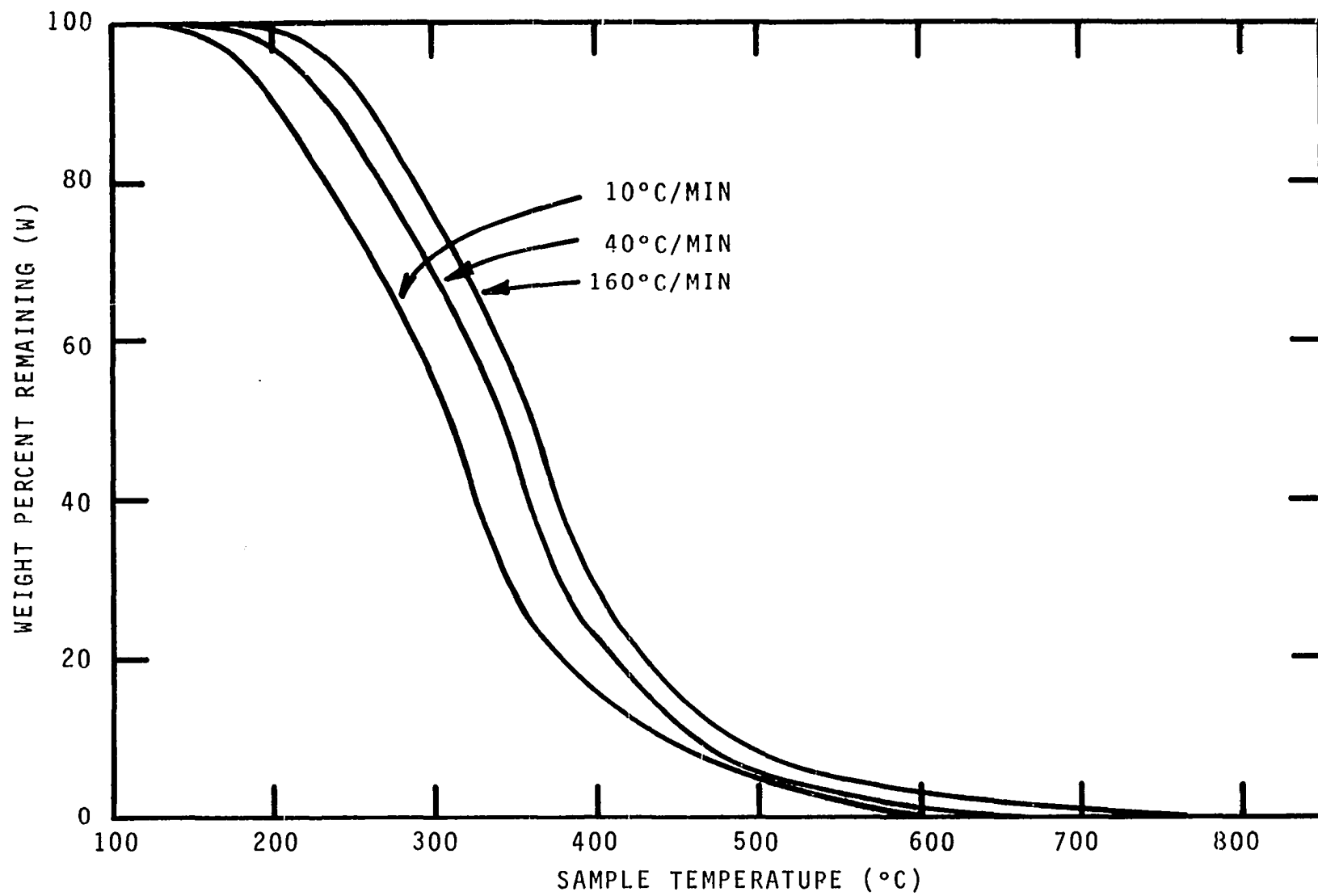


Figure IV-3. Weight Loss of Freeze-Dried Ponderosa Pine Needles.

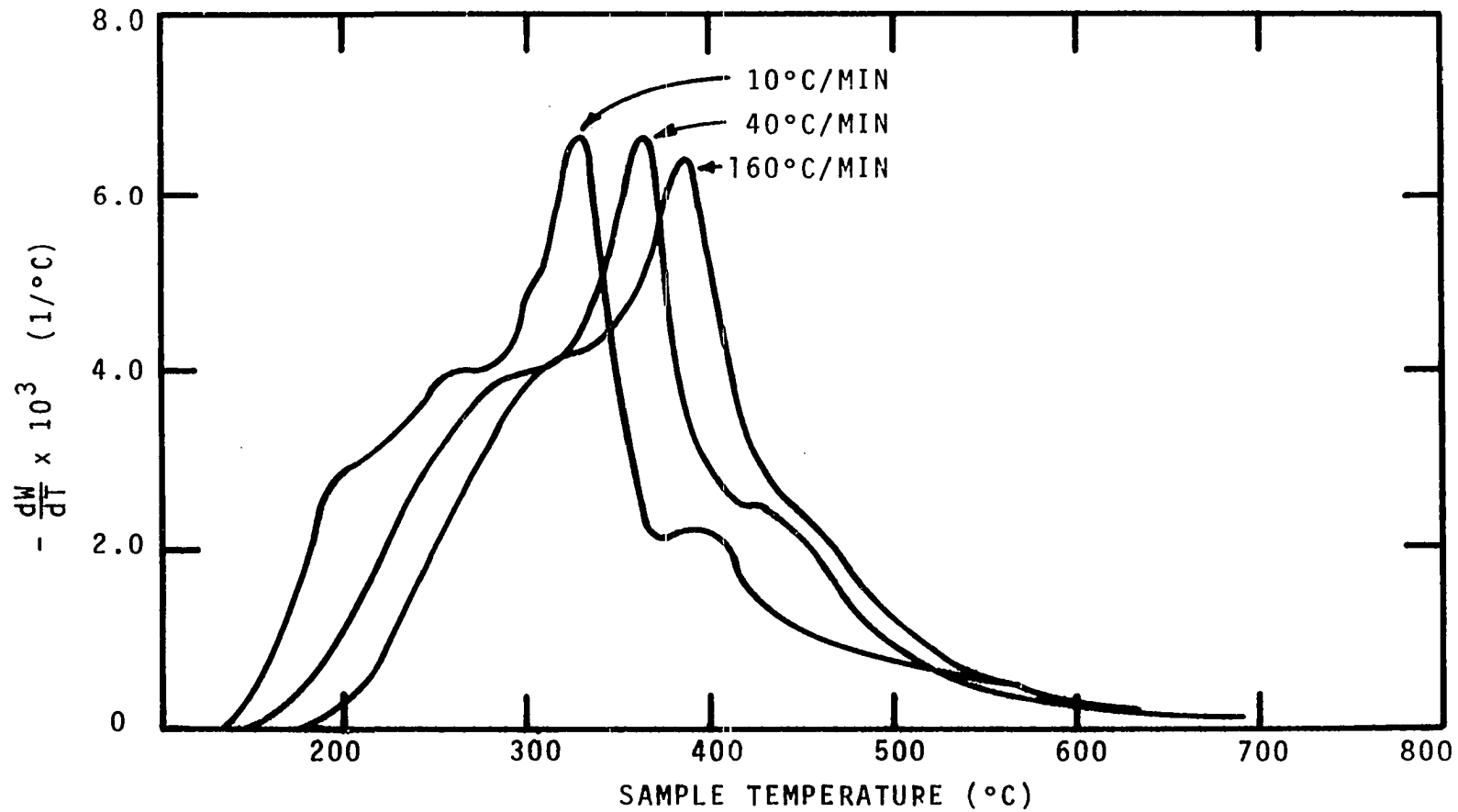


Figure IV-4. Rate of Weight Loss of Freeze-Dried Ponderosa Pine Needles.

each derivative curve should approximately equal one. As in the weight loss curves, as the heating rate increases the rate of weight loss curves are shifted to a higher temperature. Furthermore, as heating rate increases, the rate of weight loss curves appear to be "smoothed out." That is, the higher heating rates result in less definition in the rate of weight loss curve.

It was initially hoped that the weight loss results could be modeled with an equation similar to Equation II-24; however, the large percentage of extractives in the freeze-dried samples would require additional data which is not available at this time. Furthermore, the use of cellulose kinetic parameters to model the holocellulose decomposition does not appear to be justifiable based on the experimental results shown in Figure IV-5. The holocellulose sample used was from Ponderosa pine needles. The use of punky wood kinetic parameters to model the decomposition of lignin is another source of error. Rate of weight loss results for freeze-dried chamise foliage, manzanita leaves, Douglas fir needles, aspen leaves, and lodgepole pine needles are shown in Appendix F.

Energy measurements of the freeze-dried samples were made on the DSC-2 at 40 and 160°C/min. The differential energy of freeze-dried Ponderosa pine needles as a function of temperature is shown in Figures IV-6 and IV-7, for heating rates of 40 and 160°C/min, respectively. The differential

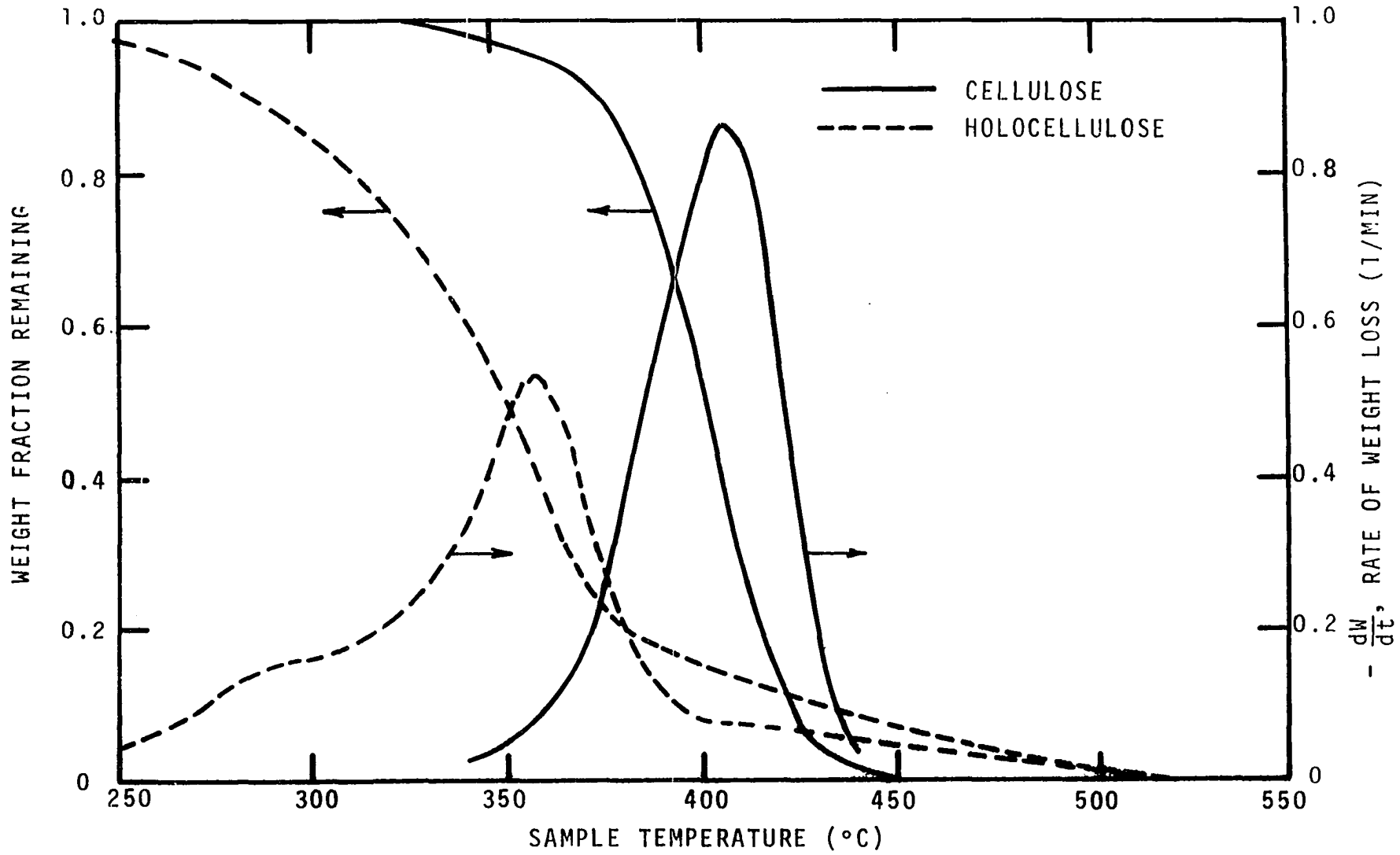


Figure IV-5. Weight Loss and Rate of Weight Loss for Cellulose and Holocellulose. Heating Rate, 40°C/min.

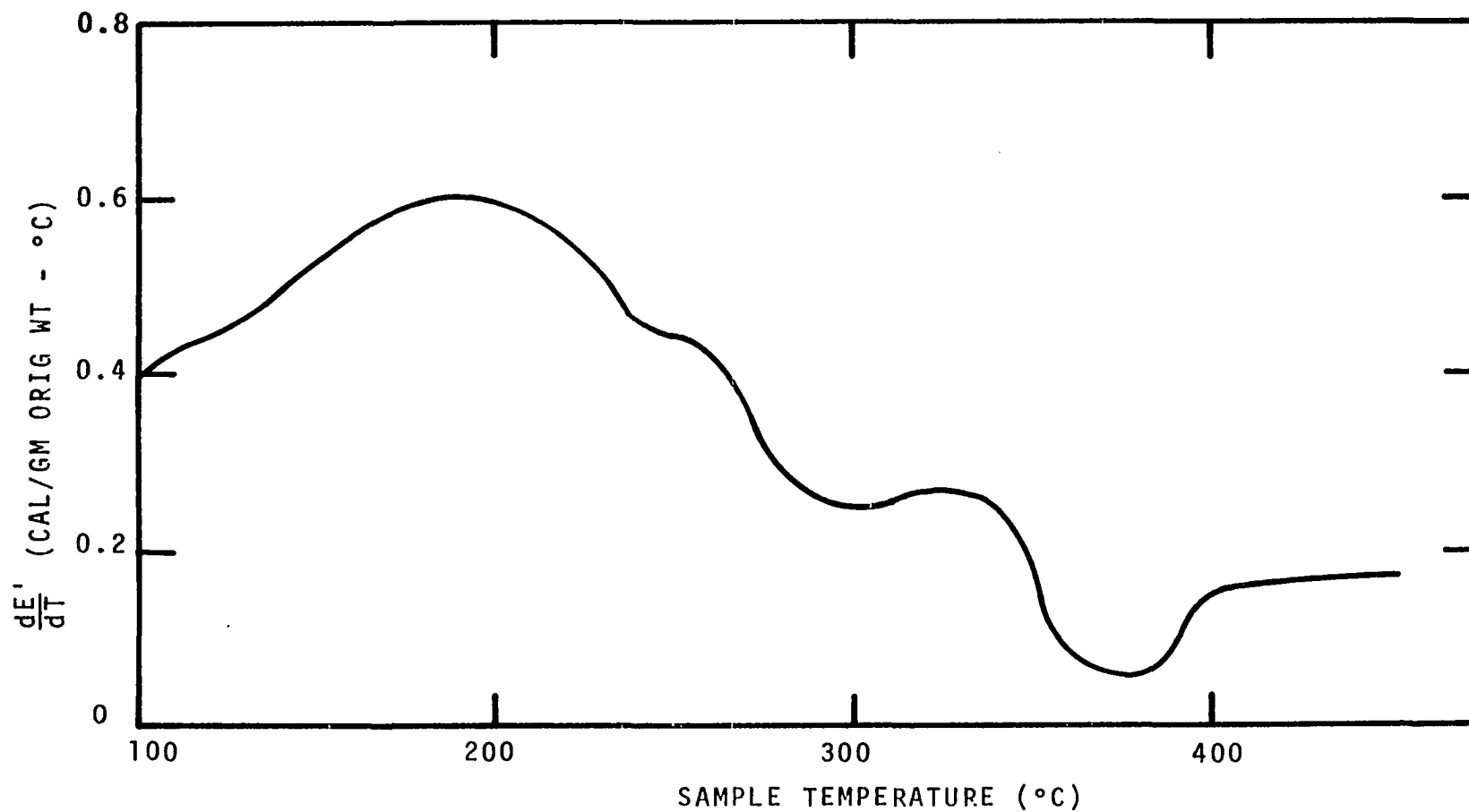


Figure IV-6. Differential Energy of Freeze-Dried Ponderosa Pine Needles. Heating Rate, 40°C/min.

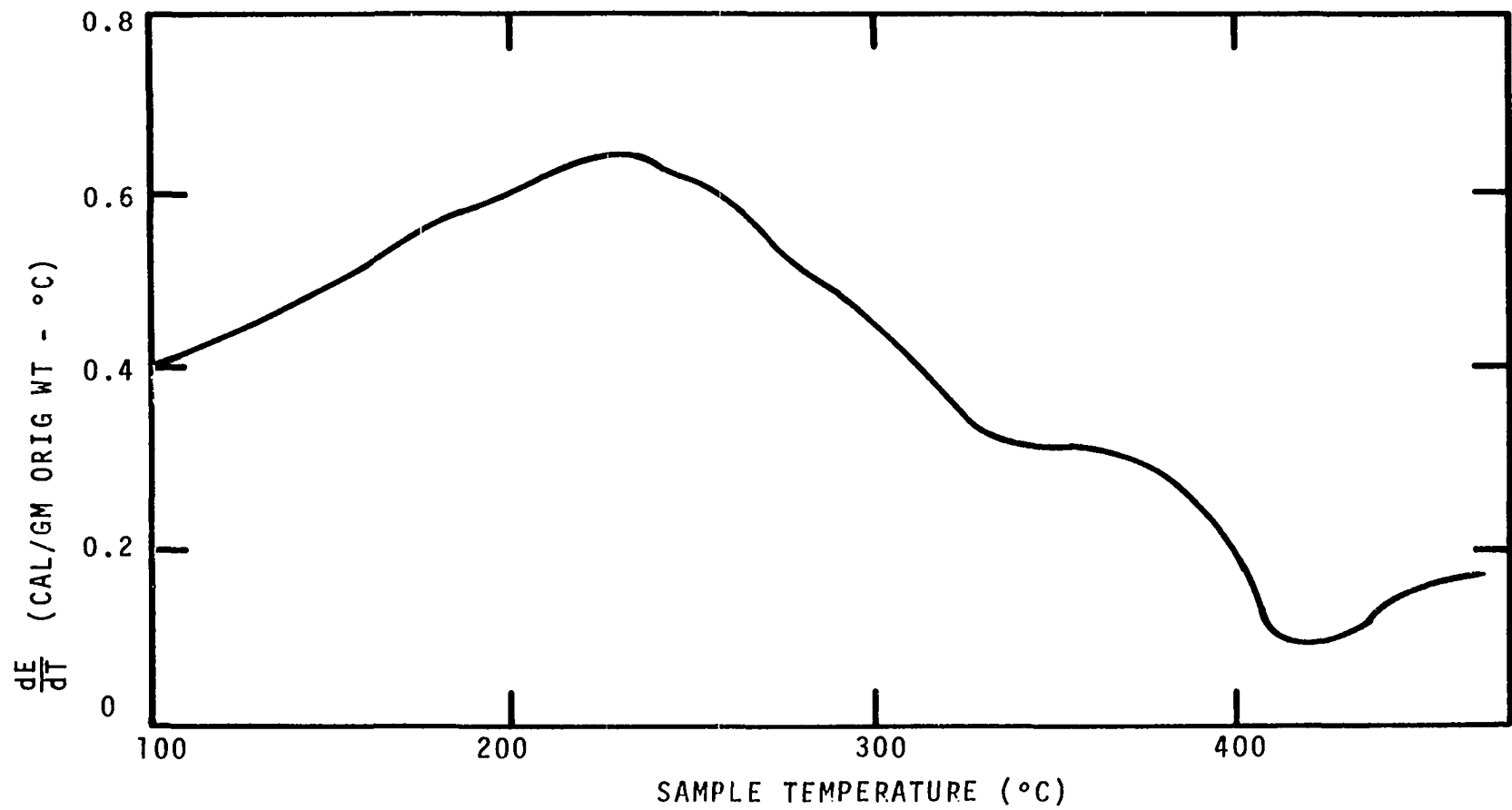


Figure IV-7. Differential Energy of Freeze-Dried Ponderosa Pine Needles. Heating Rate, 160°C/min.

energy,  $dE'/dT$ , is graphed on an original weight basis, thereby facilitating the calculations and yet showing the desired information. As in the weight loss results, the higher heating rate shifts the differential energy curve to a higher temperature. Furthermore, as in the weight loss measurements, the higher heating rate results in less definition in the differential energy measurements.

The value of  $dE'/dT$  at  $100^{\circ}\text{C}$  gives the value of the specific heat which is approximately  $0.40 \text{ cal/gm-}^{\circ}\text{C}$ . This is comparable to the value of  $0.44 \text{ cal/gm-}^{\circ}\text{C}$  for dead Ponderosa pine needles found by Duvvuri (7). The specific heats of all the freeze-dried plant samples varied from  $0.38 \text{ cal/gm-}^{\circ}\text{C}$  to  $0.42 \text{ cal/gm-}^{\circ}\text{C}$ . Havens (14) and Brown (4) reported similar values for pine and oak wood samples.

The overall shape of the differential energy curves for the freeze-dried samples is considerably different than those obtained for wood and dead plant samples (4, 7, 14). This difference is felt to be due to increased amount of extractives in the freeze-dried plant samples. The Northern Forest Fire Laboratory reports freeze-dried Ponderosa pine needles are 37.96 percent extractives when extracted with a 2 to 1 mixture of benzene and ethanol (41). Furthermore, an energy measurement of the extractives of freeze-dried Ponderosa pine needles reveals a large exothermic transition from approximately  $175^{\circ}\text{C}$  to  $275^{\circ}\text{C}$  as shown in Figure IV-8. A similar exotherm has been shown on all measurements of

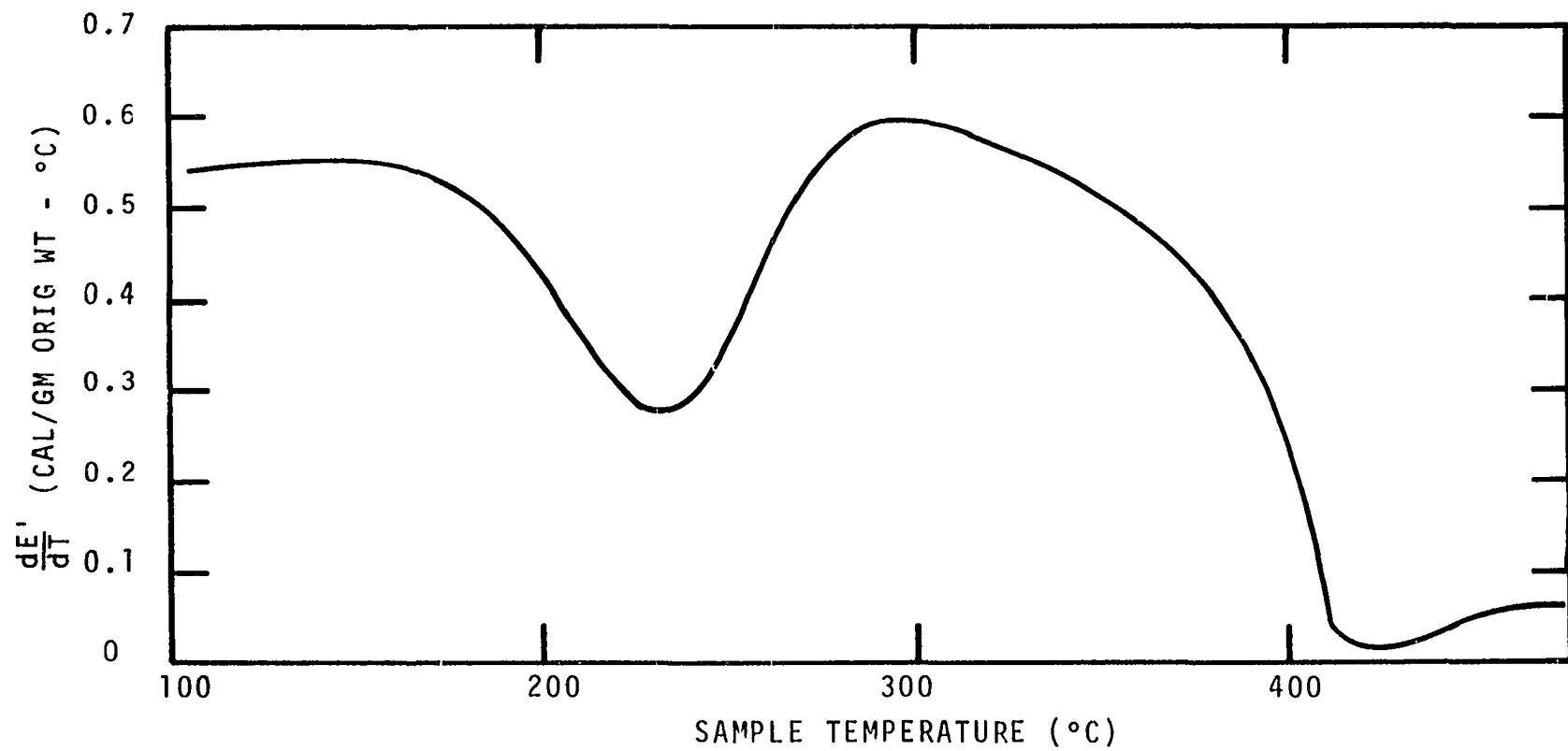


Figure IV-8. Differential Energy of Living Ponderosa Pine Needle Extractive. Heating Rate, 160°C/min.

freeze-dried plant extractives while only endothermic transitions have been found on extractives of dead plant samples. The freeze-dried samples apparently have retained a plant constituent not found in the dead plant samples. Differential energy curves of the remaining freeze-dried plant samples are shown in Appendix G.

Figures IV-9 and IV-10 show the total energy curves of living Ponderosa pine needles heating at 40 and 160°C/min, respectively. These curves are obtained by integrating the differential energy curves from 0°C. These measurements assume that the specific heat is essentially constant below 100°C. The values of the total energy are generally lower than those obtained by Duvvuri (7) from dead plant samples. This result is to be expected in light of the large exotherm due to the extractive from the freeze-dried sample. Total energy curves for the other freeze-dried samples are found in Appendix H.

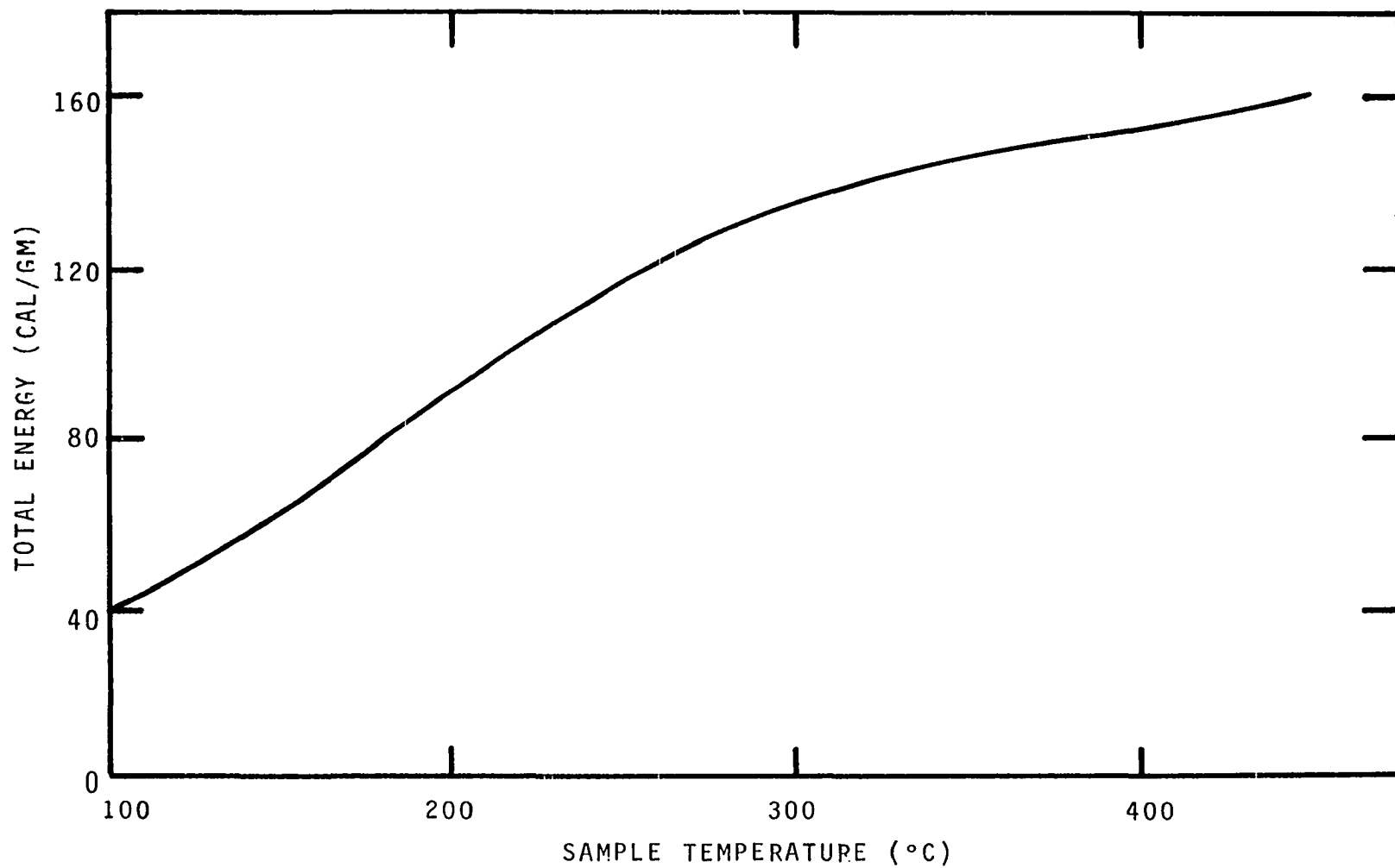


Figure IV-9. Total Energy of Freeze-Dried Ponderosa Pine Needles. Heating Rate, 40°C/min.

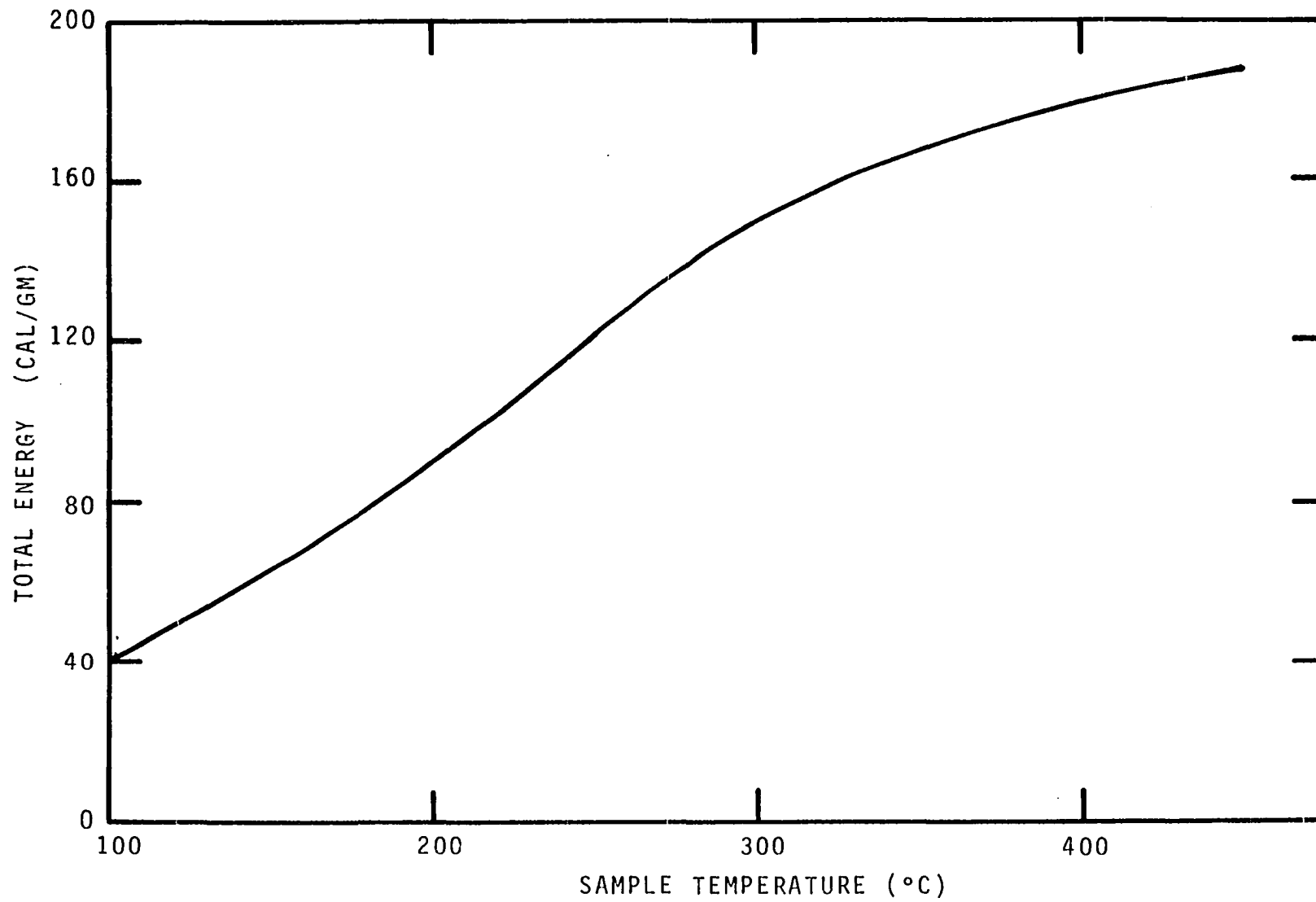


Figure IV-10. Total Energy of Freeze-Dried Ponderosa Pine Needles. Heating Rate, 160°C/min.

## CHAPTER V

### CONCLUSIONS AND SUGGESTIONS FOR FURTHER WORK

As shown in Chapter III of this work, plant samples which have been freeze-dried retain the extractives and other components (except for water) which are lost with dead plant samples. This result is verified by thermogravimetric analysis. Furthermore, initial chemical analysis results indicate the level of extractives to be considerably higher for freeze-dried samples.

Contrary to the conclusion of Duvvuri (7), heating rate does have an effect on the kinetic parameters of cellulose and punky wood in the heating rate range of 10°C/min to 160°C/min. When the kinetic parameters are plotted against heating rate on logarithmic paper, the available data describe a straight line. The results for cellulose are especially good. However, the punky wood may have more deviation since it is not a pure substance and may not be perfectly homogeneous.

Weight loss and rate of weight loss data were obtained for freeze-dried Ponderosa pine needles, Douglas fir needles, lodgepole pine needles, chamise foliage, manzanita leaves, and aspen leaves. In all samples the pyrolysis occurred

primarily between 200°C and 450°C, with the peak rates of pyrolysis occurring between 280°C and 390°C.

Energy measurements were obtained on the freeze-dried samples through the use of a differential scanning calorimeter (DSC). The overall shape of the differential energy curve appears to be changed somewhat by the large amount of extractives which have a large exothermic transition. This exotherm is not found with samples of dead plant extractives. The total energy for all samples varied from 153 cal/gm to 188 cal/gm at 450°C.

There appears to be a need for more work in the following areas:

1. Basic kinetic data for holocellulose and lignin need to be obtained and the decompositions modeled.
2. The decomposition of the various extractives needs to be studied by thermogravimetry and calorimetry.
3. The effect of inorganic components of plants needs to be studied.

## BIBLIOGRAPHY

1. Bamford, C. H.; Crank, J.; and Malan, D. H. "The Combustion of Wood, Part I." Proc. of Cambridge Phil. Soc., 42 (1946): 166-182.
2. Beall, F. C. "Differential Calorimetric Analysis of Wood and Wood Components." Forest Products Laboratory, Madison, Wisconsin, Wood Science and Technology, 5 (1971): 159-175.
3. Broido, A. "Thermogravimetric and Differential Thermal Analysis of Potassium Bicarbonate Contaminated Cellulose." WSCI Paper No. 66-20, 1966 Spring Meeting, Western States Section, The Combustion Institute, Denver Research Institute, April 1966.
4. Brown, L. E. "An Experimental and Analytical Study of Wood Pyrolysis." Ph. D. dissertation, University of Oklahoma, Norman, Oklahoma, 1972.
5. Browne, F. L. "Theories of the Combustion of Wood and Its Control." U.S. Forest Products Laboratory, Report 2136 (1958).
6. \_\_\_\_\_, and Tang, W. K. "Thermogravimetric and Differential Thermal Analysis of Wood and of Wood Treated with Inorganic Salts During Pyrolysis." Fire Research Abstracts and Reviews, 4, 3 (1962): 76-91.
7. Duvvuri, M. S. "The Pyrolysis Energy of Wildland Fuels." Ph.D. dissertation, University of Oklahoma, Norman, Oklahoma, 1974.
8. Frandsen, W. H. "Fire Spread Through Porous Fuels from the Conservation of Energy." Combustion and Flame, 16 (1971): 9-16.
9. Freeman, Eli S., and Carroll, Benjamin. "The Application of Thermoanalytical Techniques to Reaction Kinetics: The Thermogravimetric Evaluation of the Kinetics of the Decomposition of Calcium Oxalate Monohydrate." Journal of Physical Chemistry, 62 (1958): 394-397.

10. Friedman, H. L. "Kinetics of the Thermal Degradation of Char-Forming Plastics from Thermogravimetry. Application to a Phenolic Plastic." J. Polymer Science, C, 6 (1965): 183-195.
11. Garn, Paul D. Thermoanalytical Methods of Investigation. New York: Academic Press, 1965.
12. Ginnings, D. C., and Furukawa, T. "Heat Capacity Standards for the Range 14 to 1200°K." J. Amer. Chem. Soc., 75 (1953): 522-524.
13. Goldfarb, I. J.; McGuchan, R.; and Meeks, A. C. "Kinetic Analysis of Thermogravimetry. Part II. Programmed Temperatures." Air Force Materials Laboratory, Wright-Patterson Air Force Base, Ohio. ARL-TR-68-181, Part 2 (1968).
14. Havens, J. A. "Thermal Decomposition of Wood." Ph.D. dissertation, University of Oklahoma, Norman, Oklahoma, 1969.
15. Havens, J. A., et al. "A Mathematical Model of the Thermal Decomposition of Wood." Combustion Science and Technology, 5 (1972): 91-98.
16. Koch, Peter. "Specific Heat of Oven Dry Spruce Pine Wood and Bark." Wood Science, 1, 4 (1969): 203-214.
17. Kung, H. C., and Kalelkar, Ashok S. "On the Heat of Reaction in Wood Pyrolysis." Combustion and Flame, 20 (1973): 91-103.
18. Lapidus, Leon. Digital Computation for Chemical Engineers. New York: McGraw-Hill Book Company, 1962.
19. Leu, Jin Chian. "Modeling of the Pyrolysis and Ignition of Wood." Ph.D. dissertation, University of Oklahoma, Norman, Oklahoma, 1975.
20. MacLean, J. D. "Thermal Conductivity of Wood." Heating, Piping and Air Conditioning, July 1940, pp. 459-464.
21. McMillin, C. W. "Specific Heat of Overdry Loblolly Pine Wood." Wood Science, 2, 2 (1969): 107-111.
22. McMillin, C. W. "Specific Heat of Some Overdry Chemical Constituents of Loblolly Pine Wood." Wood Science, 3, 1 (1970): 52-53.
23. Mita, I.; Imai, I.; and Kambe, H. "Determination of Heat of Mixing and Heat of Vaporization with a Differential Scanning Calorimeter." Thermochemica Acta, 2 (1971): 337-344.

24. Murty, K. A., and Blackshear, P. L., Jr. "An X-Ray Photographic Study of the Reaction Kinetics of Alpha-Cellulose Decomposition." Pyrodynamics, 4 (1966): 285-298.
25. Perkin-Elmer Corp. "When is a DSC not a DSC and How Does It Work Anyway?" Thermal Analysis Newsletter, 9, 1970.
26. Perkin-Elmer Corp. "New High Performance Differential Scanning Calorimeter Introduced at Pittsburgh Conference 1972." Thermal Analysis Newsletter, 10, 1972.
27. Philpot, C. W. "Mineral Content and Pyrolysis of Selected Plant Materials." Intermountain Forest and Range Experiment Station, Ogden, Utah. USDA Forest Service Research Note INT-84 (1968).
28. Philpot, C. W. "The Effect of Reduced Extractive Content on the Burning Rate of Aspen Leaves." Intermountain Forest and Range Experiment Station, Ogden, Utah. USDA Forest Service Research Note INT-92 (1969).
29. Philpot, C. W. "Influence of Mineral Content on the Pyrolysis of Plant Materials." Forest Science, 16, 4 (1970).
30. Philpot, C. W. "The Pyrolysis Products and Thermal Characteristics of Cottonwood and Its Components." Intermountain Forest and Range Experiment Station, Ogden, Utah. USDA Forest Service Research Paper INT-107 (1971).
31. Philpot, C. W. "The Pyrolytic Effect of Treating Cottonwood with Plant Ash." Intermountain Forest and Range Experiment Station, Ogden, Utah. USDA Forest Service Research Note INT-139 (1971).
32. Ramiah, M. V. "Thermogravimetric and Differential Thermal Analysis of Cellulose, Hemicellulose, and Lignin." J. of Applied Polymer Science, 14 (1970): 1323-1337.
33. Roberts, A. F., and Clough, G. "Thermal Decomposition of Wood in an Inert Atmosphere." Ninth Symposium (International) on Combustion. New York: Academic Press, 1963.
34. Rogers, R. N., and Morris, E. D., Jr. "Determination of Emissivities with a Differential Scanning Calorimeter." Analytical Chemistry, 38, 3 (1966): 410-412.

35. Rothermel, Richard C. "A Mathematical Model for Predicting Fire Spread in Wildland Fuels." Intermountain Forest and Range Experiment Station, Ogden, Utah. USDA Research Paper INT-115 (1972).
36. Sardesai, U. V. "Thermogravimetric Analysis of Cellulose." M.S. Thesis, University of Oklahoma, Norman, Oklahoma, 1973.
37. Stamm, A. J. "Thermal Degradation of Wood and Cellulose." Industrial and Engineering Chemistry, 49 (1956): 413-417.
38. Tang, W. K. "Effect of Inorganic Salts on Pyrolysis of Wood, Alpha-Cellulose, and Lignin." U.S. Forest Service Research Paper FPL 71, January 1967.
39. Tang, W. K., and Eickner, H. W. "Effect of Inorganic Salts on Pyrolysis of Wood, Cellulose, and Lignin Determined by Differential Thermal Analysis." U.S. Forest Service Research Paper FPL-82, January 1968.
40. Tang, W. K., and Neill, W. K. "Effects of Flame Retardants on Pyrolysis and Combustion of Alpha-Cellulose." J. Polymer Science, Part C, 6 (1964): 65-81.
41. Wallace, Walter H., Jr. Private communication, March 21, 1975.
42. Woodard, W. M. "Thermal Decomposition of Synthetic Polymers." Ph.D dissertation, University of Oklahoma, Norman, Oklahoma, 1973.

## APPENDICES

## APPENDIX A

### WEIGHT LOSS AND RATE OF WEIGHT LOSS CURVES

Weight loss and rate of weight loss curves for fresh and freeze-dried samples of holly leaves and spruce needles.

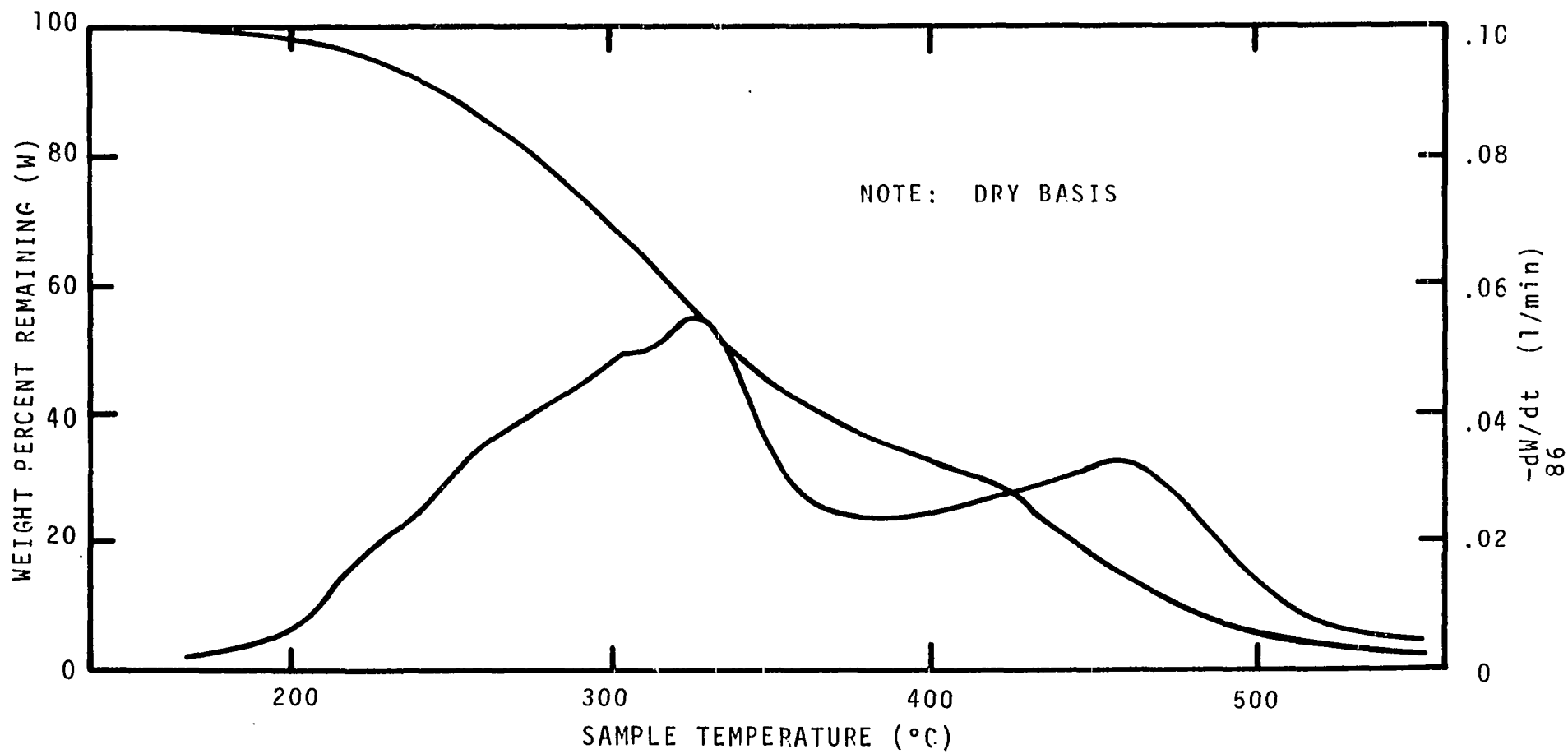


Figure A-1. Weight Loss and Rate of Weight Loss for Fresh Holly Leaves. Heating Rate, 10°C/min.

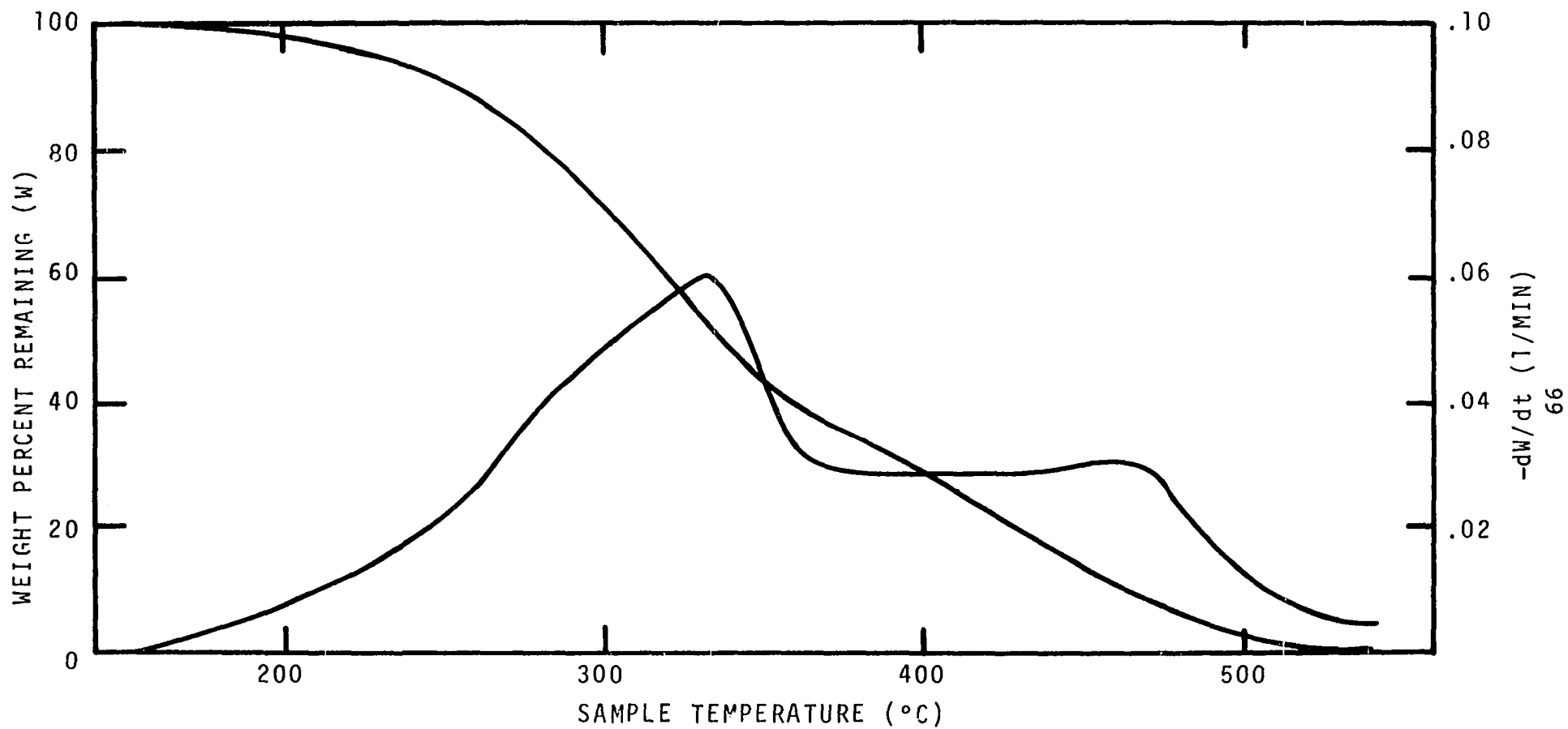


Figure A-2. Weight Loss and Rate of Weight Loss for Freeze-Dried Holly Leaves. Heating Rate, 10°C/min.

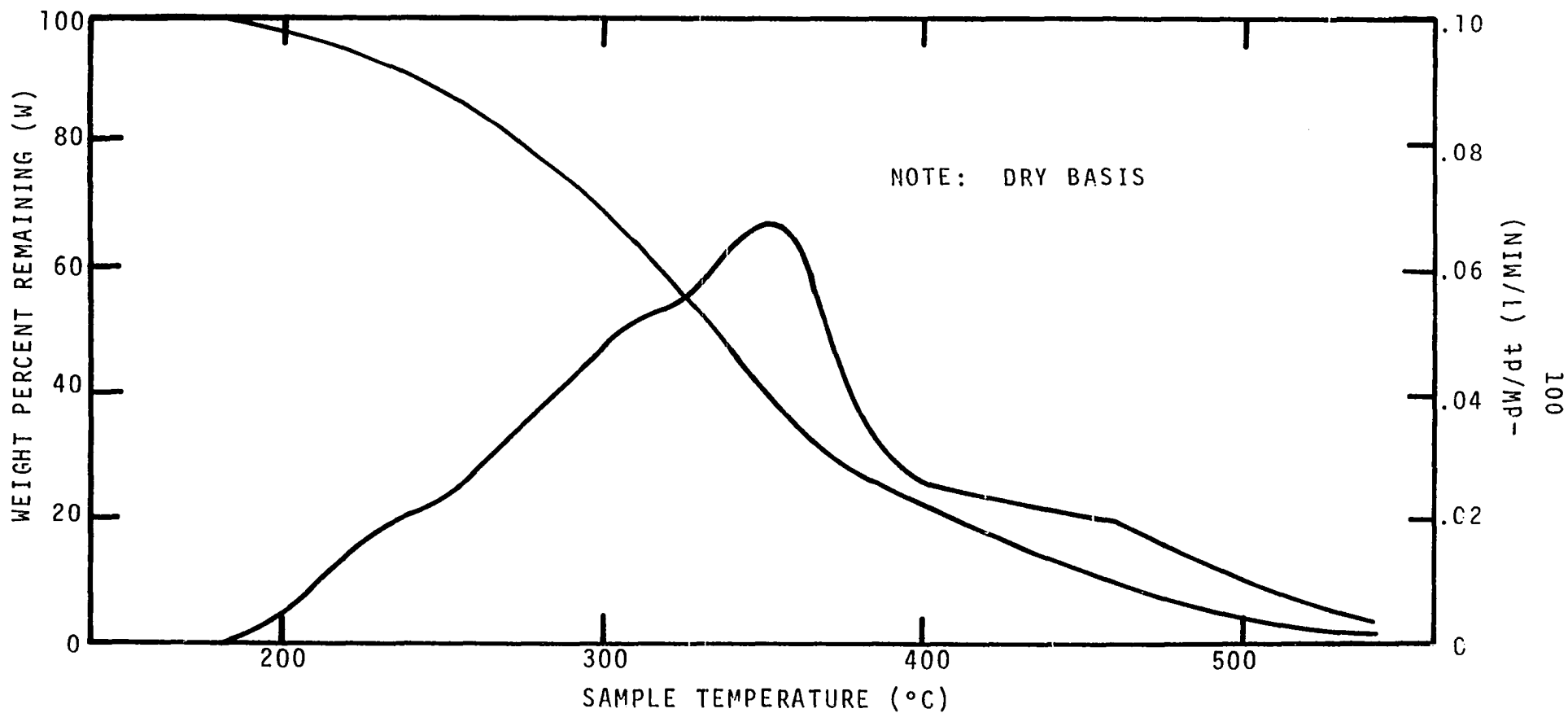


Figure A-3. Weight Loss and Rate of Weight Loss for Fresh Spruce Needles. Heating Rate, 10°C/min.

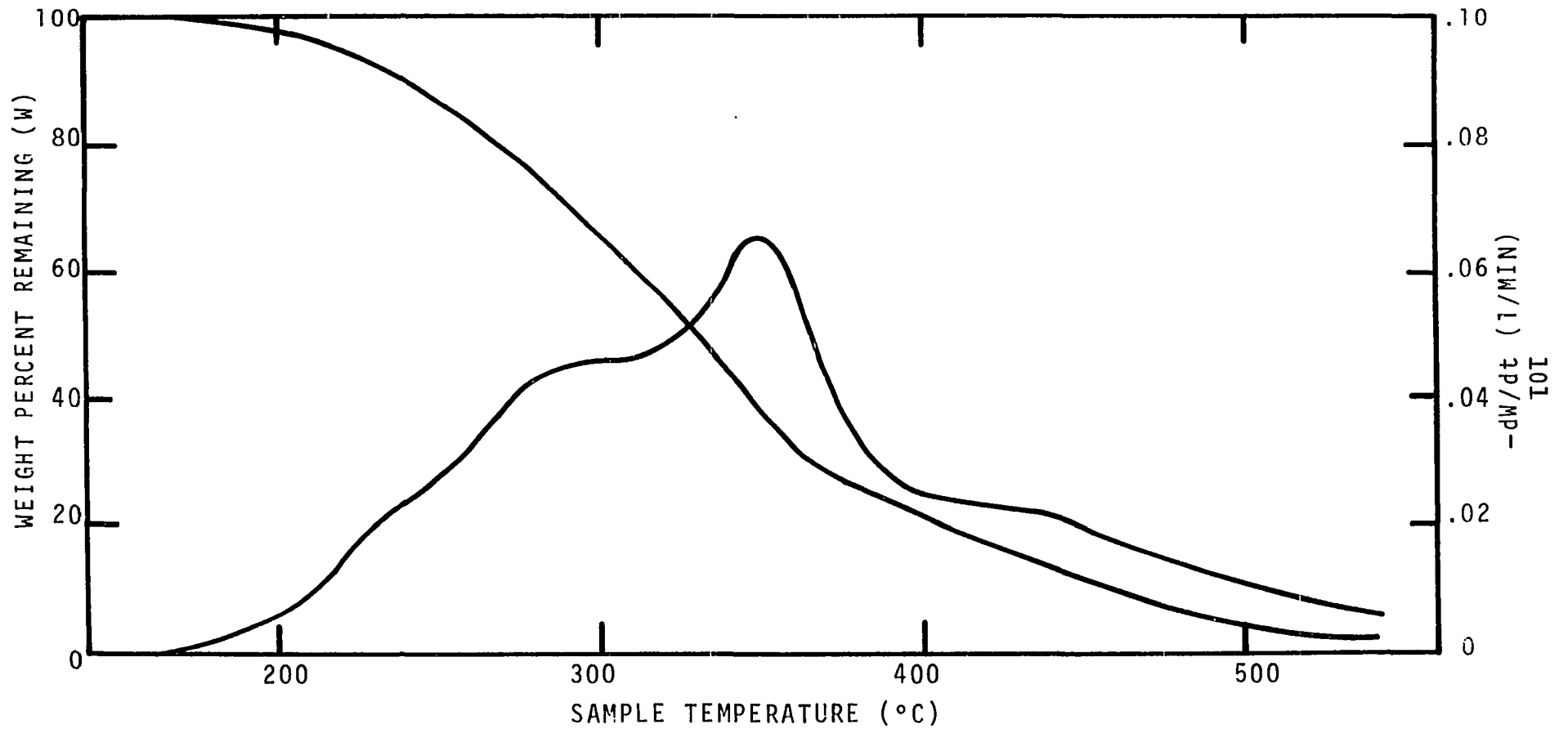


Figure A-4. Weight Loss and Rate of Weight Loss for Freeze-Dried Spruce Needles. Heating Rate, 10°C/min.

APPENDIX B

DATA ON FREEZE-DRIED SAMPLE COLLECTION

DATA ON FREEZE-DRIED SAMPLE COLLECTION

Sample	Date	Time	Elevation	Tree Size	Location
Ponderosa Pine Needles	8/7/74	4:00 pm	--	54.6 ft tall, 16.7 in dia	1/4 mi southwest of Grant Creek ranch headquarters, Missoula Montana
Quaking Aspen Leaves	8/7/74	4:00 pm	--	40.2 ft tall, 4.9 in dia	As above
Douglas fir needles	8/7/74	2:00 pm	4600-4800 ft	27.3 ft tall, 4.1 in dia	Maximum elevation of Snow Bowl Rd north of Missoula, Montana
Lodgepole pine needles	8/7/74	2:00 pm	4600-4800 ft	20.1 ft tall, 4.1 in dia	As above
Chamise foliage	8/74	--	--	--	Near Riverside, Calif.
Eastwood manzanita (Arctostaphylos glandulosa)	8/74	--	--	--	As above

APPENDIX C

DATA FROM WEIGHT LOSS MEASUREMENTS

DATA FROM WEIGHT LOSS MEASUREMENTS

Heating Rate	Initial Weight	Final Weight	Maximum Rate of Wt Loss	Maximum Rate of Wt Loss	Temp at Max Rate of Wt Loss
°C/min	mg	mg	min <sup>-1</sup>	°C <sup>-1</sup>	°C
<u>Freeze-Dried Ponderosa Pine Needles</u>					
10	1.75	0.49	0.0662	0.0066	328
40	1.61	0.40	0.2658	0.0066	362
160	1.61	0.40	1.0269	0.0064	386
<u>Freeze-Dried Aspen Leaves</u>					
10	1.49	0.34	0.0638	0.0064	320
40	1.72	0.35	0.2552	0.0064	354
160	1.25	0.28	1.0069	0.0063	375
<u>Freeze-Dried Douglas Fir Needles</u>					
10	1.70	0.48	0.0676	0.0068	336
40	1.56	0.42	0.2457	0.0061	375
160	1.78	0.46	0.8542	0.0053	392
<u>Freeze-Dried Lodgepole Pine Needles</u>					
10	1.81	0.51	0.0716	0.0072	341
40	1.82	0.46	0.2799	0.0070	373
160	1.63	0.39	0.9447	0.0059	392
<u>Freeze-Dried Chemise Foliage</u>					
10	1.69	0.43	0.0553	0.0055	279
40	1.52	0.35	0.2158	0.0054	325
160	1.76	0.38	0.8887	0.0056	342

TABLE---Continued

Heating Rate	Initial Weight	Final Weight	Maximum Rate of Wt Loss	Maximum Rate of Wt Loss	Temp at Max Rate of Wt Loss
°C/min	mg	mg	min <sup>-1</sup>	°C <sup>-1</sup>	°C
<u>Freeze-Dried Manzanita Leaves</u>					
10	1.59	0.47	0.0505	0.0051	279
40	1.83	0.49	0.1991	0.0050	310
160	1.75	0.43	0.7900	0.0049	325

APPENDIX D

DATA OF ENERGY MEASUREMENTS

DATA OF ENERGY MEASUREMENTS

Heating Rate (°C/min)	Initial Weight (mg)	Final Weight (mg)	C <sub>p</sub> at 100°C (cal/gm-°C)	Max dE'/dT (cal/gm-°C)	Temp at Max dE'/dT (°C)
<u>Freeze-Dried Ponderosa Pine Needles</u>					
40	4.052	1.38	0.395	0.602	190
160	2.670	0.86	0.405	0.640	230
<u>Freeze-Dried Aspen Leaves</u>					
40	2.676	0.80	0.390	0.550	188
160	4.023	1.34	0.385	0.572	222
<u>Freeze-Dried Douglas Fir Needles</u>					
40	3.858	1.24	0.417	0.610	200
160	4.107	1.32	0.390	0.622	225
<u>Freeze-Dried Lodgepole Pine Needles</u>					
40	4.272	1.48	0.395	0.624	187
160	2.699	0.76	0.400	0.596	228
<u>Freeze-Dried Chamise Foliage</u>					
40	4.719	1.58	0.385	0.595	185
160	2.235	0.64	0.375	0.588	210
<u>Freeze-Dried Manzanita Leaves</u>					
40	4.794	1.76	0.385	0.650	210
160	3.306	1.00	0.385	0.628	242

APPENDIX E

WEIGHT LOSS CURVES FOR FREEZE-DRIED ASPEN LEAVES, DOUGLAS  
FIR NEEDLES, LODGEPOLE PINE NEEDLES, CHAMISE FOLIAGE,  
AND MANZANITA LEAVES

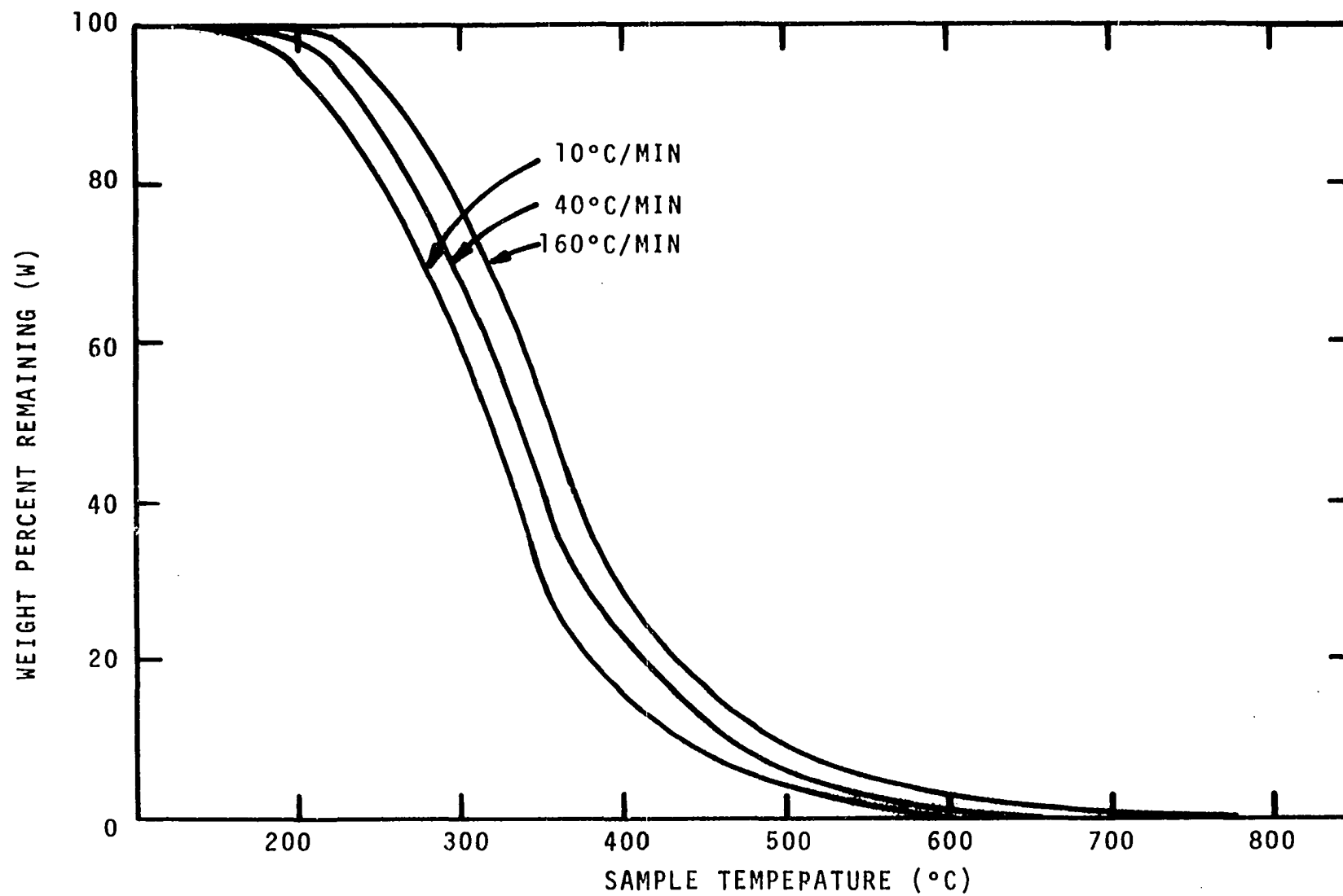


Figure E-1. Weight Loss of Freeze-Dried Aspen Leaves.

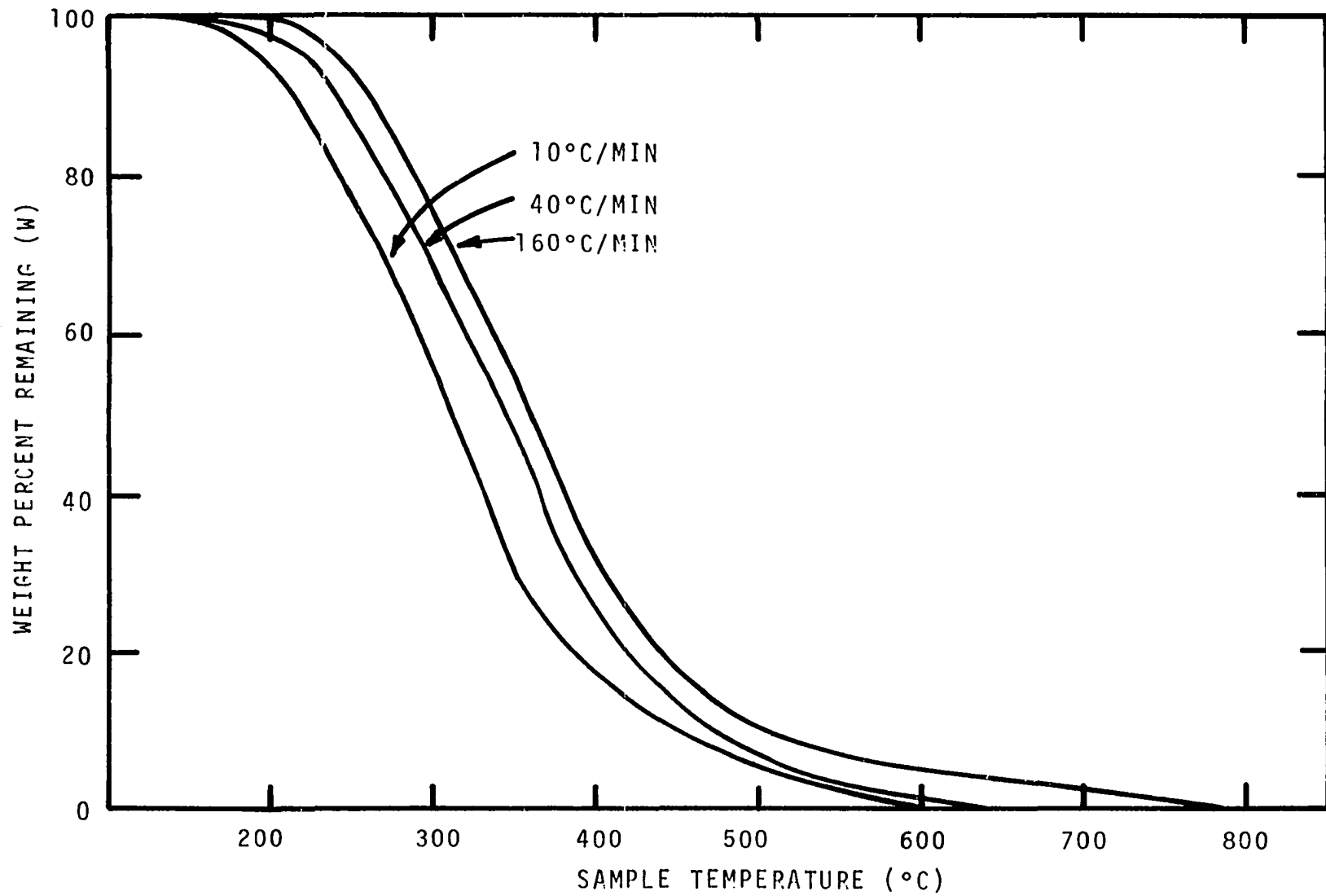


Figure E-2. Weight Loss of Freeze-Dried Douglas Fir Needles.

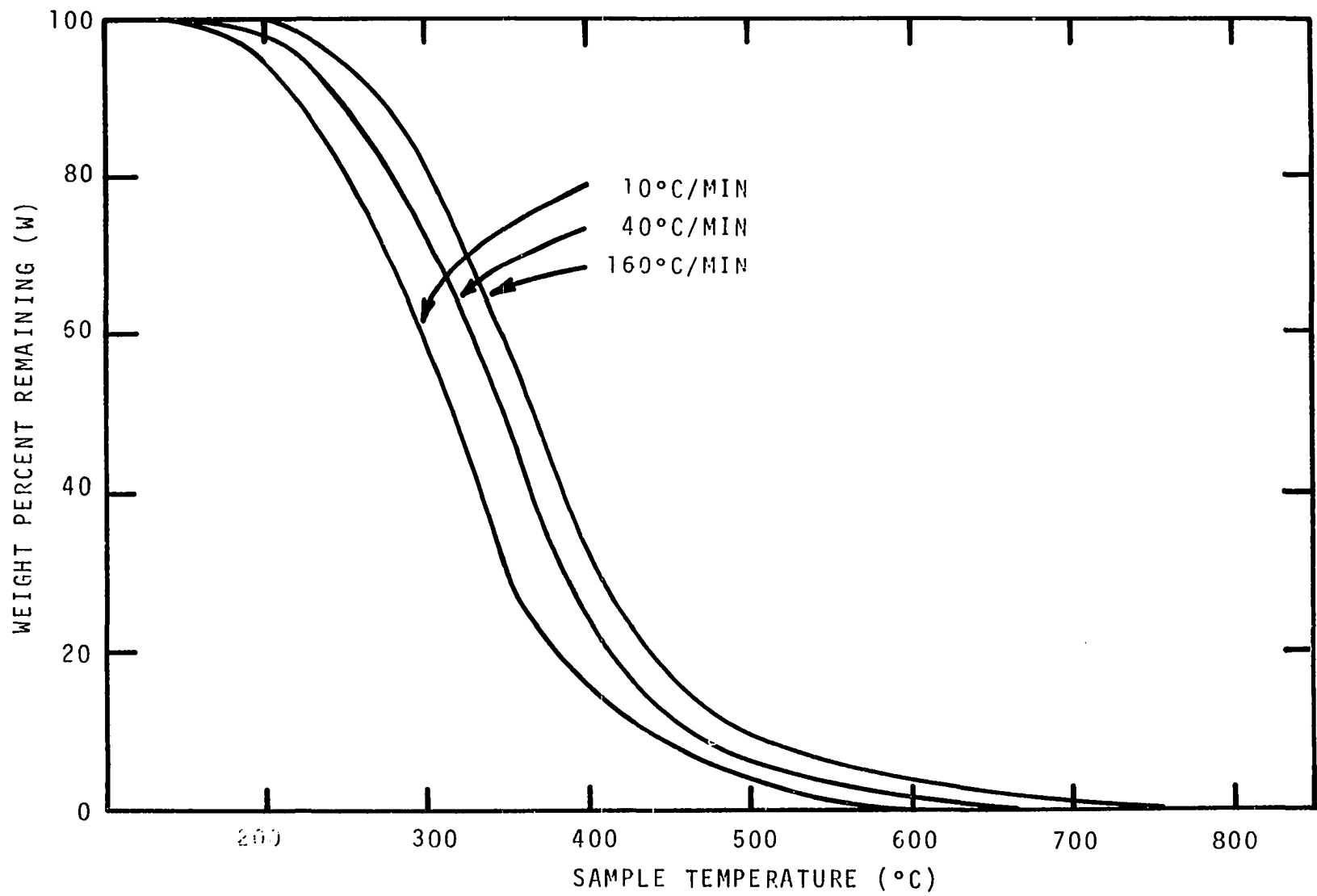


Figure E-3. Weight Loss of Freeze-Dried Lodgepole Pine Needles.

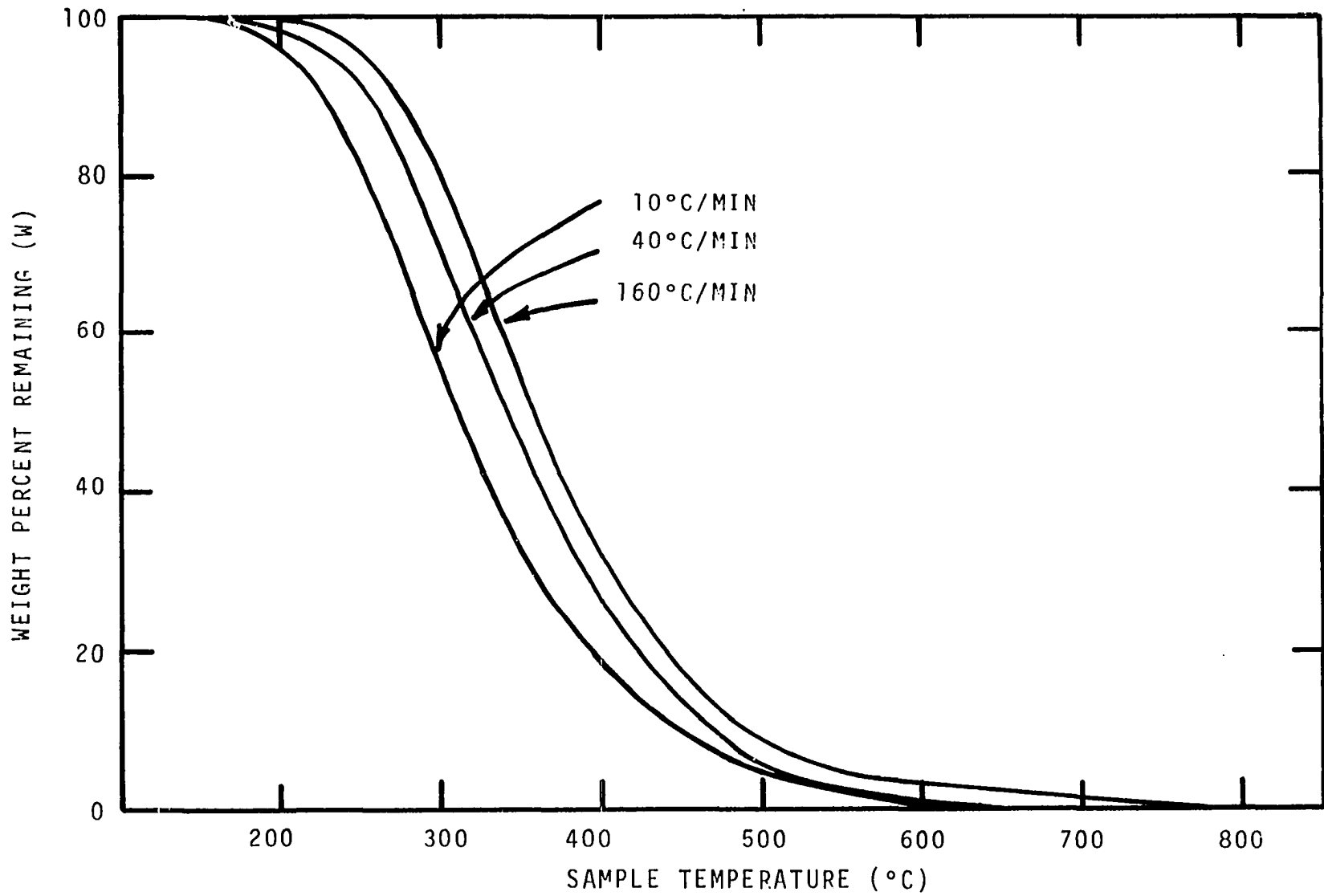


Figure E-4. Weight Loss of Freeze-Dried Chamise Foliage.

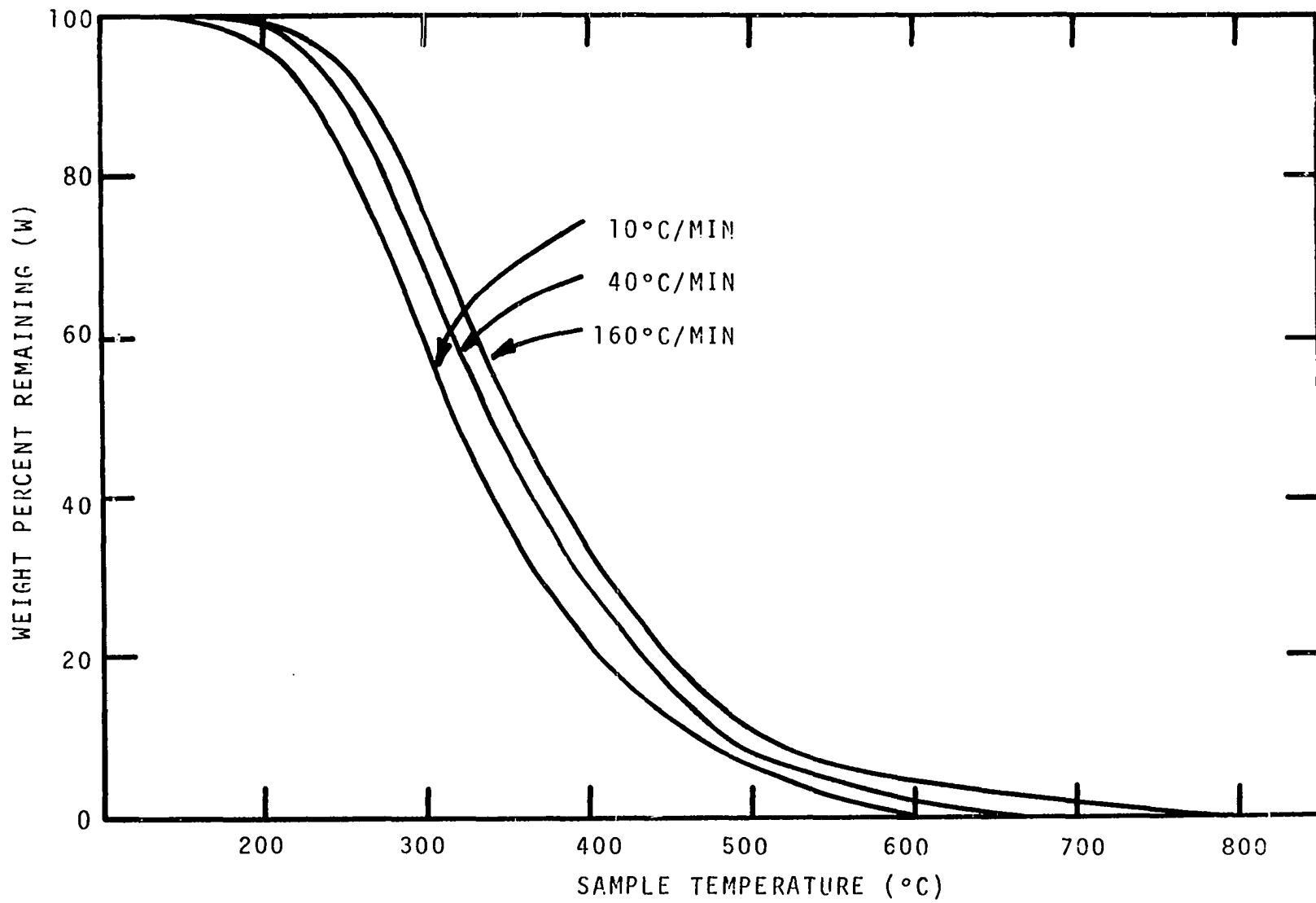


Figure E-5. Weight Loss of Freeze-Dried Manzanita Leaves.

APPENDIX F

RATE OF WEIGHT LOSS CURVES FOR FREEZE-DRIED ASPEN LEAVES,  
DOUGLAS FIR NEEDLES, LODGEPOLE PINE NEEDLES, CHAMISE  
FOLIAGE, AND MANZANITA LEAVES

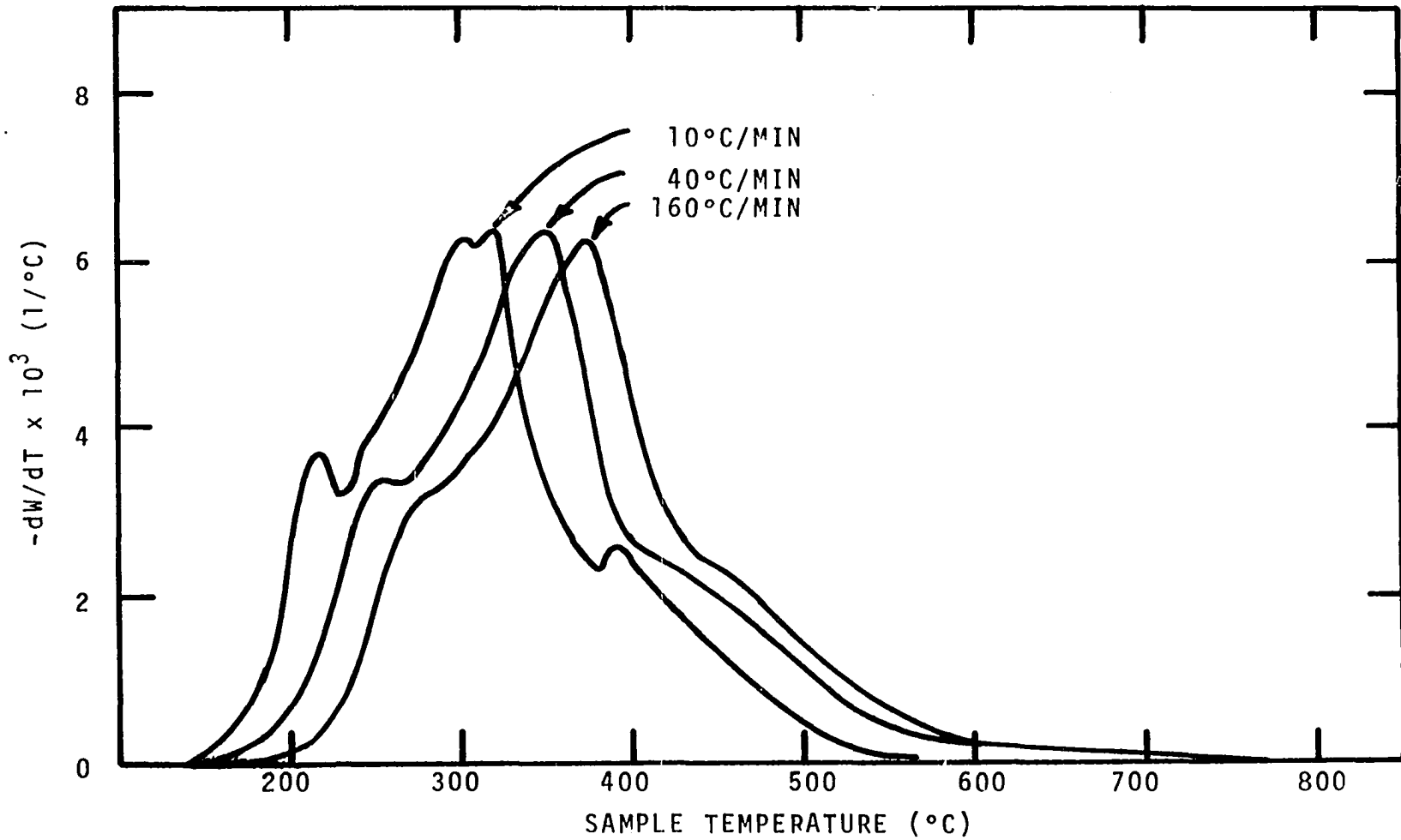


Figure F-1. Rate of Weight Loss of Freeze-Dried Aspen Leaves.

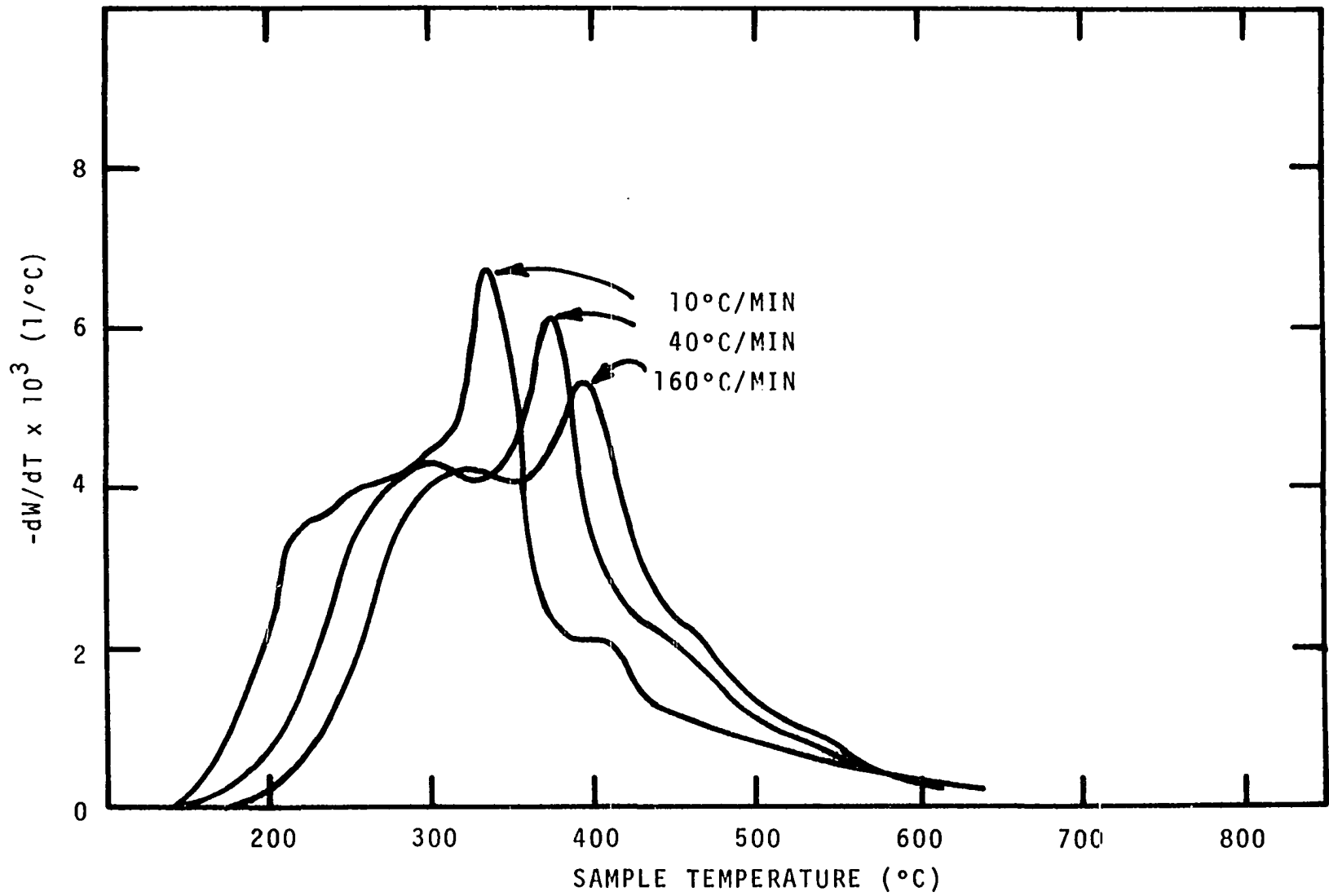


Figure F-2. Rate of Weight Loss of Freeze-Dried Douglas Fir Needles.

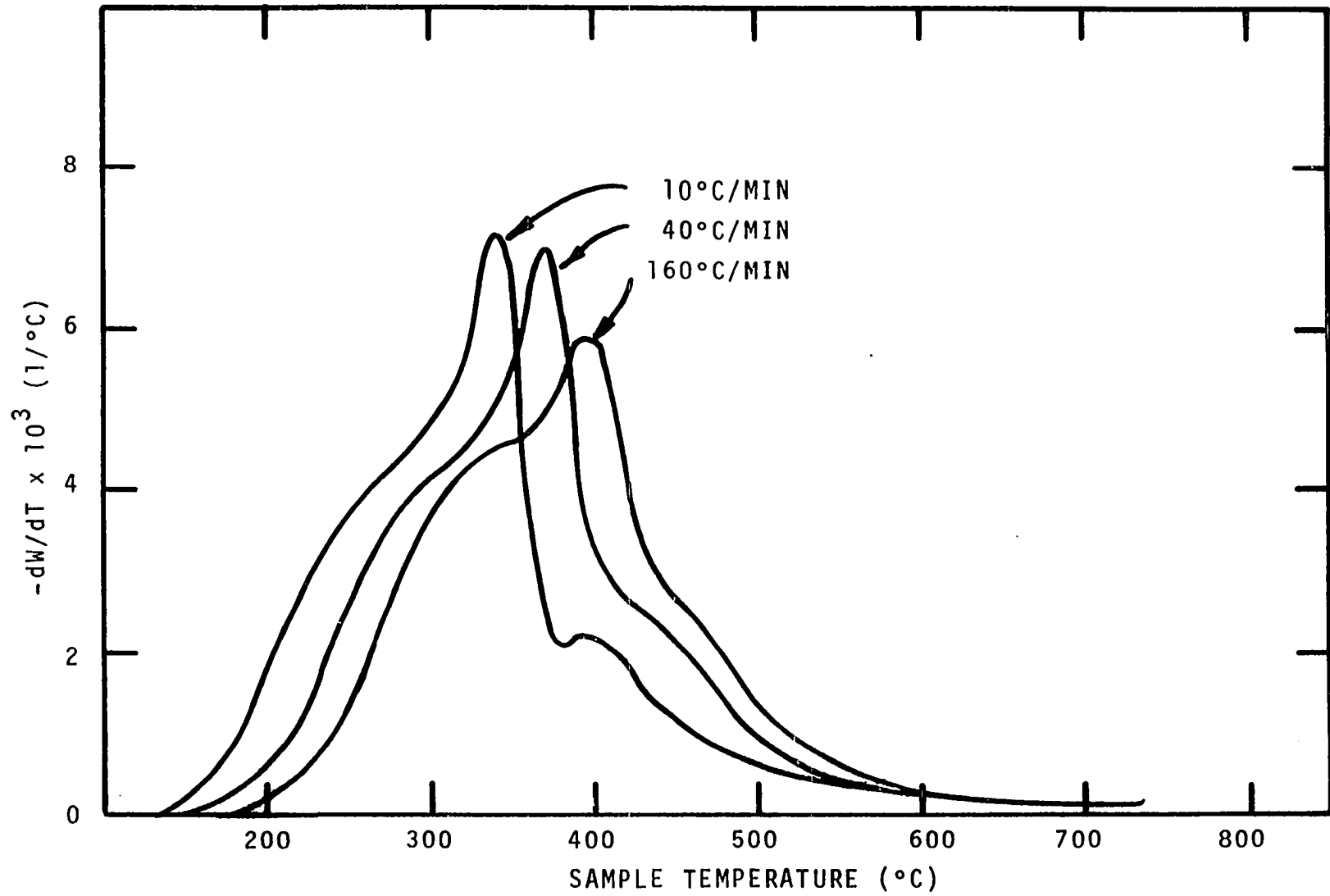


Figure F-3. Rate of Weight Loss of Freeze-Dried Lodgepole Pine Needles.

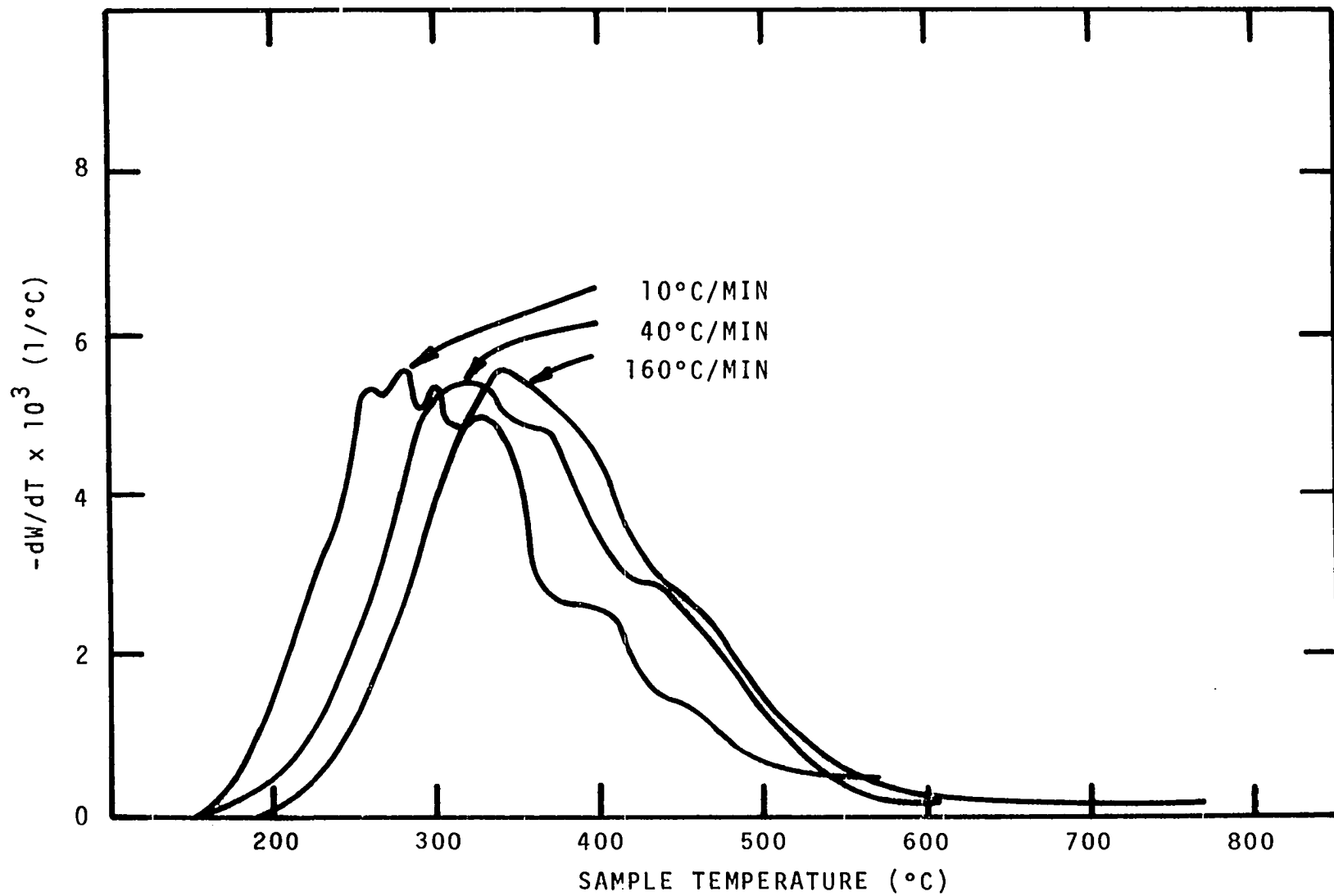


Figure F-4. Rate of Weight Loss of Freeze-Dried Chamise Foliage.

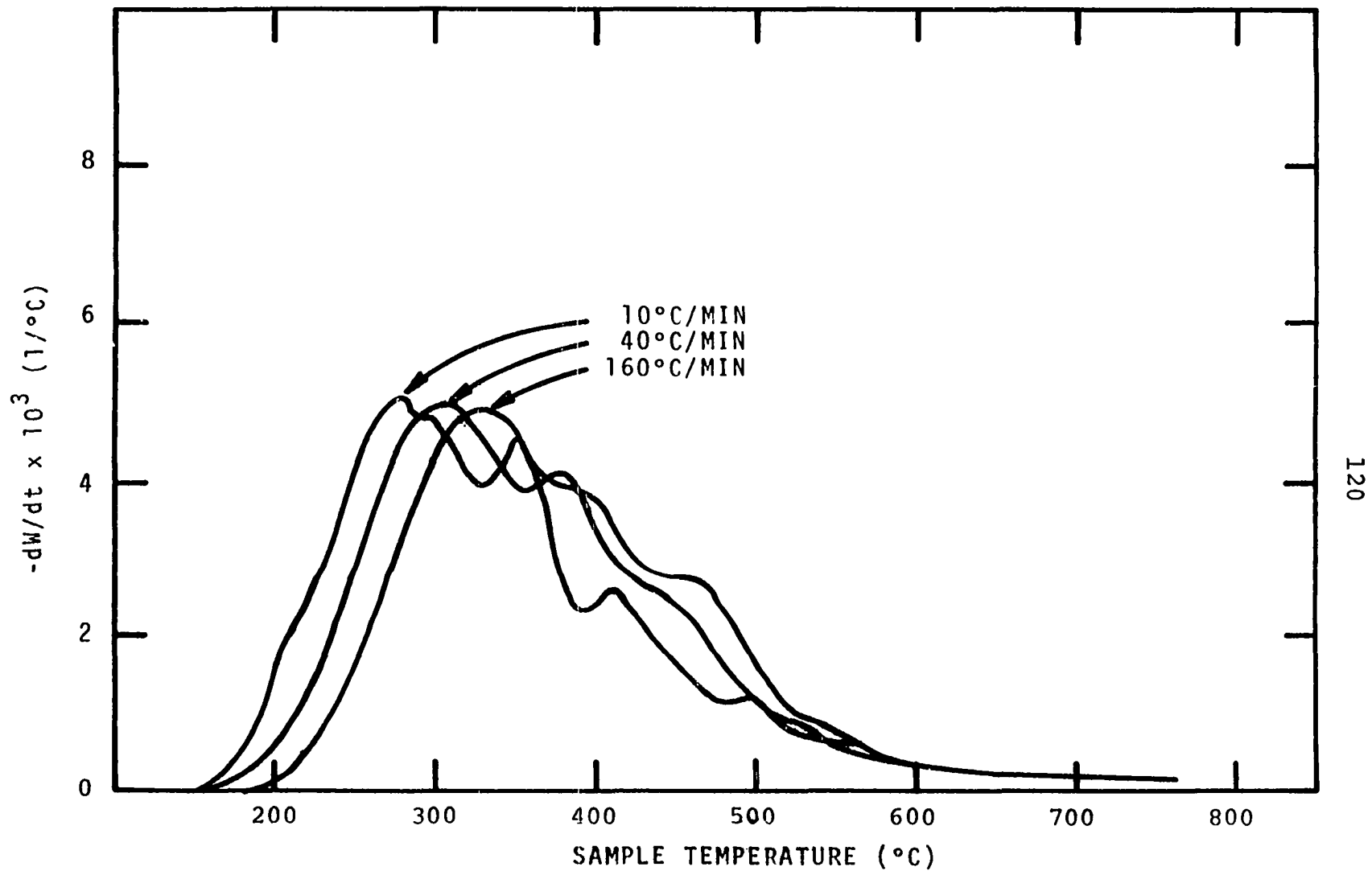


Figure F-5. Rate of Weight Loss of Freeze-Dried Manzanita Leaves.

APPENDIX G

DIFFERENTIAL ENERGY CURVES OF FREEZE-DRIED ASPEN LEAVES,  
DOUGLAS FIR NEEDLES, LODGEPOLE PINE NEEDLES, CHAMISE  
FOLIAGE, AND MANZANITA LEAVES

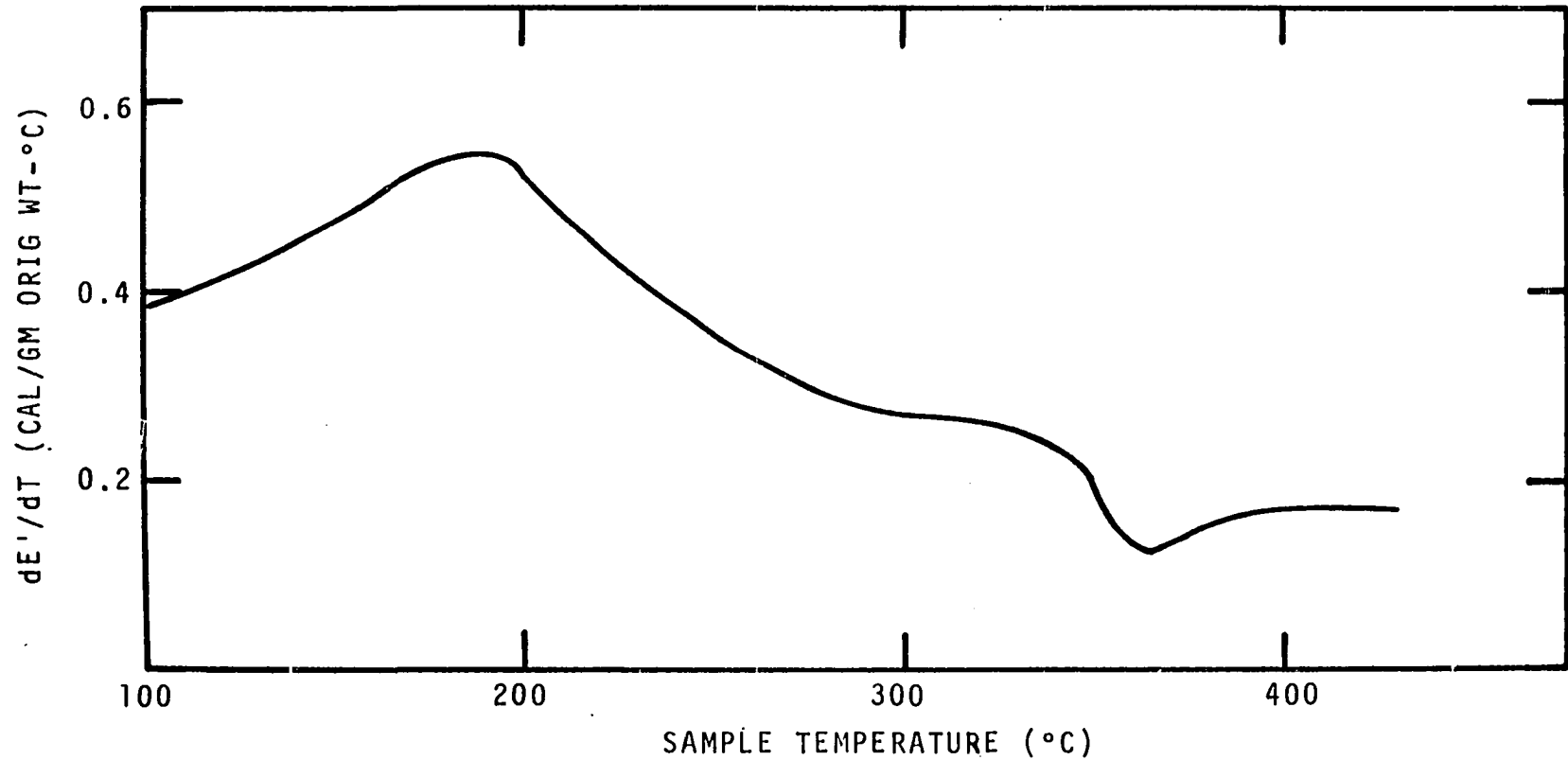


Figure G-1. Differential Energy of Freeze-Dried Aspen Leaves. Heating Rate, 40°C/min.

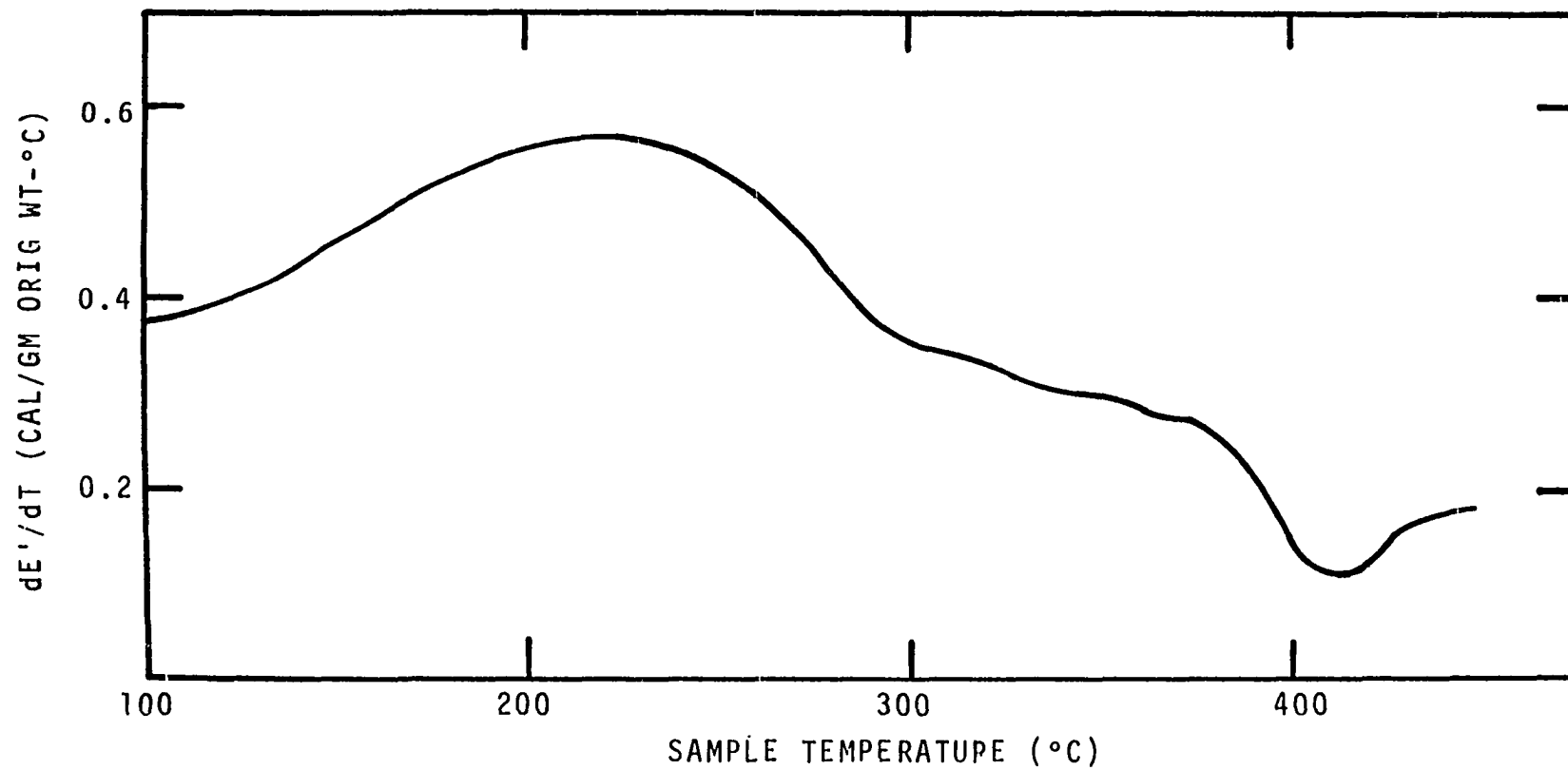


Figure G-2. Differential Energy of Freeze-Dried Aspen Leaves.  
Heating Rate, 160°C/Min.

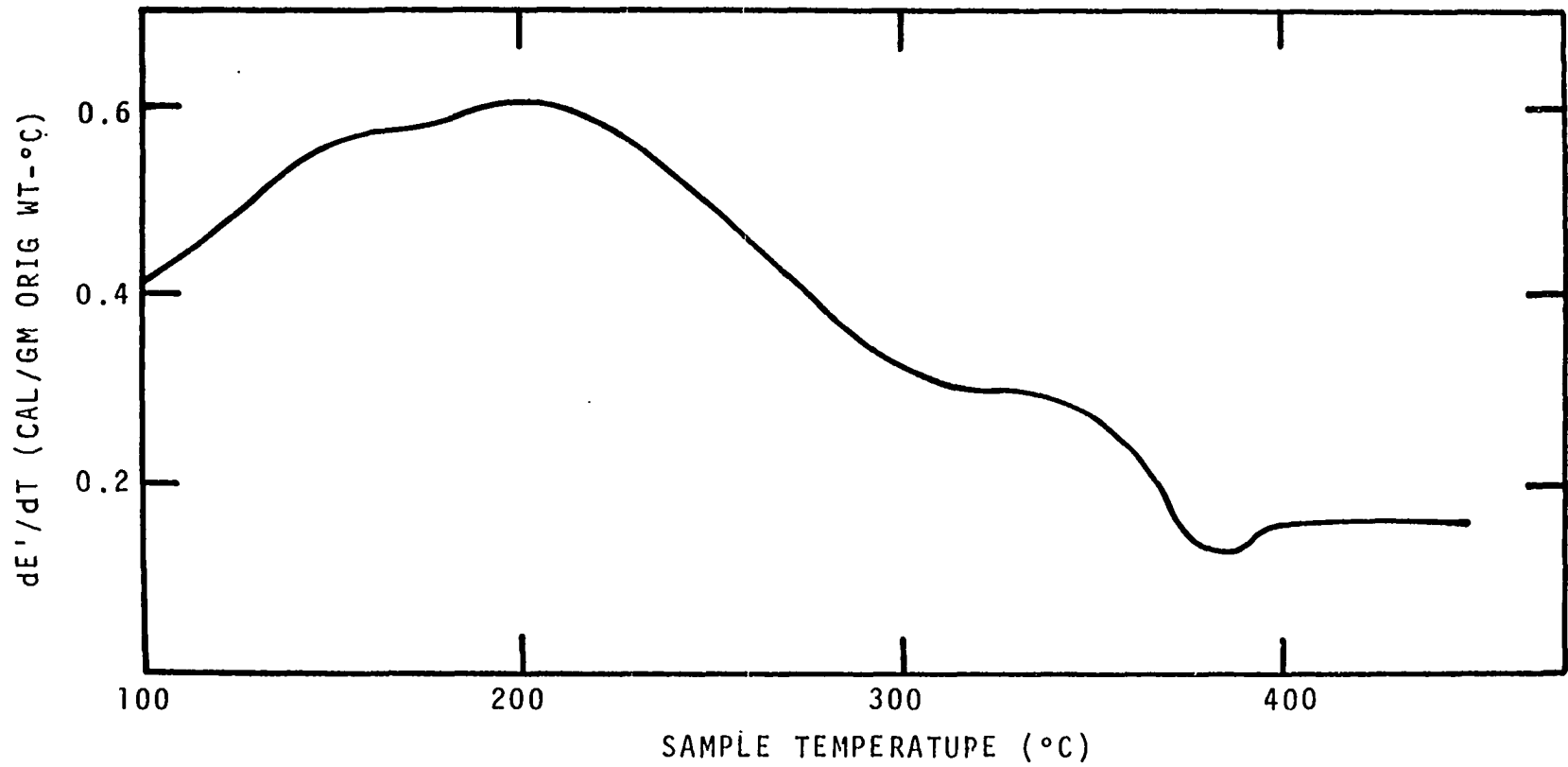


Figure G-3. Differential Energy of Freeze-Dried Douglas Fir Needles. Heating Rate, 40°C/min.

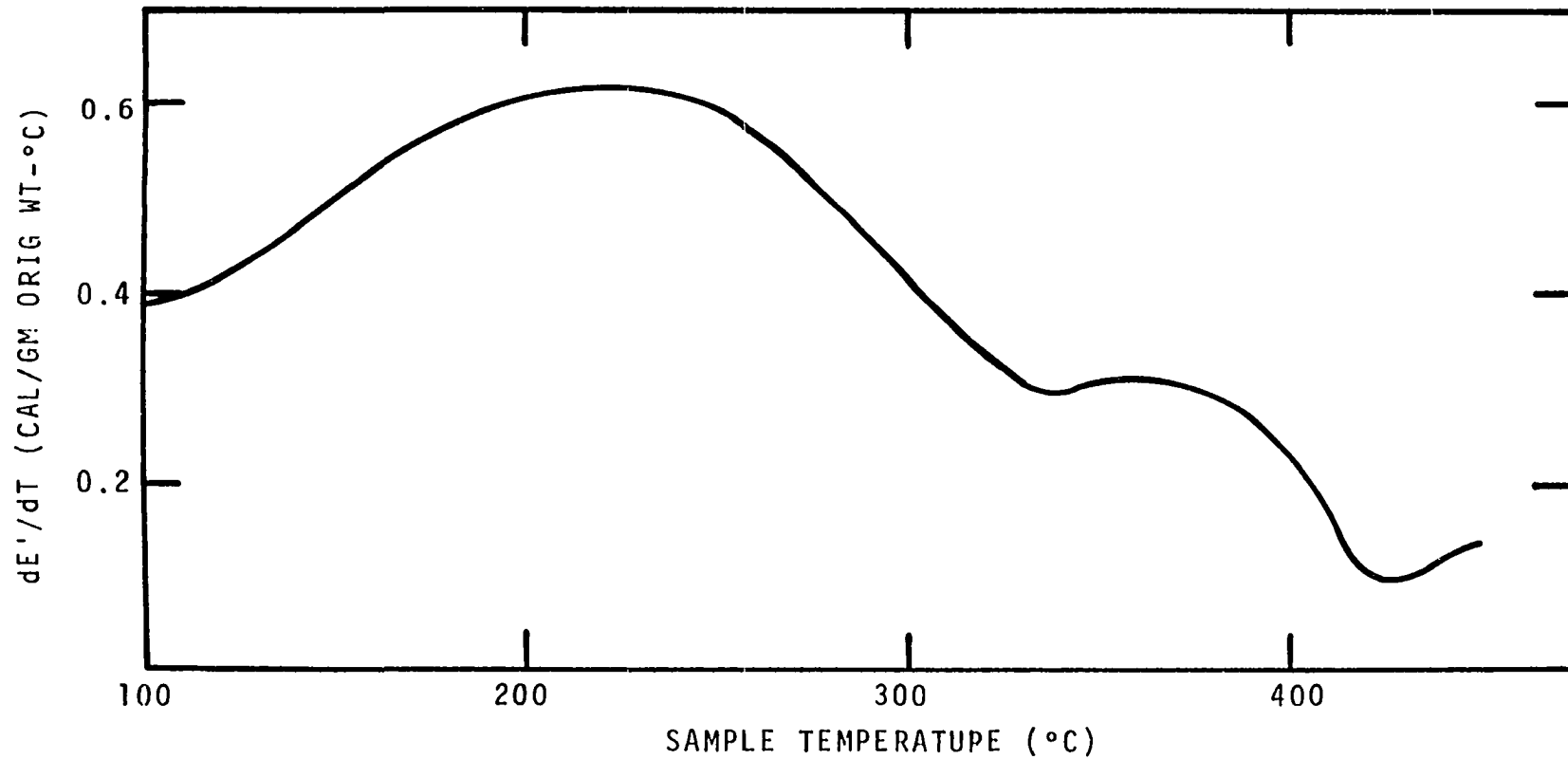


Figure G-4. Differential Energy of Freeze-Dried Douglas Fir Needles. Heating Rate, 160°C/min.

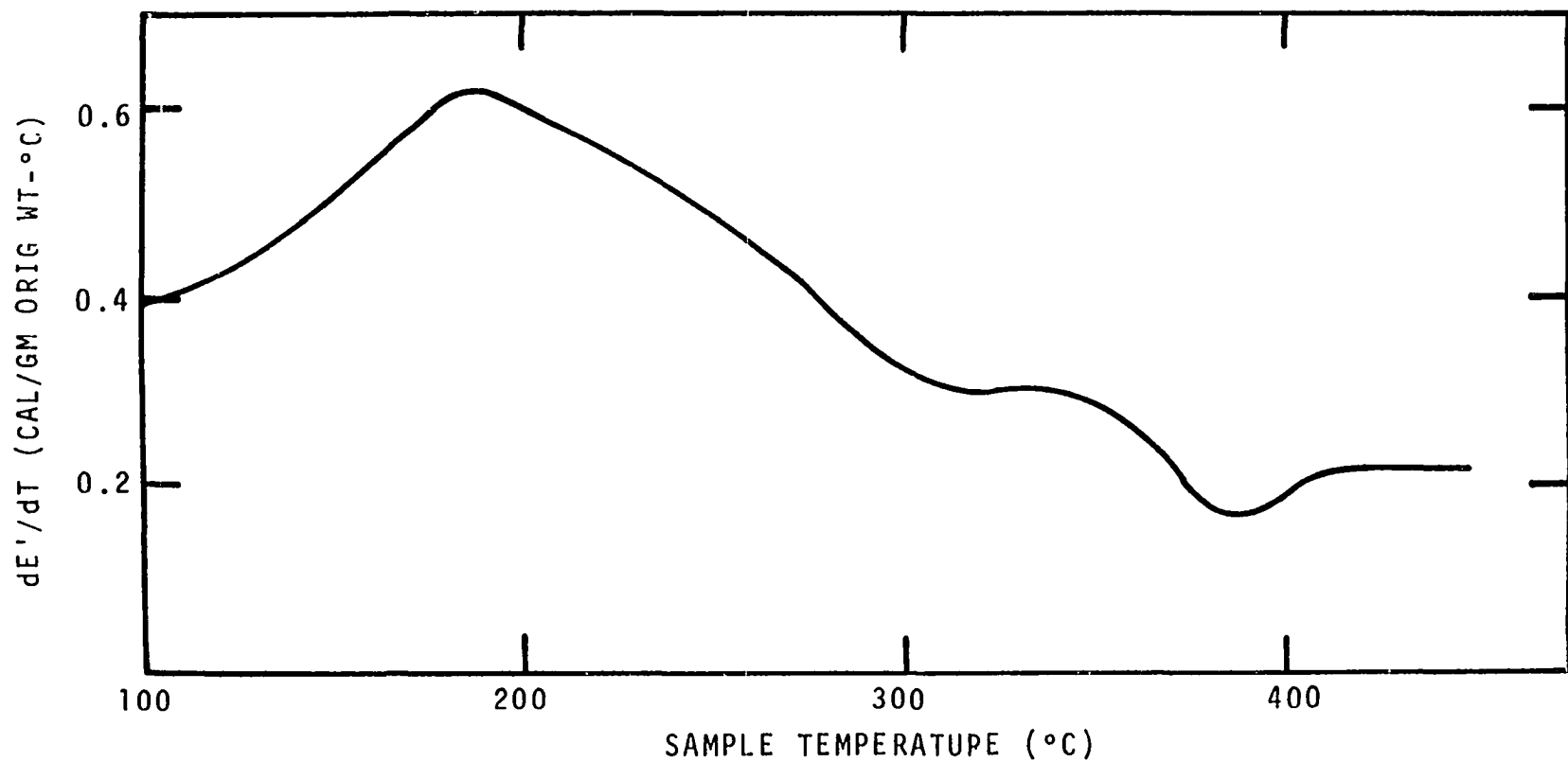


Figure G-5. Differential Energy of Freeze-Dried Lodgepole Pine Needles. Heating Rate, 40°C/min.

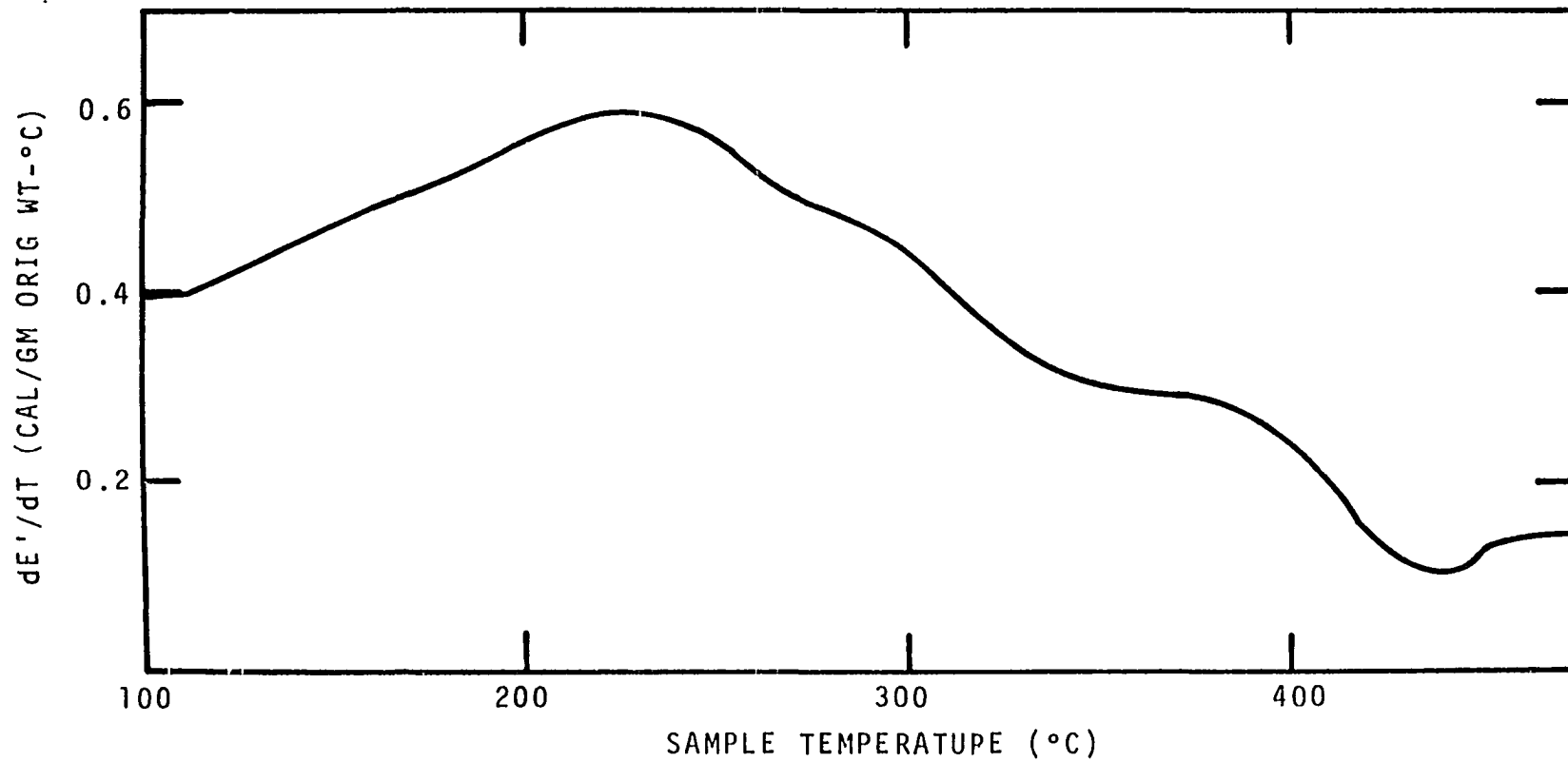


Figure G-6. Differential Energy of Freeze-Dried Lodgepole Pine Needles. Heating Rate, 160°C/min.

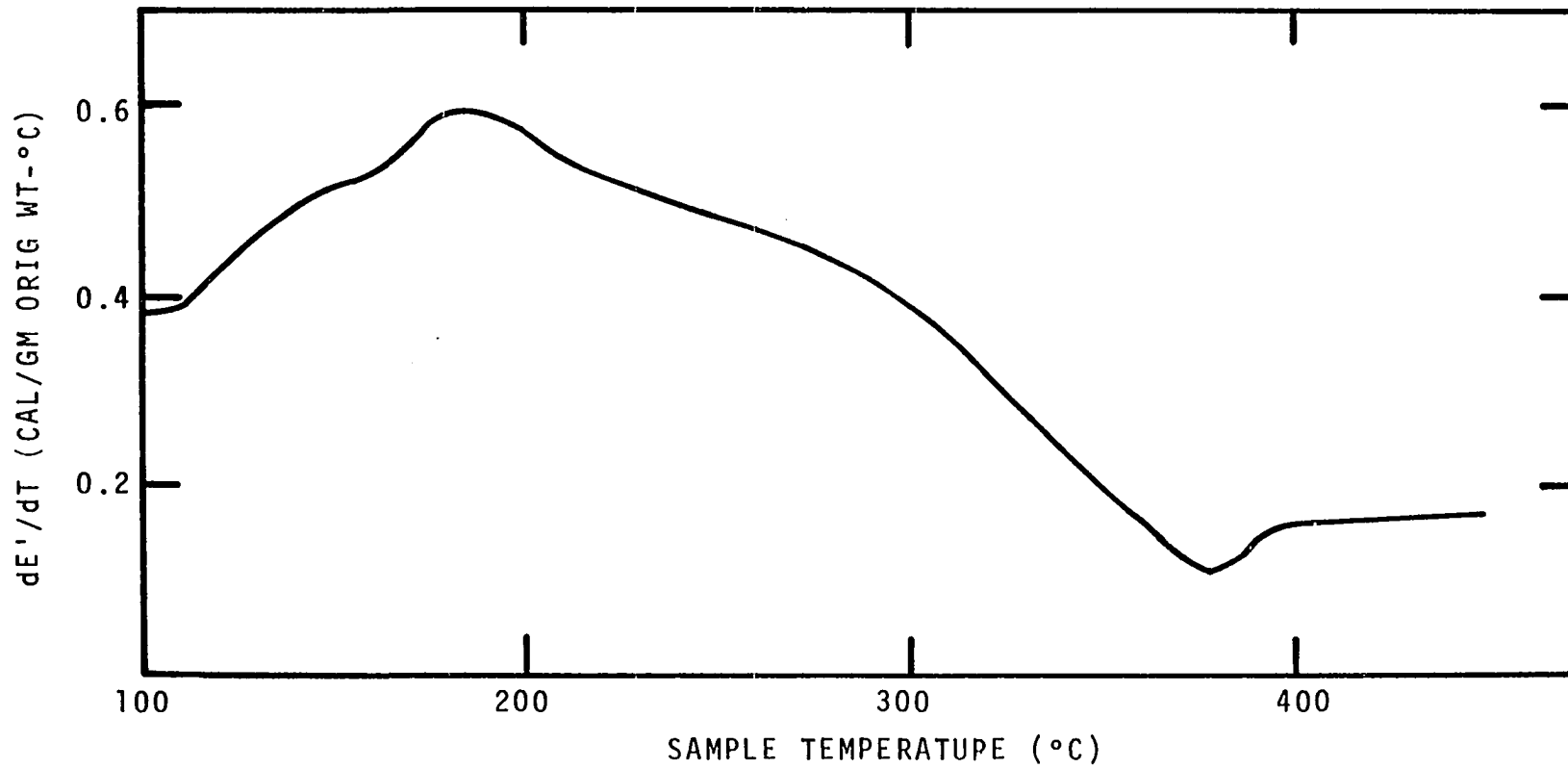


Figure G-7. Differential Energy of Freeze-Dried Chamise Foliage. Heating Rate, 40°C/min.

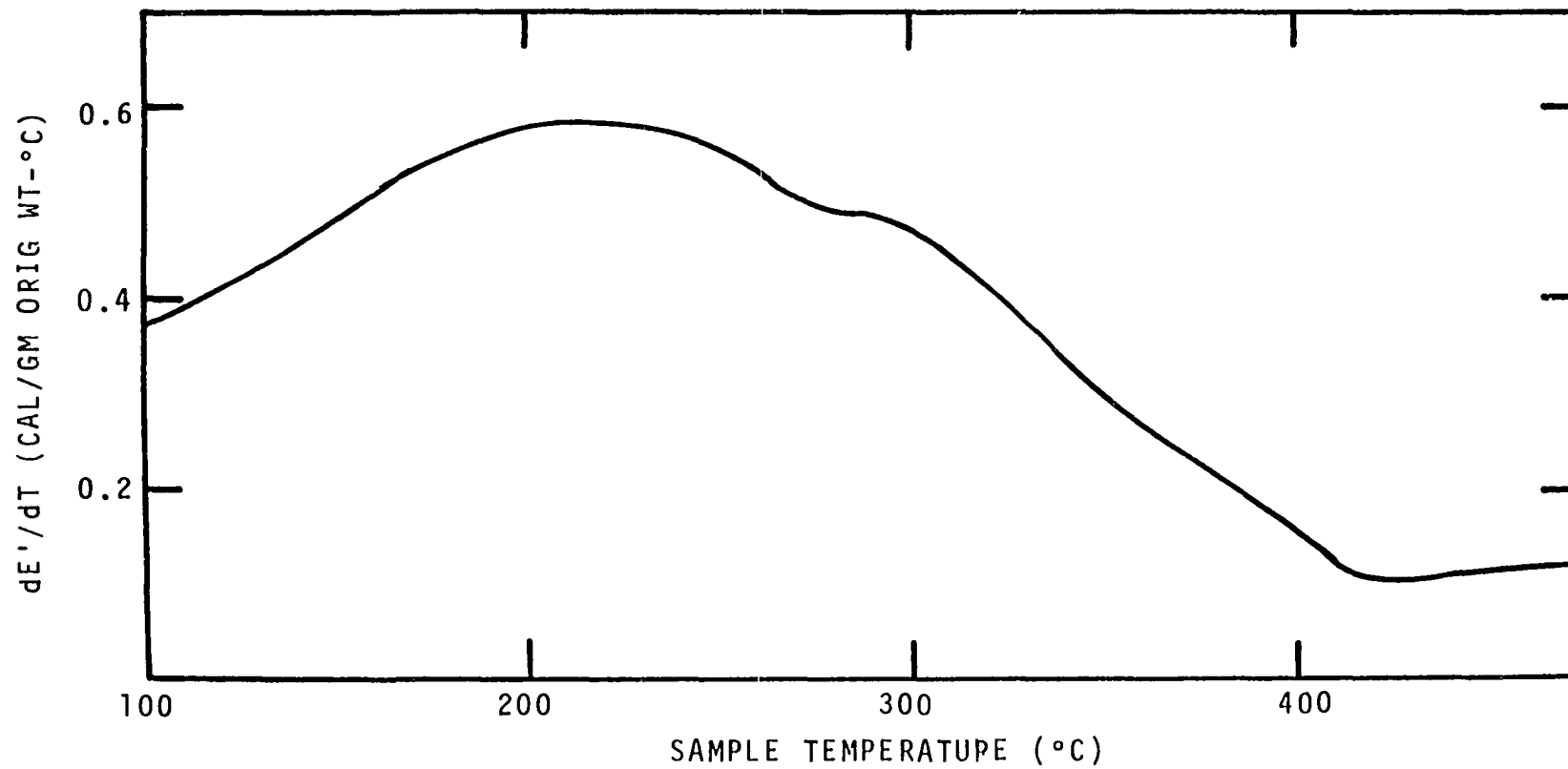


Figure G-8. Differential Energy of Freeze-Dried Chamise Foliage.  
Heating Rate, 160°C/min.

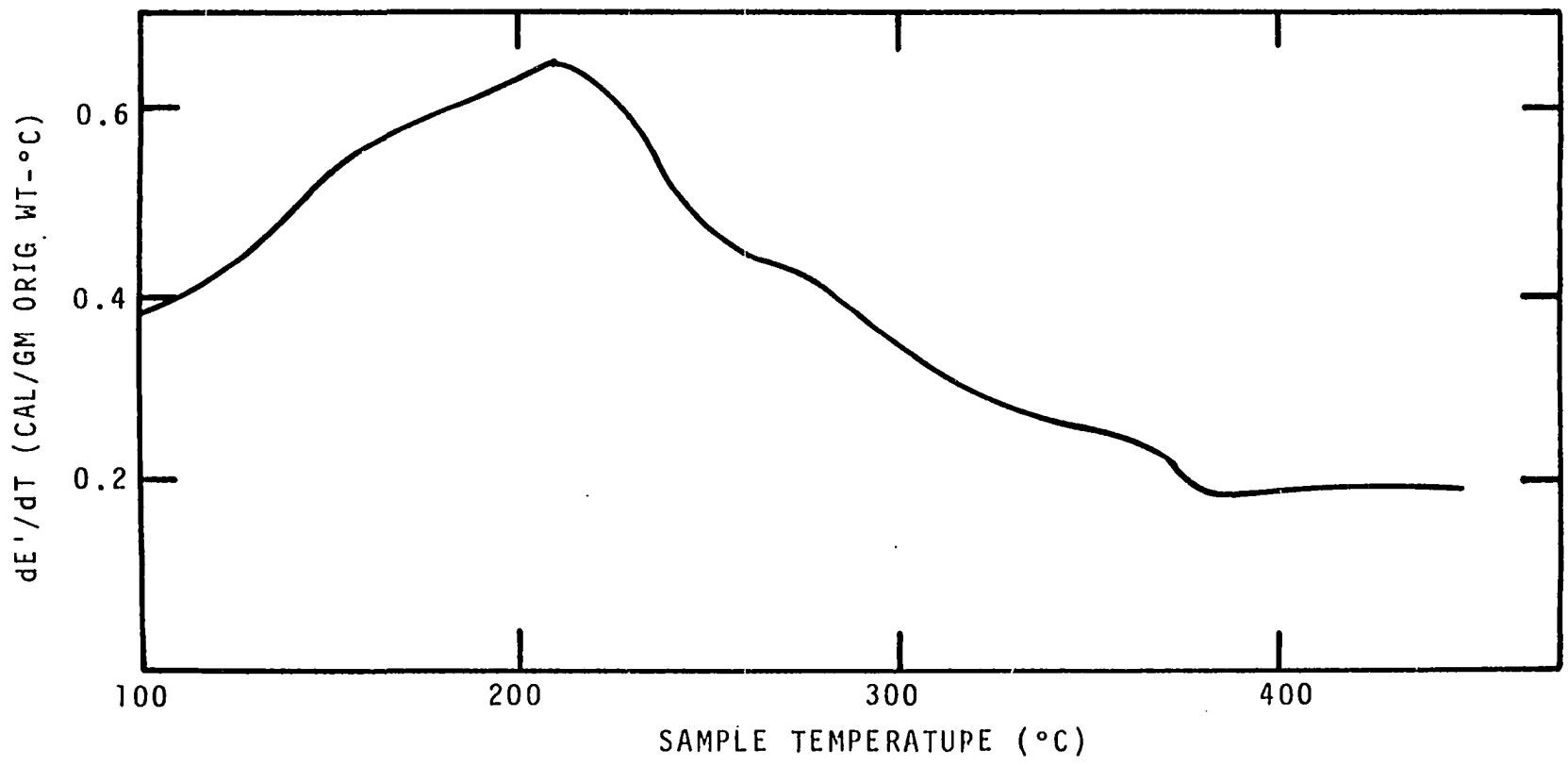


Figure G-9. Differential Energy of Freeze-Dried Manzanita Leaves. Heating Rate, 40°C/min.

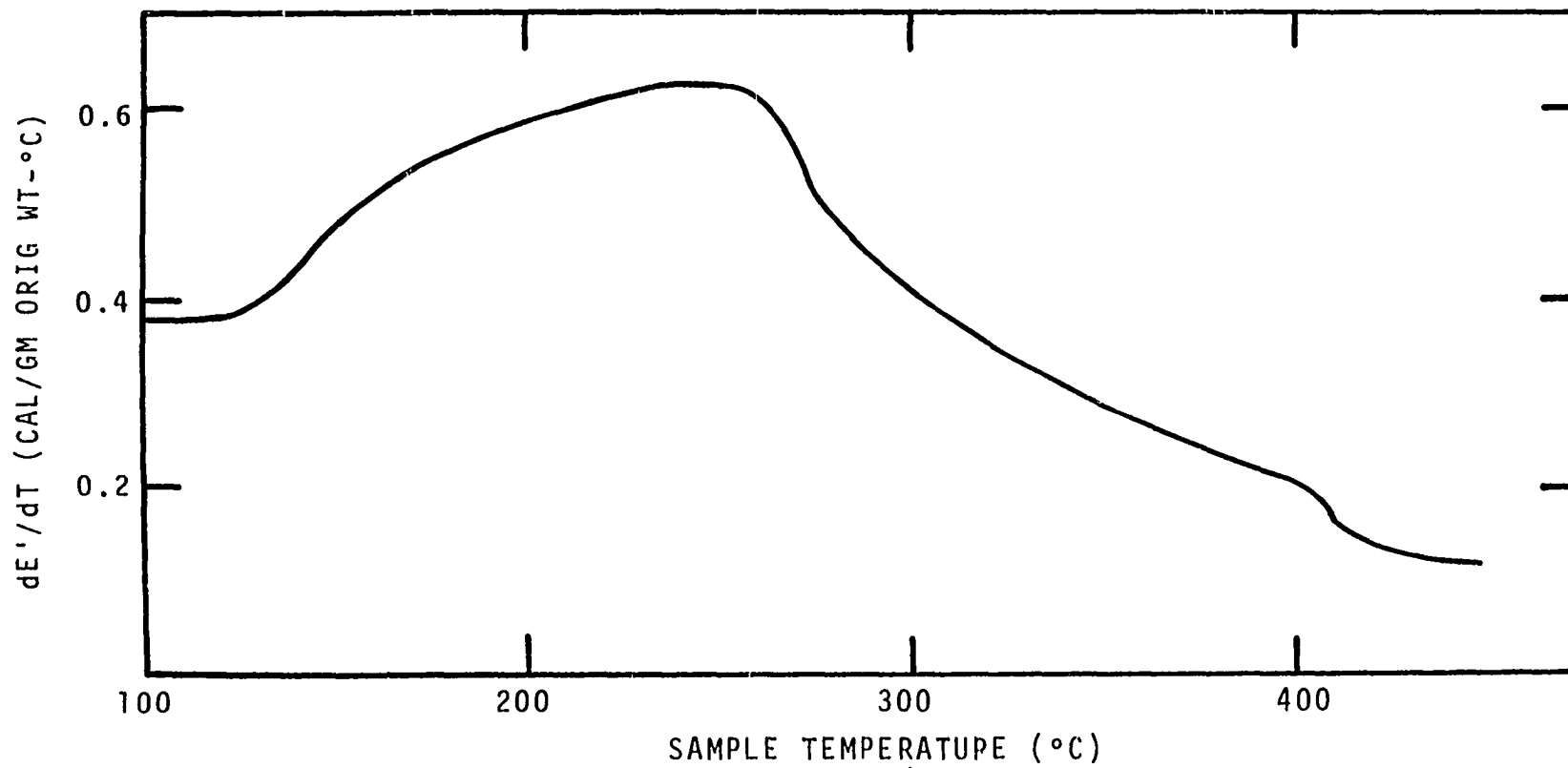


Figure G-10. Differential Energy of Freeze-Dried Manzanita Leaves. Heating Rate, 160°C/min.

APPENDIX H

TOTAL ENERGY CURVES OF FREEZE-DRIED ASPEN LEAVES, DOUGLAS  
FIR NEEDLES, LODGEPOLE PINE NEEDLES, CHAMISE FOLIAGE,  
AND MANZANITA LEAVES

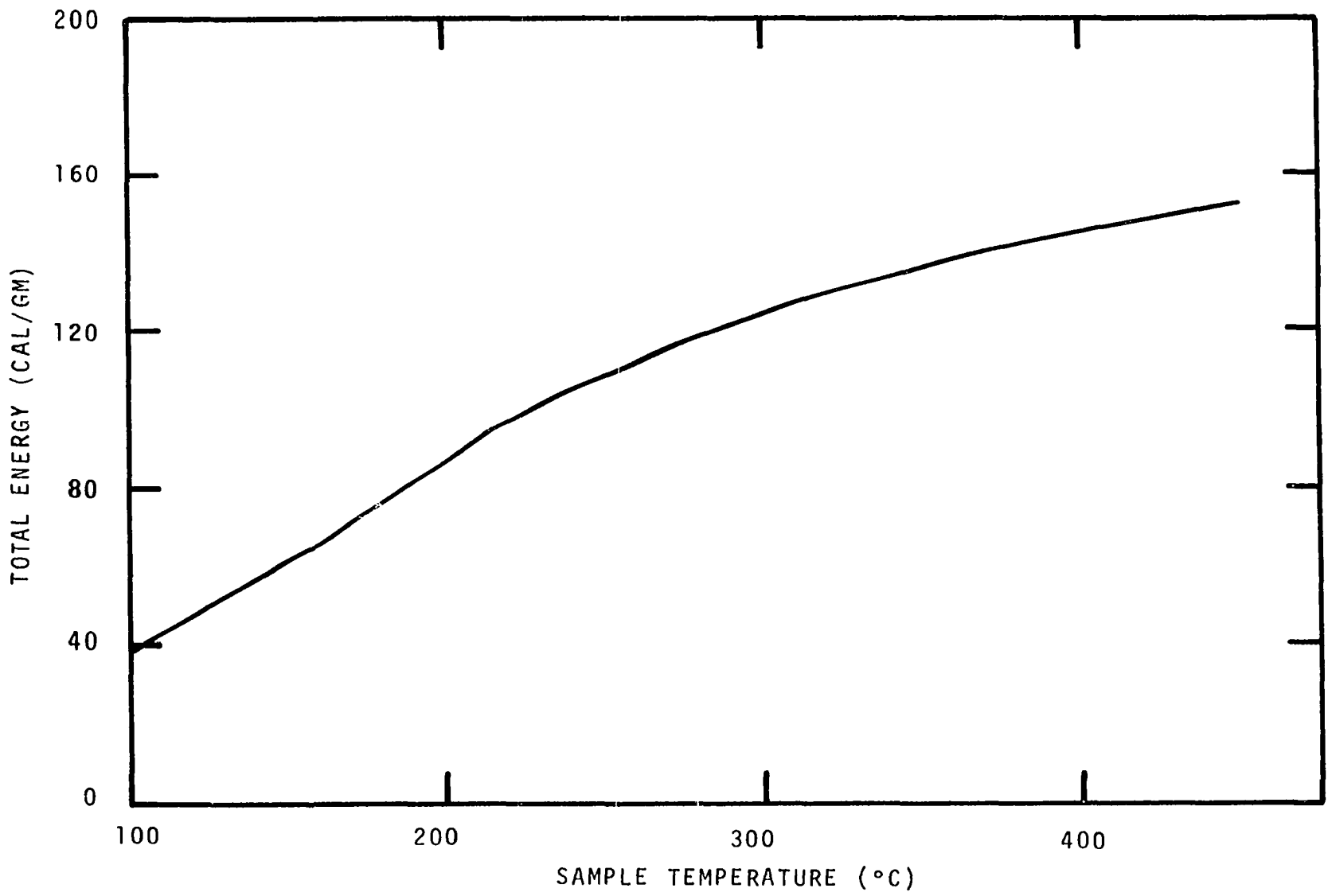
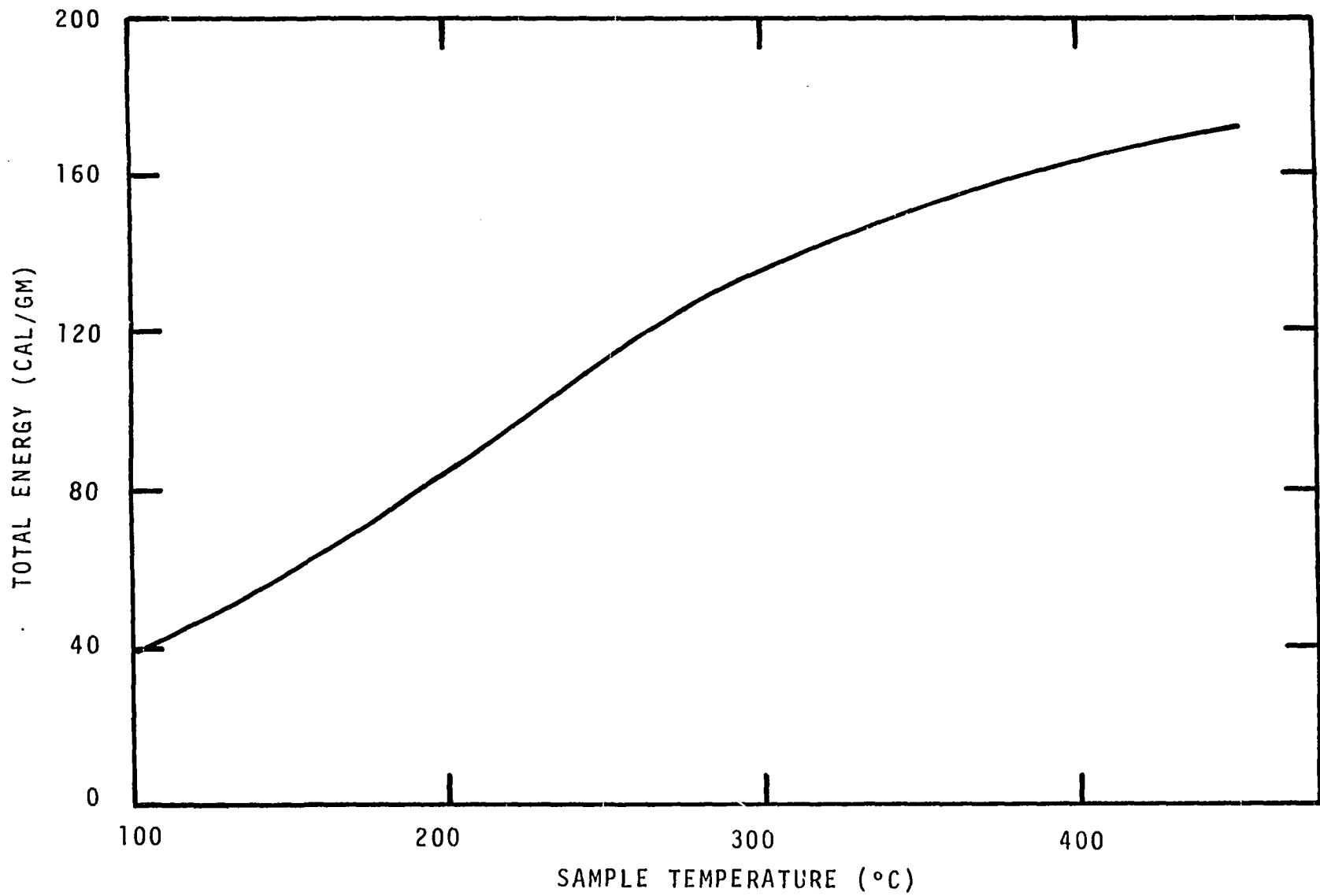


Figure H-1. Total Energy of Freeze-Dried Aspen Leaves. Heating Rate, 40°C/min.



134

Figure H-2. Total Energy of Freeze-Dried Aspen Leaves.  
Heating Rate, 160°C/min.

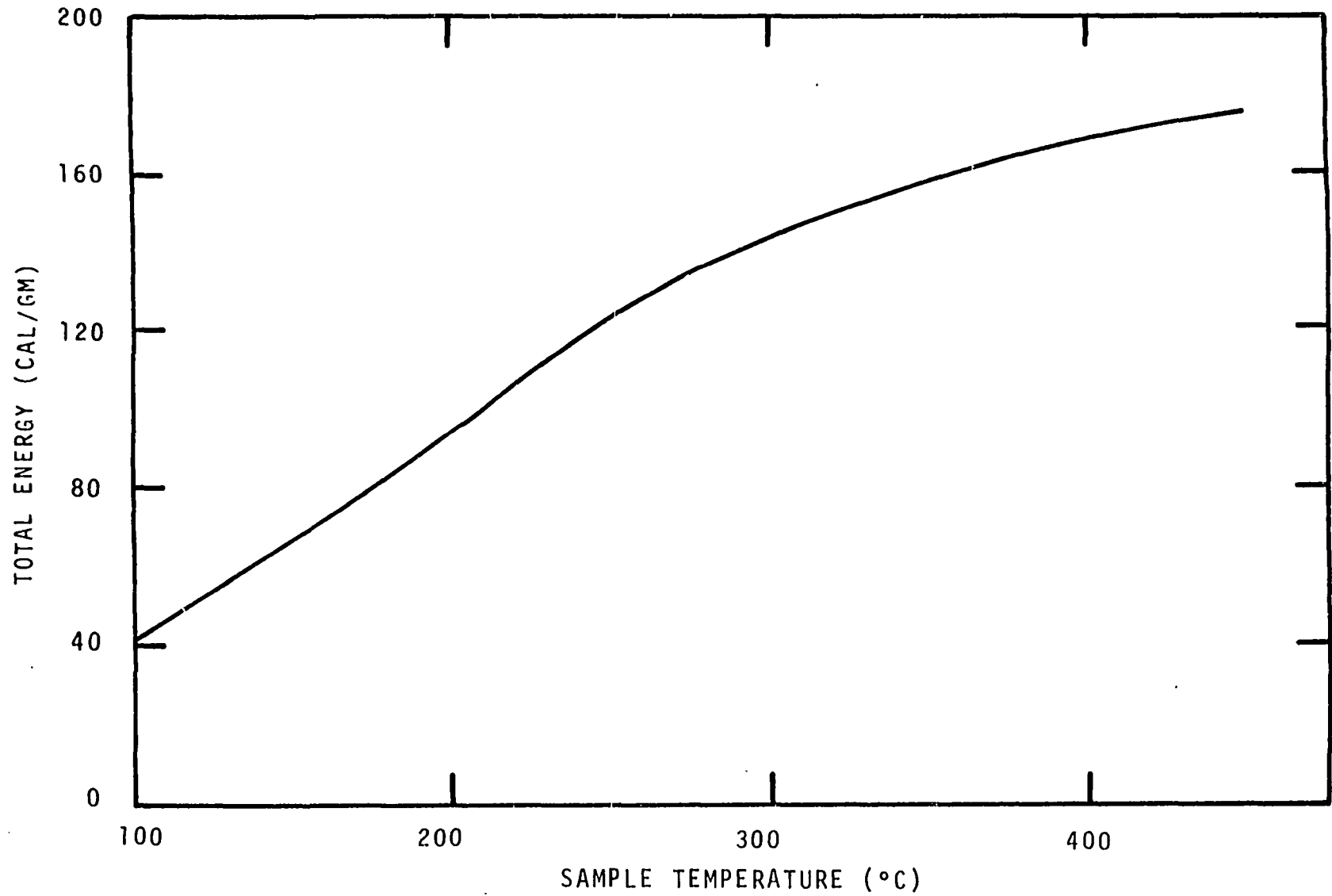


Figure H-3. Total Energy of Freeze-Dried Douglas Fir Needles. Heating Rate, 40°C/min.

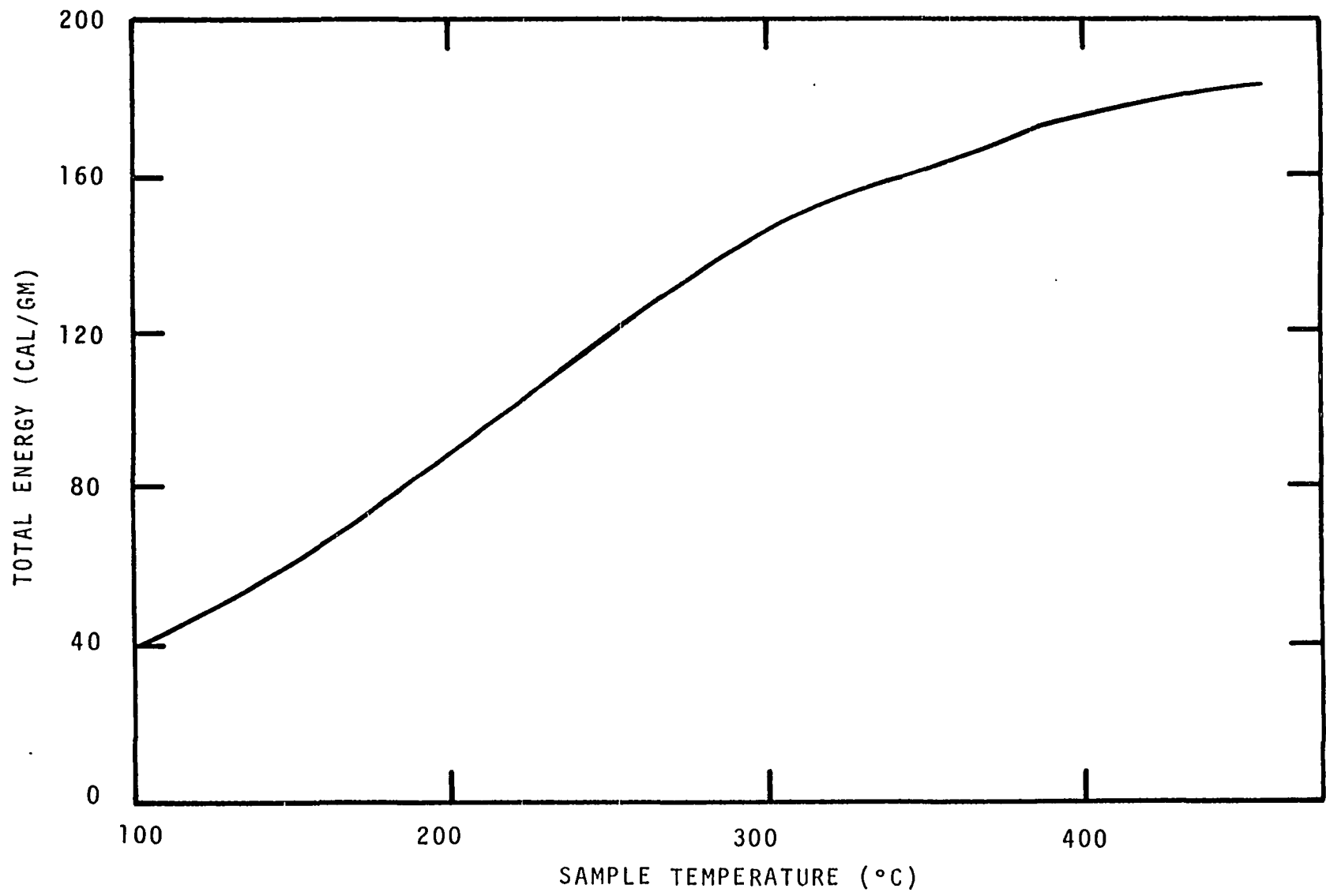


Figure H-4. Total Energy of Freeze-Dried Douglas Fir Needles. Heating Rate, 160°C/min.

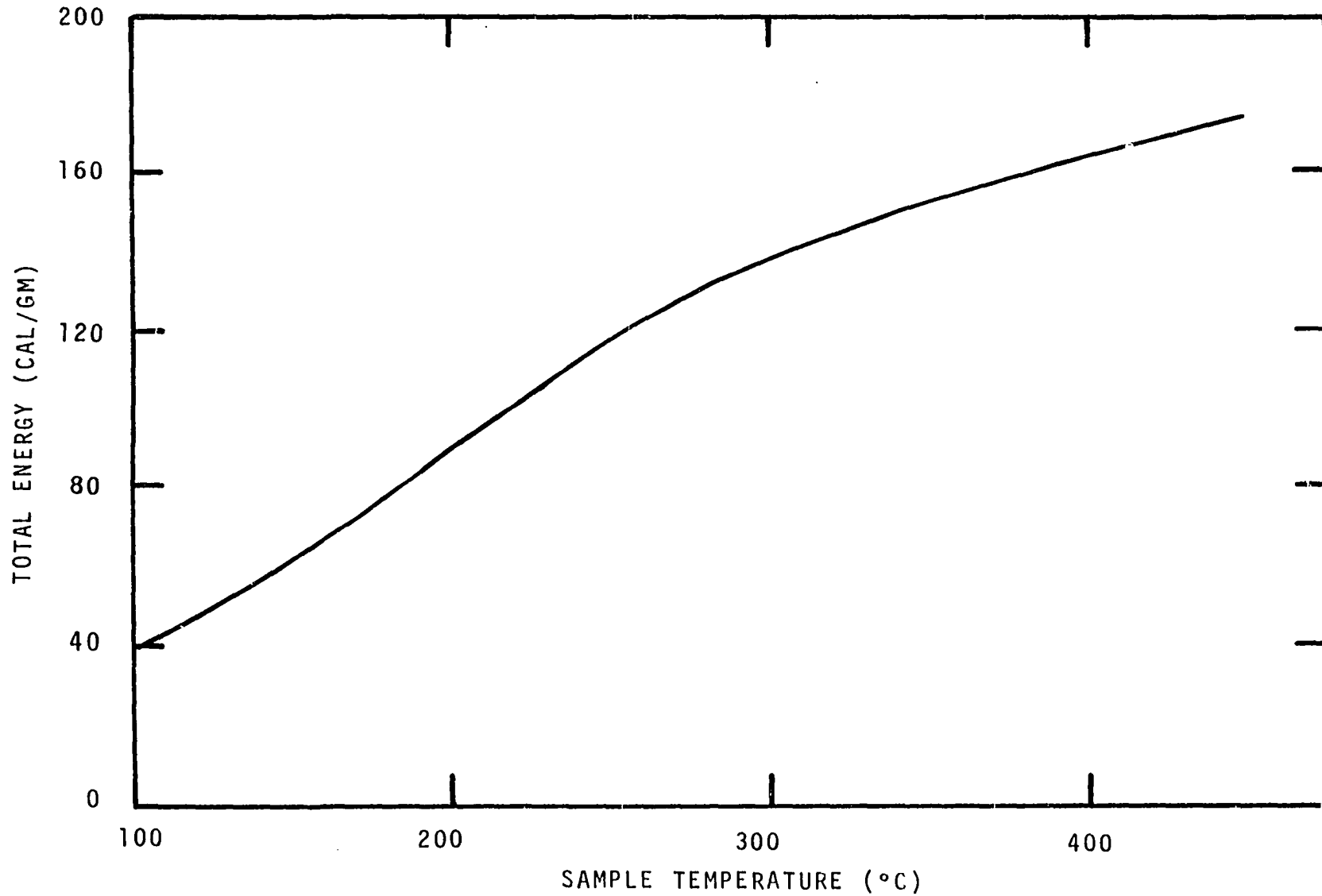


Figure H-5. Total Energy of Freeze-Dried Lodgepole Pine Needles. Heating Rate, 40°C/min.

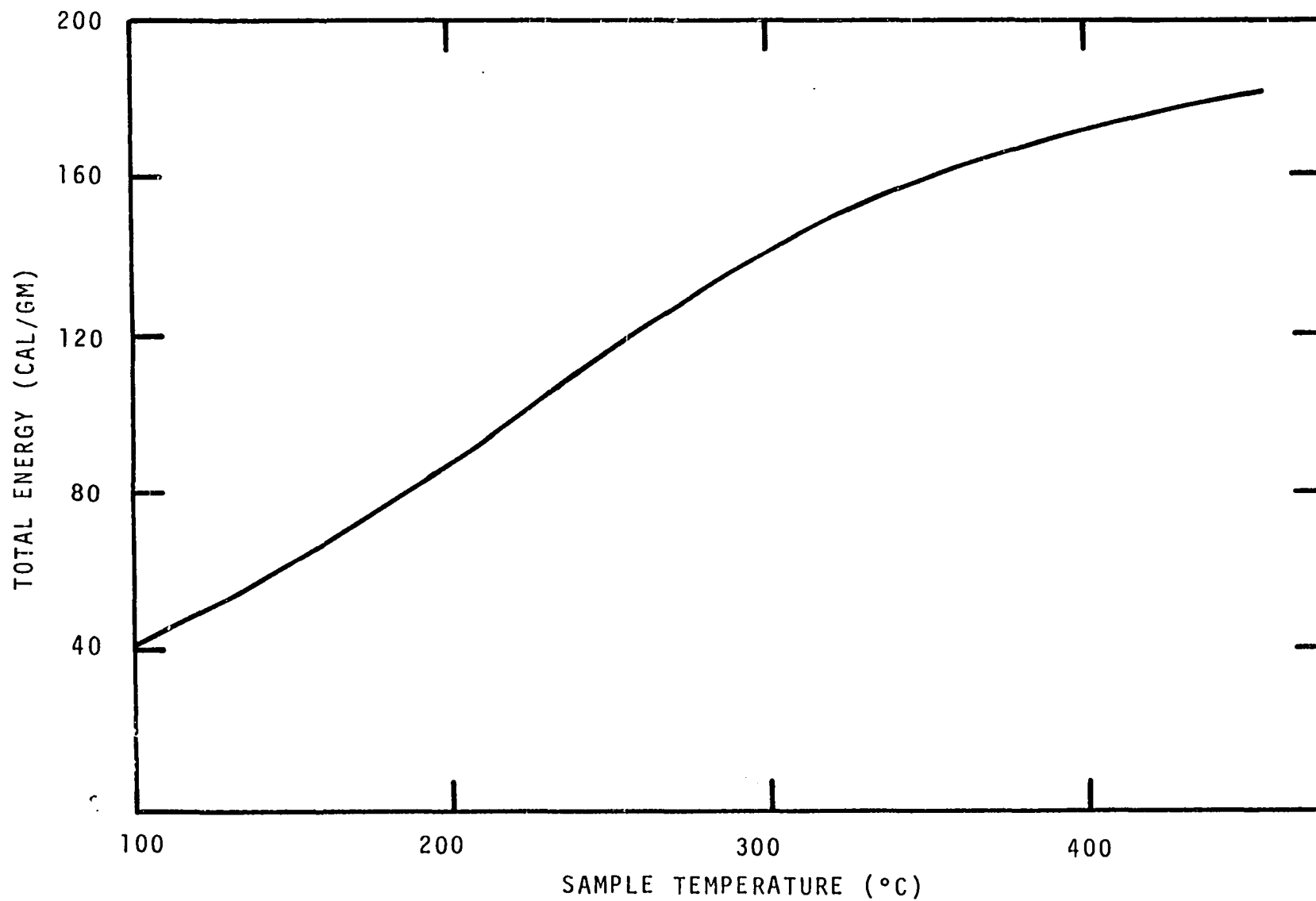


Figure H-6. Total Energy of Freeze-Dried Lodgepole Pine Needles. Heating Rate, 160°C/min.

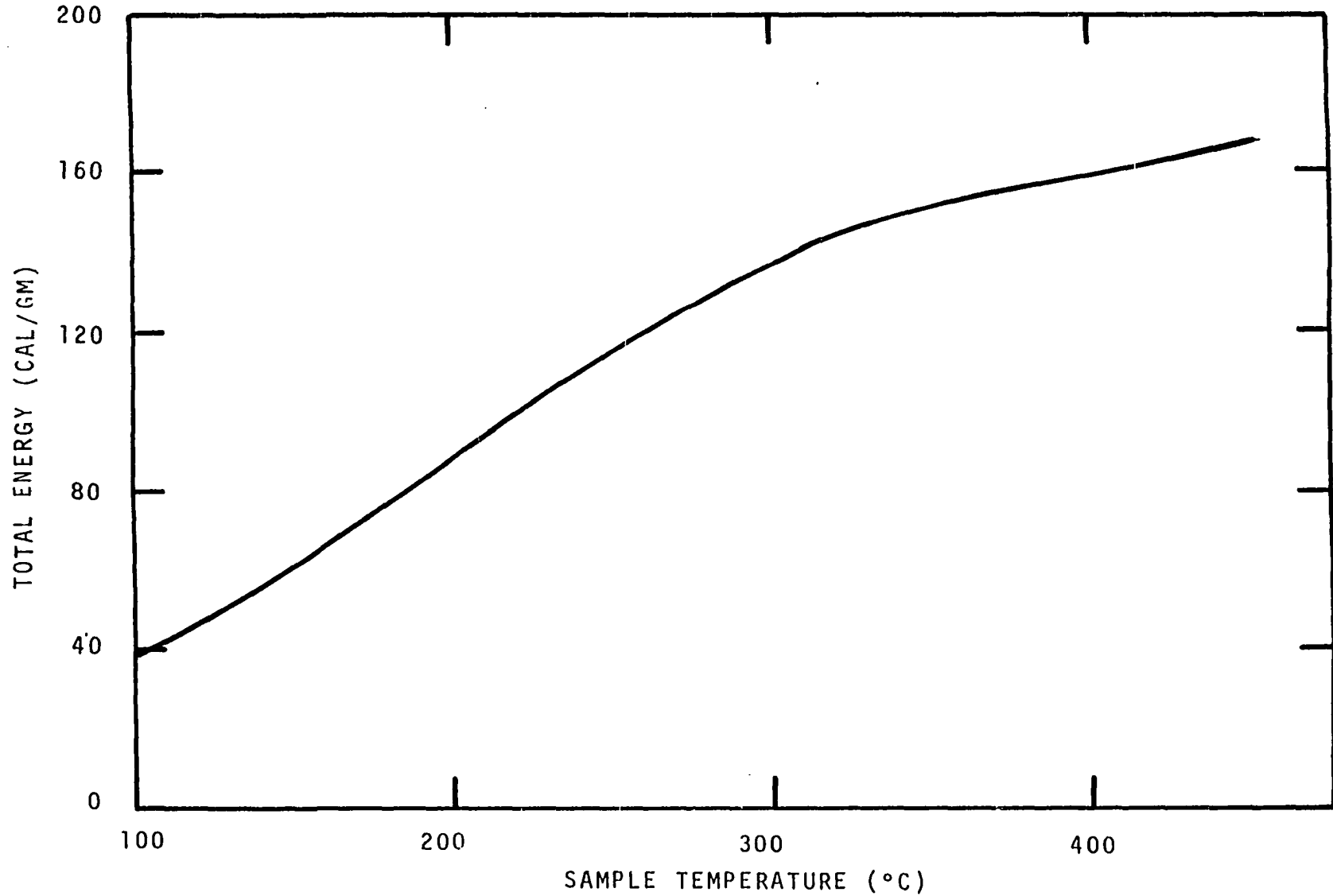


Figure H-7. Total Energy of Freeze-Dried Chamise Foliage. Heating Rate, 40°C/min.

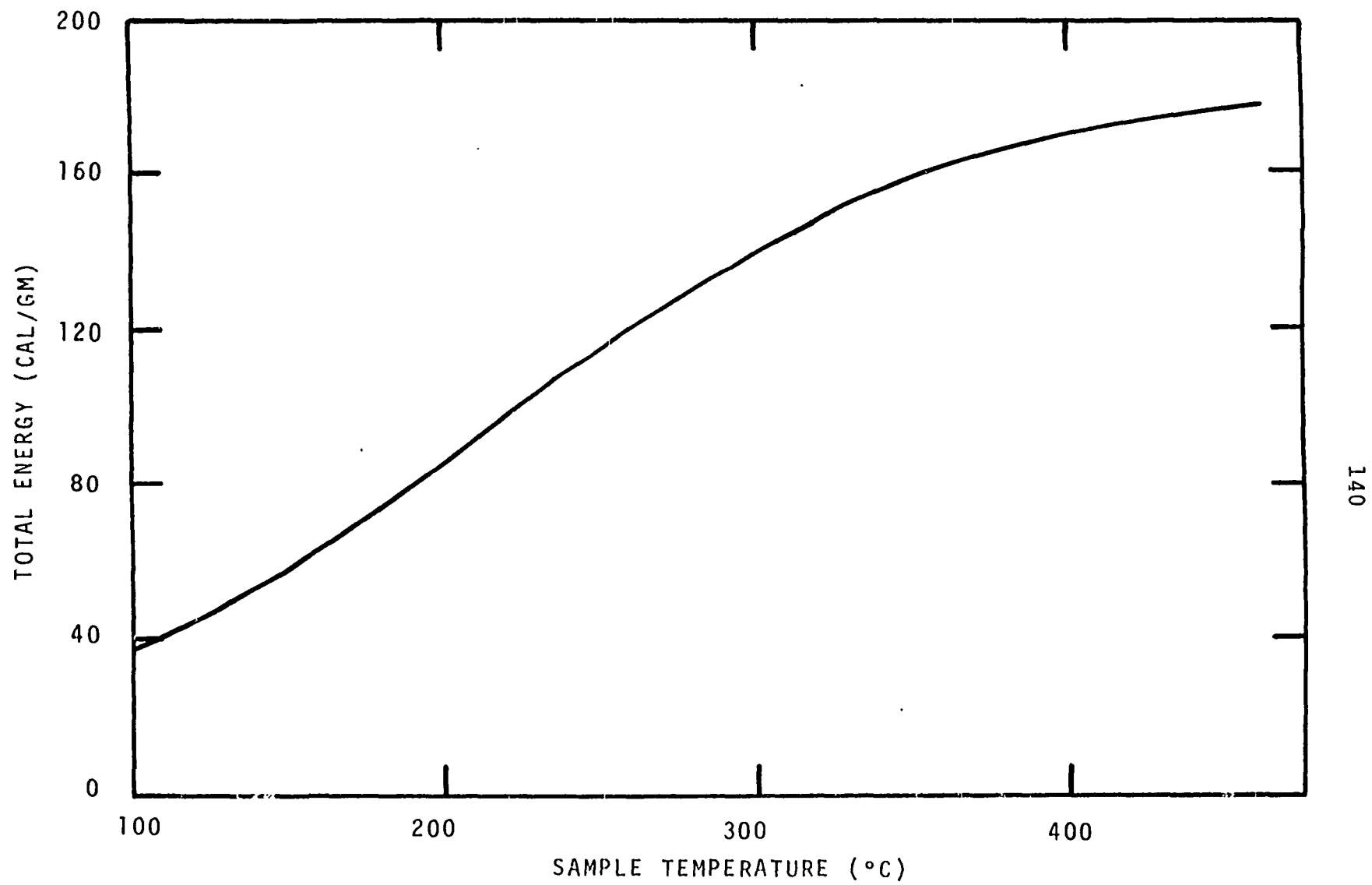


Figure H-8. Total Energy of Freeze-Dried Chamise Foliage. Heating Rate, 160°C/min.

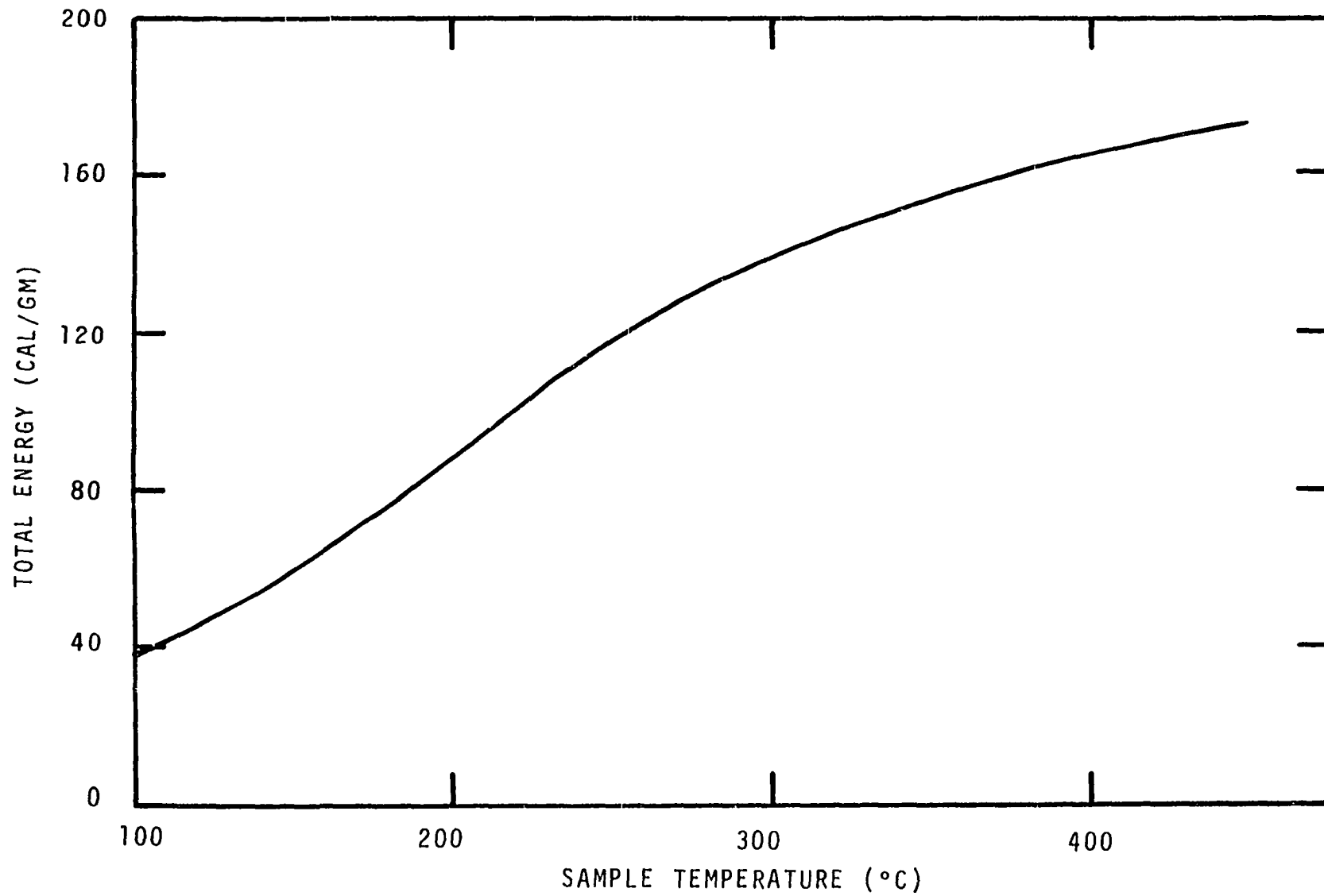


Figure H-9. Total Energy of Freeze-Dried Manzanita Leaves.  
Heating Rate, 40°C/min.

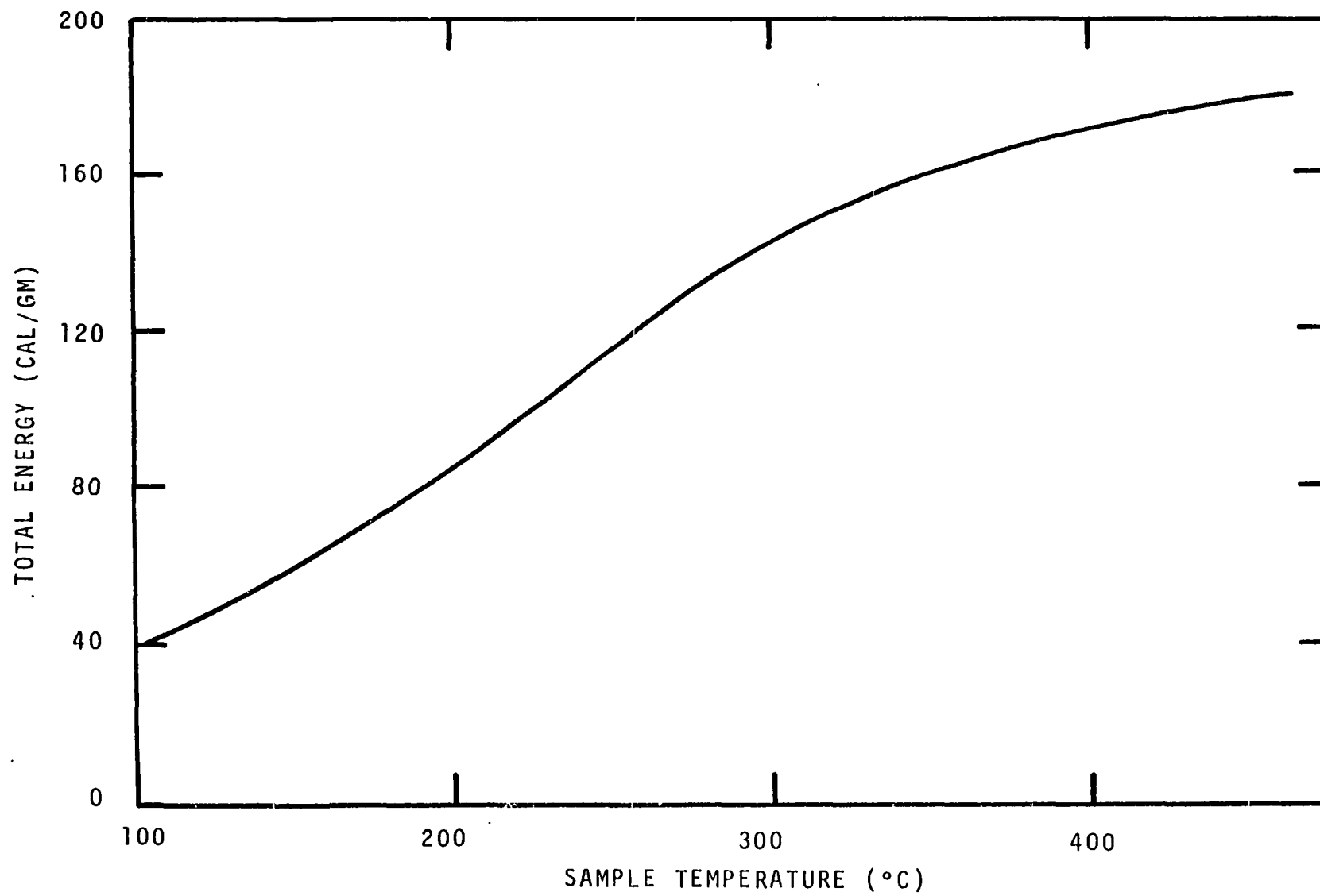


Figure H-10. Total Energy of Freeze-Dried Manzanita Leaves. Heating Rate, 160°C/min.